ACIBADEM MEHMET ALI AYDINLAR UNIVERSITY
INSTITUTE OF HEALTH SCIENCES

LONG-TERM STABILITY AND FORCED DEGRADATION STUDIES OF A THERAPEUTIC MONOCLONAL ANTIBODY

MERVE ÇELİK YAMACI

PH.D. THESIS

DEPARTMENT OF MEDICAL BIOTECHNOLOGY

SUPERVISOR
Prof. Dr. Özge CAN

ISTANBUL-2023

ACIBADEM MEHMET ALI AYDINLAR UNIVERSITY
INSTITUTE OF HEALTH SCIENCES

LONG-TERM STABILITY AND FORCED DEGRADATION STUDIES OF A THERAPEUTIC MONOCLONAL ANTIBODY

MERVE ÇELİK YAMACI

PH.D. THESIS

DEPARTMENT OF MEDICAL BIOTECHNOLOGY

SUPERVISOR
Prof. Dr. Özge CAN

ISTANBUL-2023

Department:	Medical Biotechnology
Program:	Medical Biotechnology Doctorate Program
Thesis Title:	Long-Term Stability and Forced Degradation Studies of a Therapeutic Monoclonal Antibody
Student's name and Surname:	Merve Çelik Yamacı
Date of Defense:	23 / 01 / 2023

This is to certify that I have examined this copy of Ph.D. thesis. I have found that she prepared after fulfilling the specified requirements in the associated legislation before the final examining committee, whose signatures are below.

Jury Member (Head of the Defense)	Prof. Dr., Tanıl Kocagöz Acıbadem Mehmet Ali Aydınlar University	_____
Jury Member (Thesis Supervisor)	Prof. Dr., Özge Can Acıbadem Mehmet Ali Aydınlar University	_____
Jury Member	Asst. Prof., Dr. Özgül Gök Acıbadem Mehmet Ali Aydınlar University	_____
Jury Member	Prof. Dr., Gizem Dinler Doğanay İstanbul Technical University	_____
Jury Member	Prof. Dr., Demet Cansaran Duman Ankara University	_____

DECLARATION

I declare that this thesis work is my own work, I had no unethical behavior at any stage from the planning to the writing of the thesis, I obtained all the information in this thesis in accordance with academic and ethical rules, and I cited all the information and comments that were not obtained with this thesis work, and I provided resources in the list of references. I also declare that there was no violation of any patents and copyrights during the study and writing of this thesis.

23 / 01 / 2023

Merve Çelik Yamacı

PREFACE AND ACKNOWLEDGEMENT

First and foremost, I would like to thank my advisor Prof. Dr. Özge Can, who shared his valuable knowledge and time with me during this thesis. It was an honor to be his student.

I would like to thank Assist. Prof. Ahmet Emin Atik, Berna Somuncu Ph.D., M.sc. Gülipek Güven, and M.sc. Zeynep Zülfiye Yıldırım Keleş for their help in my thesis. I would like to express my gratitude to Turgut İlaçları A.Ş. for financially supporting this study.

I am grateful to my Acıbadem family, Ozan Savaşan, Esma Aybakan, Tayyip Karaman and Merve Aydın, for always being there for me no matter what.

Special thanks to my besties, M.sc. Ceren Pamukcu and Yiğit Erdemgil Ph.D., who did not spare their help and support at every stage of this thesis and gave me the maximum level of fun and laughter throughout this journey. They always have a special place in my heart.

I would like to thank my dear mother Ayten Çelik and my father Mevlüt Çelik, who believed in me and was always there for me; I owe every success I have achieved to their love and support. And I would like to thank my mother-in-law Sibel Yamacı and father-in-law Halil Yamacı, who always motivated and appreciated me.

Last but by no means least, I would like to thank the person who supported me the most during this thesis, my wonderful husband, İlker Yamacı. If he hadn't sat with me in front of the computer on the weekends, I wouldn't have had the strength to write this thesis.

TABLE OF CONTENTS

LIST OF ABBREVIATIONS AND SYMBOL

α	Alpha
Å	Angstrom
BEH	Ethylene Bridged Hybrid
βME	βetamercaptoethanol
BS	Biosimilar mAb
CDR	Complementarity-determining Region
CE	Capillary Electrophoresis
CHO	Chinese Hamster Ovary
cm	Centimeter
CpB	Carboxypeptidase ß
CQA	Critical Quality Attribute
δ	Delta
DNA	Deoxyribonucleic Acid
DP	Drug Product
DS	Drug Substance
ε	Epsilon
EEA	European Economic Area
ELISA	Enzyme-Linked Immunosorbent Assay
EMA	European Medicines Agency
F/T	Freeze/Thaw
Fab	Antigen-binding Fragment
Fc	Crystallizable Fragment
FDA	United States Food and Drug Administration
γ	Gamma
Fv	Variable Fragment
GMP	Good Manufacturing Practice
H_2O_2	Hydrogen Peroxide
HC	Heavy Chain
HCl	Hydrochloric Acid
HMW	High Molecular Weight

ICH	International Conference on Harmonization
Ig	Immunoglobulin
IgG	Immunoglobulin G
i.d.	Internal Diameter
icIEF	Imaged Capillary Isoelectric Focusing
κ	Kappa
kDa	Kilodaltons
λ	Lambda
LC	Light Chain
LMW	Light Molecular Weight
Lys	Lysine
µg	Microgram
µL	Microliter
µm	Micrometer
M	Molarity
mAb	Monoclonal Antibody
mg	Milligram
mL	Milliliter
mM	Millimolar
µ	Mu
N	Normal
nm	Nanometer
nrCE-SDS	Non-Reduced Capillary Electrophoresis-Sodium Dodecyl Sulfate
NS0	Murine Myeloma
OR	Originator
PCR	Polymerase Chain Reaction
PDA	Photodiode Array Detector
pH	Potential of Hydrogen
pI	Isoelectric point
pNPP	p-Nitrophenyl Phosphate
PTM	Post Translational Modification
QA	Quality Attributes

rCE-SDS	Reduced Capillary Electrophoresis-Sodium Dodecyl Sulfate
RH	Relative Humidity
rpm	Revolutions Per Minute
RT	Room Temperature
SD	Standard Deviation
SDS	Sodium Dodecyl Sulfate
SDS-Mw	Sodium Dodecyl Sulfate Molecular Weight
SDS-PAGE	Sodium Dodecyl Sulfate Polyacrylamide Gel Electrophoresis
SEC	Size Exclusion Chromatography
SE-UPLC	Size Exclusion Ultra High-Performance Liquid Chromatography
Tm	Melting Temperature
UV/Vis	Ultraviolet/Visible Spectroscopy
V	Volt
WHO	World Health Organization

LIST OF FIGURES

LIST OF TABLES

ÖZET

Terapötik Monoklonal Bir Antikorun Uzun Süreli Stabilitesi ve Hızlandırılmış Degradasyon Çalışmaları

Biyobenzer mAb (BS) için uzun vadeli stabilite çalışmaları yapmak, yapılarının karmaşıklığından dolayı özellikle önemlidir. Stabilite çalışması, BS örneğinin üç farklı saklama koşulu üzerinde gerçekleştirilmiştir. Stabilite çalışması boyunca, 5.0±3.0˚C'de saklanan BS örneği için toplam HMW veya monomer yüzdesinde önemli bir değişiklik olmamıştır. Ancak ≤-65°C'de monomer pikinde önemli bir azalma ve HMW seviyesinde bir artış gözlenir. Bu durum, ürünün dondurularak saklamaya uygun olmadığını gösterir (≤-65°C). BS örneklerinin yük varyantı profilleri, safsızlık seviyeleri ölçüldü ve kompleman analizi yapıldı. Tüm zaman noktalarındaki sonuçlar spesifikasyon aralığı içindedir. Ek veri olarak orijinatör (OR) ürün, 24 ay boyunca 5.0±3.0°C'de saklandı ve 5.0±3.0°C'deki BS örneği ile karşılaştırıldı. Sonuç olarak tüm analiz sonuçlarında BS ve OR örneklerinin 5.0±3.0°C arasında anlamlı bir değişim gözlenmedi. BS ve OR örneklerine stres uygulamak, klinik çalışmalardan önce değerli bilgiler sağlayabilir. Bu zorunlu bozunma çalışmalarında, SE-UPLC, icIEF, CE-SDS ve kompleman analizi ile BS ve OR örneklerindeki bozunma ürünlerinin değişimi araştırıldı. Stres boyunca lineer eğrilerin eğimleri istatistiksel olarak karşılaştırıldı. Buna göre, BS ve OR örneklerinin bozunma oranlarının benzer olduğu sonucuna varılmıştır. Sonuç olarak, bu tez kapsamında tamamlanan zorunlu bozunma ve uzun vadeli stabilite çalışmaları, BS örneğinin yapısının ve biyolojik aktivitesinin karakterize edilmesine yardımcı olmuştur.

Anahtar Sözcükler: Biyobenzer, karakterizasyon, monoklonal antikor, stabilite çalışması, zorunlu bozunma çalışmaları

ABSTRACT

Long-Term Stability and Forced Degradation Studies of a Therapeutic Monoclonal Antibody

Performing long-term stability studies for biosimilar mAb (BS) is particularly important due to the complexity of their structures. The stability study was performed on three different storage conditions of the BS. Throughout the stability study, there was no significant change in the percentage of total HMW or the monomer for BS stored at 5.0±3.0˚C. However, a significant decrease in monomer peak and an increase in HMW level are observed ≤-65°C. It indicates that the product is not suitable for freezing storage (≤-65°C). The charge variant profiles, impurity levels, and relative potency of the BS samples were also measured. Results at all time points are within the specification range. As additional data, the originator (OR) was stored at 5.0±3.0˚C for 24 months and compared with the BS at 5.0±3.0˚C. As a result, no significant change was observed between the 5.0±3.0˚C of BS and OR samples in all analysis results. Applying stress to BS and OR can provide valuable information before clinical studies. These forced degradation studies investigated the change of degradation products in BS and OR by SE-UPLC, icIEF, CE-SDS, and complement assay. The slopes of the linear curves throughout the stress were statistically compared. Accordingly, it was concluded that the degradation rates of BS and OR were similar. In conclusion, forced degradation and long-term stability studies completed as part of this thesis helped to characterize the structure and biological activity of BS.

Keywords: Biosimilar, characterization, monoclonal antibody, stability study, forced degradation studies

1 INTRODUCTION AND AIM

Since the end of the 20th century, with the rapid development of biotechnology and significant advances in disease treatment, drug development has shifted towards biopharmaceuticals rather than small-molecule drugs (1). In Turkey, the total market size of biotechnological drugs reached 8.7 billion Turkish Liras in 2020, accounting for 18.2% of the total pharmaceutical market value, and almost all of these drugs are imported (2). In the light of these data, many pharmaceutical companies take steps to enter the field of biotechnology every year.

Monoclonal antibodies (mAbs), which dominated the top 10 best-selling drugs in 2017, have seen a steady increase in market share (3). However, many biotechnological drug patents have expired, opening up a multi-billion-dollar market to competitors for biosimilars (4). Competing with a biosimilar of comparable quality, safety, and efficacy to the reference product can reduce treatment costs and help increase patient access to treatment (5). Even if the same process is applied as the originator product, changes during the manufacture, transportation, and storage conditions may alter the quality of the therapeutic products (4).

Due to the differences in their structures, separate approaches have been established for each biotechnological product. State-of-the-art analytical tools can characterize their physicochemical structures, biological activities, and impurity properties (6,7).

Stability studies under forced degradation and storage conditions are essential for mAbs to assess sensitivity to factors that impacts efficacy, safety, and quality (4,8). The stress conditions for forced degradation studies are much more severe than the physical and chemical stress to which products are subjected during production, transportation, and storage (9). Therefore, forced degradation studies enrich impurity levels, accelerate protein degradation, and demonstrate the ability of the methods to distinguish between impurities, degradation products, and the desired product (10).

The behavior of biosimilar and originator products can be monitored under applied stress conditions, and their stability can be compared during long-term storage. Examination of therapeutic mAbs under stressful conditions provides structural information about the product's quality, safety, and efficacy in a relatively short time (9). Any changes in physicochemical properties, structure, aggregation, biological activity, visual appearance, and impurities are essential for the product's development phase (9,10). With this thesis, results from stability and degradation studies provide valuable data for the similarity comparison of biosimilar and originator products.

2 BACKGROUND

2.1 Biotechnology and Biopharmaceuticals

Biotechnology is the branch of applied science that uses living organisms to make or modify products or processes for specific use (11) The term "biotechnology" was coined in 1919 by Hungarian engineer Karl Ereky in a book based on converting raw materials into valuable products using living organisms. (12) Biotechnology is a multidisciplinary field that uses biology and various technologies such as chemistry, molecular biology, genetic engineering, immunology, cell culture, physiology, etc. (11,12)

The power of biotechnology affects all aspects of daily life and has a remarkable impact on the world economy and community (13). Conventional biotechnology is used for specific purposes, such as fermented products or bread production. On the other hand, modern biotechnology techniques include recombinant DNA for gene cloning, tissue culture, polymerase chain reaction (PCR), monoclonal antibody (mAb) techniques, and large-scale fermentation processes (14).

Technological advances have significantly increased the value of biotechnological drugs, which represent most of all drugs worldwide in the pharmaceutical industry (13). With the contribution of these developments, major pharmaceutical companies have adopted biotechnology to develop new drugs (15). Pharmaceutical biotechnology is a relatively new and rapidly growing field in which biotechnology principles play an essential role and one of the most important fields for developing safer and more effective biotechnological drugs (15,16).

Biotechnological drugs, also known as biopharmaceuticals, constitute most of the new drugs developed to treat many diseases, especially cancer, heart diseases, metabolic disorders, and diabetes, which are common in the community (16). Due to the rapid development of the biopharmaceutical market and the demand for these drugs, it is believed to have great potential for further dynamic growth (17,18).

Humulin, recombinant human insulin, was the first biopharmaceutical approved by the FDA in 1982 for human therapeutic uses (15). Since the approval of mAbs like Proleukin and Zenapax in the 1990s and Humira in 2003, the number of biopharmaceuticals has rapidly increased (16). Recombinant proteins, mAbs, blood/plasma-derived products, peptides, vaccines, nucleic acids, cytokines, and cell and tissue cultures are all examples of biopharmaceuticals (12,17).

Biopharmaceutical drugs differ significantly from the more commonly prescribed chemical drugs. While chemical drugs are small molecules with stable structures produced by chemical synthesis, biopharmaceutical drugs are large molecules with complex and heterogeneous structures due to the formation of polymeric chains (18). Unlike chemical drugs, which are not or are only slightly sensitive to process changes during manufacture, biopharmaceuticals are extremely sensitive to process changes. Since they are produced using living systems such as genetically modified bacteria and mammalian cells, their synthesis is affected by many parameters during the production process (20,21). Due to biological differences between the expression systems and the conditions of the applied manufacturing process, a certain degree of variability can occur even between different batches of the same product (21).

Biopharmaceuticals have many advantages over the conventional small-molecule drugs. They are gaining increasing attention as new drugs due to their selectivity toward their respective targets. For example, they only target specific molecules and rarely cause the side effects associated with conventional small-molecule drugs (18).

Compared with conventional drugs, biopharmaceuticals exhibit high specificity and activity. The application of biopharmaceuticals has facilitated the treatment of patients with poor responses to conventional small molecules (19,20).

2.2 Biosimilars

Biotechnology has made it possible to manufacture a wide range of therapeutic proteins, allowing biopharmaceuticals to become important therapeutic options for various diseases. Due to the complex manufacturing process, biopharmaceuticals are more expensive than small-molecule chemical drugs. The production costs of biopharmaceuticals, particularly mAbs, may result in reduced patient access to the drugs (5).

With the expiration of patents and other exclusivity rights of many commercially approved drugs, developing alternative versions of biopharmaceuticals called biosimilars has provided a new market area, reducing the risks and costs (21).

The United States Food and Drug Administration (FDA) defines a biosimilar as "a biological product that is highly similar to and has no clinically meaningful differences from an existing FDA-approved reference product" (22). Also, the European Medicines Agency (EMA) defines a biosimilar as: "A biosimilar is a biological medicinal product that contains a version of the active substance of an already authorized original biological medicinal product (reference medicinal product) in the European Economic Area (EEA). Similarity to the reference medicinal product in terms of quality characteristics, biological activity, safety, and efficacy based on a comprehensive comparability exercise needs to be established" (23). Guidelines defined by these organizations establish the regulatory framework for the approval of biosimilars. In addition, product-specific biosimilar guidelines, such as mAbs, have been published. (24).

Since 2006, EMA has recommended the approval of 90 biosimilars, but 20 of those approvals have been withdrawn or refused. In total, 70 biosimilars have been approved for use in Europe, see Table 1, and mAb-based drugs constitute 50% of approved biosimilars (25).

Table 1: EMA-approved biosimilars

No	Product name	Active substance	Authorization date	Company
1	Abasaglar	insulin glargine	09 Sep 2014	Eli Lilly Nederland B.V.
2	Abevmy	bevacizumab	21 Apr 2021	Mylan (now Viatris)
3	Abseamed	epoetin alfa	27 Aug 2007	Medice Arzneimittel Pütter
4	Accofil	filgrastim	17 Sep 2014	Accord Healthcare
5	Alymsys	bevacizumab	26 Mar 2021	mAbxience Research
6	Amgevita	adalimumab	21 Mar 2017	Amgen
7	Amsparity	adalimumab	13 Feb 2020	Pfizer
8	Aybintio	bevacizumab	19 Aug 2020	Samsung Bioepis
9	Bemfola	follitropin alfa	26 Mar 2014	Finox Biotech
10	Benepali	etanercept	13 Jan 2016	Samsung Bioepis
11	Binocrit	epoetin alfa	28 Aug 2007	Sandoz
12	Blitzima	rituximab	13 Jul 2017	Celltrion
13	Byooviz	ranibizumab	18 Aug 2021	Samsung Bioepis
14	Cegfila	pegfilgrastim	19 Dec 2019	Mundipharma Biologics
15	Epoetin alfa Hexal	epoetin alfa	27 Aug 2007	Hexal
16	Equidacent	bevacizumab	24 Sep 2020	Centus Biotherapeutics
17	Erelzi	etanercept	23 Jun 2017	Sandoz
18	Filgrastim Hexal	filgrastim	6 Feb 2009	Hexal
19	Flixabi	infliximab	26 May 2016	Samsung Bioepis
20	Fulphila	pegfilgrastim	20 Nov 2018	Mylan
21	Grastofil	filgrastim	17 Oct 2013	Apotex
22	Grasustek	pegfilgrastim	20 Jun 2019	Juta Pharma (USV)
23	Hefiya	adalimumab	26 Jul 2018	Sandoz
24	Herzuma	trastuzumab	8 Feb 2018	Celltrion Healthcare
25	Hukyndra	adalimumab	17 Sep 2021	Alvotech/Stada Artnimettel
26	Hulio	adalimumab	17 Sep 2018	Fujifilm Kyowa Kirin Biologics
27	Hyrimoz	adalimumab	26 Jul 2018	Sandoz
28	Idacio	adalimumab	2 Apr 2019	Fresenius Kabi
29	Imraldi	adalimumab	24 Aug 2017	Samsung Bioepis
30	Inflectra	infliximab	10 Sep 2013	Hospira (Pfizer)
31	Inhixa	enoxaparin sodium	15 Sep 2016	Techdow Europe
32	Insulin aspart Sanofi	insulin aspart	25 Jun 2020	Sanofi-Aventis
33	Insulin lispro Sanofi	insulin lispro	19 Jul 2017	Sanofi-Aventis
34	Kanjinti	trastuzumab	16 May 2018	Amgen/Allergan
35	Kirsty	insulin aspart	5 Feb 2021	Mylan (now Viatris) / Biocon
36	Lextemy	bevacizumab	25 Feb 2021	Mylan (now Viatris)
37	Libmyris	adalimumab	17 Sep 2021	Alvotech/Stada Artnimettel

Table 1: EMA-approved biosimilars (continue)

No	Product name	Active substance	Authorization date	Company
38	Livogiva	teriparatide	27 Aug 2020	Theramex Ireland
39	Movymia	teriparatide	11 Jan 2017	Stada Arzneimittel
40	Mvasi	bevacizumab	15 Jan 2018	Amgen
41	Nepexto	etanercept	25 May 2020	Mylan
42	Nivestim	filgrastim	7 Jun 2010	Hospira (Pfizer)
43	Nyvepria	pegfilgrastim	18 Nov 2020	Pfizer
44	Ogivri	trastuzumab	12 Dec 2018	Biocon/Mylan
45	Omnitrope	somatropin	12 Apr 2006	Sandoz
46	Onbevzi	bevacizumab	11 Jan 2021	Samsung Bioepis
47	Ontruzant	trastuzumab	15 Nov 2017	Samsung Bioepis
48	Ovaleap	follitropin alfa	27 Sep 2013	Teva Pharma
49	Oyavas	bevacizumab	26 Mar 2021	Stada Arzneimittel
50	Pelgraz	pegfilgrastim	21 Sep 2018	Accord Healthcare
51	Pelmeg	pegfilgrastim	20 Nov 2018	Cinfa Biotech/Mundipharma
52	Ratiograstim	filgrastim	15 Sep 2008	Ratiopharm
53	Remsima	infliximab	10 Sep 2013	Celltrion
54	Retacrit	epoetin zeta	18 Dec 2007	Hospira (Pfizer)
55	Rixathon	rituximab	15 Jun 2017	Sandoz
56	Riximyo	rituximab	15 Jun 2017	Sandoz
57	Ruxience	rituximab	1 Apr 2020	Pfizer
58	Semglee	insulin glargine	28 Mar 2018	Mylan
59	Silapo	epoetin zeta	18 Dec 2007	Stada Arzneimittel
60	Stimufend	pegfilgrastim	28 Mar 2022	Fresenius Kabi Deutschland GmbH
61	Terrosa	teriparatide	4 Jan 2017	Gedeon Richter
62	Tevagrastim	filgrastim	15 Sep 2008	Teva Generics
63	Trazimera	trastuzumab	26 Jul 2018	Pfizer
64	Truxima	rituximab	17 Feb 2017	Celltrion
65	Yuflyma	adalimumab	11 Feb 2021	Celltrion Healthcare
66	Zarzio	filgrastim	6 Feb 2009	Sandoz
67	Zercepac	trastuzumab	27 Jul 2020	Accord Healthcare
68	Zessly	infliximab	18 May 2018	Sandoz
69	Ziextenzo	pegfilgrastim	22 Nov 2018	Sandoz
70	Zirabev	bevacizumab	14 Feb 2019	Pfizer

Because small molecule drugs are chemically synthesized, developing and manufacturing identical (generic) products are relatively simple (24). After the patent expiration of the approved product, it is sufficient to demonstrate that the generic product contains the same chemical composition as the originator product and that the pharmacokinetic properties are similar. In contrast, biopharmaceuticals are produced mainly by living systems and are difficult to manufacture, much more complex than small-molecule drugs (21). Biosimilars are not generic equivalents of originator products and therefore require a much more detailed approval process than a generic drug. Although the focus of the originator biological development process is clinical data, due to the complexity of the structure and manufacturing process, the biosimilar development process requires more extensive analytical characterization (15,24).

Physical, chemical, biological, and microbiological properties are the best ways to describe the complexity of biosimilars. The properties required to ensure the desired product quality are known as critical quality attributes (CQA) and should be routinely monitored and controlled within a specified limit, range, or distribution (4,26,27). Selecting quality attributes (QAs) based on molecular structure, mechanism of action, safety, and efficacy, as well as defining analytical methods to test them, are the first steps in establishing CQAs for biosimilar products. Quantitative and qualitative methods are used to assess the risk and impact of each QA (26,28).

Each production step is extremely sensitive to environmental changes and can affect the final product, including batch-to-batch variation (4). As a result, regulatory agencies must approve manufacturing processes and all modifications, confirming that they have no impact on overall clinical efficacy or safety. Although the regulatory requirements for biosimilar mAbs are more complex than for smaller biosimilars, the vast market potential has prompted many pharmaceutical companies to invest in developing biosimilar mAbs (3,5,29).

2.3 Monoclonal Antibodies and Immunoglobulins

Monoclonal antibodies have become the most widely recognized biotherapeutics in the pharmaceutical industry over the past 20 years due to their therapeutic efficacy against many diseases, such as cancer and autoimmune diseases (30). The work of Köhler and Milstein in 1975 on methods of producing murine hybridomas is considered by many to be the dawning of the era of therapeutic mAbs (31).

Following the discovery of the mAb hybridoma technology, Orthoclone OKT3w, the first commercial therapeutic antibody, was licensed by Ortho Biotech in 1986 for the inhibition of transplant rejection (20). Eight years later, the second antibody, the chimeric antibody ReoProw (abciximab), was developed by Centocor to inhibit platelet aggregation after cardiovascular surgery (32).

With the introduction of five mAb drugs into the market in 1997-1998, significant interest has emerged in the field of therapeutic mAbs. For this reason, the 1970s and 1980s had an important place in the biological revolution. Several technologies were developed during this period, which ultimately combined for the development of the therapeutic mAb industry (7). The use of restriction enzymes to clone a gene into a plasmid, the development of hybridoma technology, site-directed mutagenesis as a tool for protein engineering, and a better understanding of antibody expression genetics are all examples of these technologies. In the 1980s, recombinant antibodies were made possible by advances in phage display technology, PCR, sequencing and characterization of human germline antibody genes, and expression of antibody genes in cell cultures and Escherichia coli (7,31,32).

An international nomenclature has been proposed using a specific suffix corresponding to the origin and source of mAbs to facilitate the distinction between the various mAbs. The suffix "-omab" is added to mouse mAbs (33). In 2003, the FDA approved Tositumomab (Bexxar) for treating non-Hodgkin's lymphoma (34).

Chimeric antibodies are humanized mAbs with the suffixes "-ximab" (chimeric antibodies that are approximately 65% human) or "-zumab" (humanized antibodies that are approximately 95% human) (33). The FDA approved Cetuximab (Erbitux) as a chimeric antibody in 2004 to treat colorectal, head, and neck cancers. Bevacizumab (Avastin) is a humanized antibody approved by the FDA in 2004 to reduce tumors by inhibiting the formation of new blood vessels (32,35).

The suffix "-mumab" is added to human mAbs, produced either by hybridomas derived from transgenic mice with human antibody genes replaced or by a process known as phage display (33). Adalimumab (Humira), the first human mAb developed using phage display technologies, was approved by the FDA to treat various immune system diseases (36).

Monoclonal antibodies are secreted by certain immune system cells that precisely bind to specific sites (epitopes) on the surface of foreign invaders, allowing them to be destroyed or neutralized (37). B lymphocytes are immune cells that secrete antibodies and fusing these antibody-producing cells with myelomas (B-cell tumor cells) results in a hybridoma. This immortal cell can grow indefinitely in culture and secrete large amounts of a specific antibody. mAbs are produced by hybridoma cells that can bind to only one site on a specific target. They are powerful clinical and industrial tools, and biotechnology companies can produce them in large quantities for various applications by growing hybridoma cell lines in bioreactors (38,39).

Monoclonal antibodies belong to the immunoglobulin (Ig) superfamily, and immunoglobulins (Igs) are Y-shaped glycoproteins divided into five major classes based on their biological properties and effector functions: IgA, IgD, IgE, IgG, and IgM; these antibodies differ in their heavy chain sequences, with heavy chain types α, δ, ε, γ and μ, respectively (40). The main functions and structures of Igs are summarized in Table **2**. Light chains are classified into two types, called κ and λ, and differ in their C region but have no functional differences (41).

Table 2: Immunoglobulin subclasses

Subclasses	IgA	IgD	IgE	IgG	IgM
Structure	 Dimer	 Monomer	 Monomer	 Monomer	 Pentamer
Heavy chain type	α	δ	ε	γ	μ
Molecular weight (Daltons)	405,000	180,000	190,000	150,000	970,000
Percentage in serum	13%	0.2%	0.002%	80%	6%
Half-life (days)	6	3	2	IgG1: 21 IgG2: 20 IgG3: 7 IgG4: 21	5
Function	Protects mucous membranes	Supports antigen recognition	Protects against parasites	Secondary response antibody	Primary response antibody

Many therapeutic mAbs are in the immunoglobulin G (IgG) class. The general structure of an IgG is shown in Figure **1**. IgGs are large tetrameric glycoproteins with four polypeptide chains and weigh about 150 kDa (40). The structure consists of two identical heavy chains (H, 50 kDa) and two identical light chains (L, 25 kDa) linked by interchain disulfide bonds at the hinge region (42). Each chain consists of structural domains that give constant, variable, and hypervariable regions according to their size and function. The H chains contain one variable (V_H) domain and three constant (C_H1, C_H2, and C_H3) domains, and the L chains contain one variable (V_L) and one constant (C_L) domain (39,40,42).

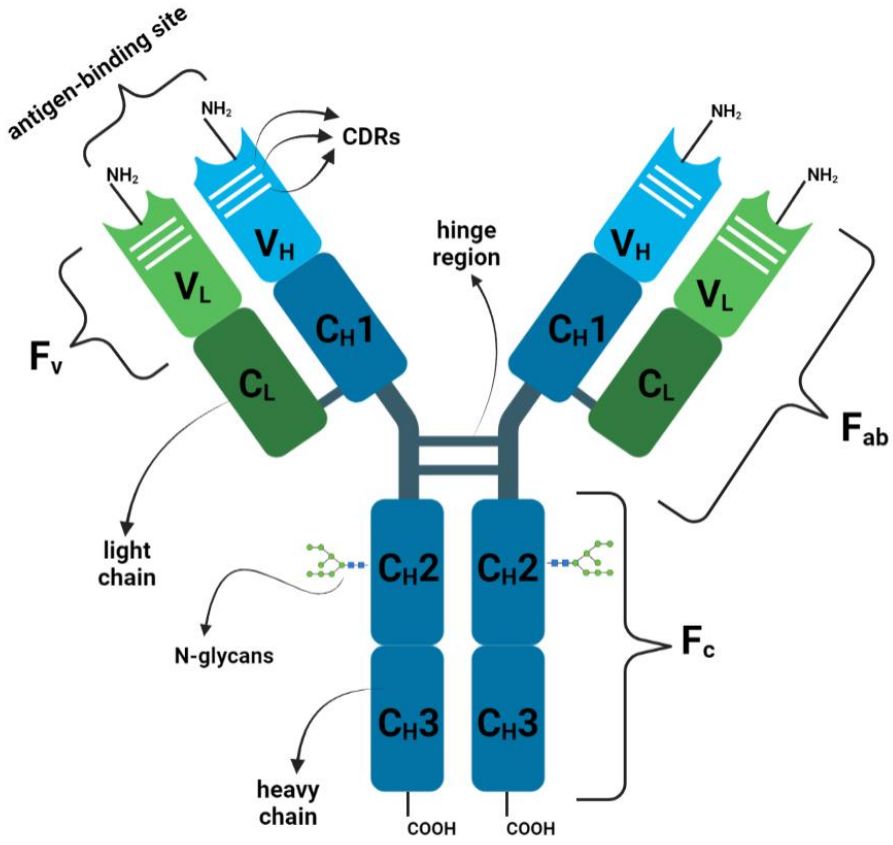

Figure 1: The general structure of an IgG

Each antibody molecule can be divided into two functionally distinct regions, each performing a different function. The antigen-binding fragment (Fab) contains complete light chains and V_H and C_H1 domains of the heavy chains and is responsible for antigen recognition and binding (38). The two identical sites in the Fab, consisting of the variable domains at the N-terminal ends of the H chain and the L chain, are called the antigen-binding sites (43). These variable domains, which are subregions of the Fab and bind to the antigen, may also be referred to as the variable fragment or F_V (42). Each F_V contains three hypervariable regions called complementarity-determining regions (CDRs), which are responsible for antigen recognition (37). The crystallizable fragment (Fc) region contains the remaining heavy chain C domains (C_H2 and C_H3) and is responsible for the effector functions like interaction with cell surface receptors and complementary proteins (7,38). The Fc region carries a pair of oligosaccharides (N-glycans) responsible for significant effects on the activity and efficacy of IgGs (37,42).

Differences in the number and location of interchain disulfide bonds and the length of the hinge region divide IgG into IgG1, IgG2, IgG3, and IgG4 subclasses (41). These differences affect their ability to bind an antigen and induce effector functions. IgG1 is the most preferred subclass for therapeutic antibodies due to its effector function and a longer serum half-life. Because it exhibits a short half-life in circulation, the IgG3 subclass is not used for therapeutic antibodies (44,45). A mAb with the desired effector function can be designed for therapeutic treatment using antibody engineering. Because IgG2 and IgG4 are the least effective subclasses, they can be combined in design, such as IgG2/4, in which IgG2's C_H1 domain and hinge region are fused to IgG4's C_H2 and C_H3 domains (45,46).

Post-translational modifications (PTM) are enzymatic and chemical modifications that occur at the amino acid side chains or C- or N-terminal ends of proteins (47,48). Because mAbs are produced by living cells, even if the differences in their production are minor, they lead to different levels of PTMs such as glycation, oxidation, glycosylation, deamidation, size variations, charge heterogeneity, and false disulfide bond formation, which in turn cause structural and functional differences between the originator product and the biosimilar (43,49).

A significant PTM that influences protein folding, conformation, stability, solubility, localization, and activity is glycosylation (50). The majority of mAbs contain an N-glycosylation site on the Fc fragment, which is known to have an impact on their effector activities, including complement-dependent cytotoxicity (CDC), antibody-dependent cellular cytotoxicity (ADCC), and antibody-dependent cellular phagocytosis (ADCP) (51–53). mAbs glycosylation can be either O-linked on serine (Ser) and threonine (Thr) residues or N-linked on asparagine (Asn) residues (54). Most of the structures of the mAbs made in CHO cell lines are biantennary, just like the human endogenous IgGs. In contrast, non-human glycan moieties like N-glycolylneuraminic acid (NGNA) and α-galactose are present in mAbs expressed in murine cell lines, such as NS0 cell lines (55,56).

Numerous factors can lead to oxidative stress, which can alter the structure of mAbs in a way that could trigger an immune response (57). Methionine, tyrosine, and cysteine are susceptible to oxidation (58). This process may take place during various stages of the development of mAbs, such as production, purification, formulation, and storage, changing their biological and physical characteristics as well as their potency and stability (57,59). mAbs that have undergone methionine oxidation may have a slight basic charge due to changes in the surface charge of the protein as well as the ionizability of nearby amino acid side chains (60,61). Capillary isoelectric focusing (cIEF) can be used to identify and quantify the resulting charge variants (62,63).

Asp deamidation is frequently seen and plays a significant part in controlling the stability and heterogeneity of mAbs (64). Asp residues on CDRs are vulnerable to deamidation, and deamidation of these residues can affect antigen binding and, thus, product potency (65,66). Asp near glycine and in flexible protein regions are more likely to deamidate, highlighting the importance of conformation in deamidation (67,68). Alkaline pH conditions and, for certain residues like Asn331 and Asn360, methionine oxidation are also factors that promote deamidation (68,69). Deamidation, like oxidation, can be detected using icIEF. Because deamidated residues are acidic in nature, icIEF can more easily resolve deamidated proteins and peptides (62).

C-terminal Lys variants are clipped modifications found at the C-terminal ends of mAbs produced in mammalian cell cultures (70,71). Because Lys residue is positively charged, modification of C-terminal lysines changes the basicity of the mAbs (72,73). The loss of C-terminal lysine causes a decrease in positive charge, resulting in charge heterogeneity of mAb products (73,74). In vivo, the removal of C-terminal lysine residues occurs to varying degrees but does not affect the effector functions such as CDC (71,75,76).

Glycation refers to the non-enzymatic addition of a monosaccharide to lysine side chains and other free amines (77,78). The reducing sugars (e.g., glucose, galactose) in cell media are the primary source of this PTM (79,80). The sample becomes more heterogeneous as a result, especially regarding the charge profile (77,81).

The number and location of disulfide bonds vary greatly between IgG subclasses and are critical for the structure, stability, and biological functions of mAbs (39,82). Incomplete disulfide bond formation results in the formation of various cysteine-related variants (82,83). Intra-chain disulfide bonds are protected from solvent exposure and are thus significantly less likely to be modified (83,84). Inter-chain disulfide bonds, on the other hand, are more susceptible to modification, and this susceptibility varies depending on the subclass of IgG (82–84).

At the N-terminus of mAbs, glutamine and glutamate spontaneously cyclize to form pyroglutamic acid (pyro-Glu) (85). The conversion of Gln to pyroGlu makes mAbs more acidic, while the conversion of Glu to pyroGlu results in a basic shift (85,86). As a result of the N-terminal cyclization, the charge heterogeneity of mAb products increases, which can be detected using charge-based techniques (70). There is no difference in half-life or potency between cyclized and non-cyclized N-terminal residues (39,86).

Since these PTMs have a significant impact on the biological activity, immunogenicity, and stability of mAbs, their characterization is essential in mAb production (87,88). Therefore, when developing a biosimilar, it is essential to carry out comprehensive physicochemical and biological characterization with robust methodologies to detect structural differences between the originator product and the biosimilar and prove their similarities (89). In addition to characterization studies, stability studies that can provide information about the reference product's shelf life, degradation pathways, and biosimilar are vital in biosimilar development (90).

2.4 Stability Studies

The physical and chemical stability of the biotherapeutics is critical throughout the product lifecycle because it affects the product's quality, safety, and efficacy. At different stages of production, shipping, and storage, biotherapeutics encounter many conditions that can impact stability and lead to loss of efficacy and are exposed to various environmental factors that cause biochemical and structural (91).

Stability studies of biopharmaceutical products can be expressed as complex procedures to establish quality, efficacy, and safety while maintaining their properties throughout their shelf life from production. The term "shelf life" is a technical term that refers to the product's stability and is expressed as an expiry date. The expiry date of biopharmaceuticals is affected by various environmental factors such as light, temperature, humidity, and radiation, as well as the type of container used and storage conditions (92,93).

Factors such as pH, reactant concentration, radiation, and time between production and use influence reactions such as hydrolysis, reduction, or oxidation and significantly affect the stability of a biopharmaceutical product (8,90,92). Moreover, these reactions may lead to the loss of active pharmaceutical ingredient (API) potency and excipient activity, forming degradation products (90).

Due to undesirable results, providing data for specific stability tests to regulatory agencies before approving a new product has become a legal requirement. Stability studies are an essential requirement for the regulatory approval of any drug (8,94). According to guidelines issued by the International Conference on Harmonization (ICH), the World Health Organization (WHO), or other agencies, these studies must be carried out (8). The “ICH Topic Q5C Quality of Biotechnological Products: Stability Testing of Biotechnological/Biological Products” and “ICH Topic Q 1 A (R2) Stability Testing of New Drug Substances and Products” guidelines provide detailed information to evaluate the stability of a drug substance (DS) and drug product (DP) (95,96).

When performing stability studies, DS or DP are tested over time under various temperature and humidity conditions (97). Accelerated stability tests determine the degradation products present after long storage at relatively high temperatures and humidity (92). Long-term stability studies are carried out by testing the product under less rigorous conditions to determine the drug's shelf life. The storage conditions are chosen following the climatic zones where the product will be sold (90,93). Table 3 shows the storage conditions specified by ICH for stability studies.

Table 3: Stability studies storage conditions

Intended Storage Condition	Type of Stability Studies	Temperature (°C)	Relative Humidity (RH) (%)	Time (Months)
Room Temperature (RT)	Long term	25°C ± 2°C	60% RH ± 5%	12
		30°C ± 2°C	65% RH ± 5%	12
	Intermediate	30°C ± 2°C	65% RH ± 5%	6
	Accelerated	40°C ± 2°C	75% RH ± 5%	6
Refrigerator	Long term	5°C ± 3°C	--	12
	Accelerated	25°C ± 2°C	60% RH ± 5%	6
Freezer	Long term	-20°C ± 5°C	--	12
		≤-65°C	--	12

Long-term stability studies establish a DS/DP stability profile based on real-time data and determine the retest period or shelf life. Depending on whether the DS or DP is stored in the freezer (≤-20°C), ultra-low freezer (≤-65°C), refrigerator (2–8°C), or room temperature (RT), stability studies vary in the respective storage conditions (95,96).

According to the ICH Q5C guideline, at least six months of stability data from the production is required, and should be extended. Stability studies are conducted quarterly in the first year, every six months in the second year, and annually in the third year, after which the frequency is determined according to the shelf life (95,96).

In addition to real-time stability studies to determine the storage conditions and expiration date of biopharmaceutical products, stability studies under stress conditions or forced degradation studies also play an essential role in different stages of development and production (8).

2.5 Forced Degradation Studies

Forced degradation refers to a series of studies involving the degradation of the biopharmaceutical drug under severe conditions, producing degradation products to determine the molecule's stability (8). Forced degradation studies have been widely used to support formulation development and comparability throughout the life cycle of mAbs. Furthermore, forced degradation studies can simulate accidental exposure of mAbs to conditions that could affect product quality, safety, and efficacy during manufacture, storage, handling, and administration (98,99). Even though these studies were conducted under relatively harsh conditions in a short period, the data obtained allows for understanding structural properties that are not observed in real-time stability studies (100).

Although forced degradation studies are an essential part of the biopharmaceutical industry, there is no standard protocol for stress conditions or test timing. Due to the lack of a standard protocol, it is the responsibility of academic and biopharmaceutical industry researchers to develop forced degradation assays that can meet all expectations from stability studies under stress conditions (10,101).

Oxidation, thermal degradation, acid and base hydrolysis, light exposure, freeze-thaw cycles, and agitation are all recommended stress factors for forced degradation studies. Nevertheless, there are no specifications in the regulatory guidelines regarding the pH, temperature, oxidizing agents, and exposure time (94,100,102).

The timing of the stress test, the type of stress, and the degree of degradation must be carefully chosen to obtain more realistic degradation pathways (103). Because over-stressing can cause excessive degradation and trigger the formation of secondary degradation products that cannot be produced during stability studies, under-stressing may result in insufficient degradation (98,101).

2.5.1 Thermal stress

Forced degradation under thermal stress is usually performed at temperatures higher than those required for storage and accelerated stability (104). The thermal stress condition for a mAb with a long-term storage temperature of 2–8°C could be 35°C or higher (100). High temperatures accelerate the degradation of various pathways in a short time. Aggregation, which includes insoluble (precipitates and particles) and covalent or non-covalent soluble aggregates, is one of the significant degradation pathways caused by high temperatures (41).

2.5.2 Agitation stress

Agitation stress is one of the significant physical stresses encountered by mAbs (99). It is critical to understand its sensitivity to agitation, as a mAb can undergo agitation such as mixing or shaking during cell culture, purification, formulation, filling, and transporting stages. Exposure of the mAb to agitation increases its contact with hydrophobic interfaces such as air-liquid or liquid-surface. The formation of insoluble and soluble aggregates, which can be covalent or non-covalent, is the primary degradation pathway caused by agitation (102,105).

2.5.3 Freeze/thaw stress

Freeze/thaw (F/T) is a stress condition to which mAb products are frequently exposed during transport and handling and are investigated as forced degradation conditions to assess the susceptibility of mAbs to temperature cycling (104). These studies are also often used to develop stability-indicating assays and better understand the protein degradation mechanism, and study conditions ranged from 3 to 5 F/T cycles between <-65°C and RT (106). Chemical degradation is not the primary degradation pathway for F/T stress; forming various aggregates and fragments is the primary degradation pathway during F/T. As a result, purity and size methodologies are the most used analytical methods for F/T studies (107,108).

2.5.4 pH stress

The pH of a protein's environment significantly impacts its function and stability (109). By disrupting the intramolecular or intermolecular forces (such as hydrogen bonds, electrostatic interactions, and hydrophobic interactions) that make up the protein's structure, extreme pH conditions can permanently denature proteins or cause them to be aggregated (91,105).

The pH range to be applied for stress studies depends on the properties of the proteins and the purpose of the study. Low-stress pH 3-5 is the most used for acidic conditions, and high-stress pH 8-9 is used for basic conditions. Hydrochloric acid or sulfuric acids are recommended for acid stress, and sodium hydroxide or potassium hydroxide for base stress (110). Titration of acid or base directly to the DS formulation or buffer exchange with another buffer at the desired pH is used to achieve the required pH (101).

Most pH stress tests are carried out at 25°C or 40°C. The stress test is usually started at room temperature and then increased to a high temperature (50–70°C) if no degradation occurs. The stress test should not last longer than seven days. Protein products can be exposed to extreme local pH environments during production processes. Understanding the effects of pH changes is crucial, as certain manufacturing conditions can cause product-related impurities and can lead to protein degradation (10,100,111).

2.5.5 Oxidation stress

mAbs are exposed to oxidizing substances like free radicals, dissolved oxygen, and oxygen in the air. Methionine (Met) is the most oxidative amino acid, and methionine sulfoxide is the main product of its oxidation with oxidizing reagents such as hydrogen peroxide (112,113).

Production, purification, formulation, and storage processes can all lead to the oxidation of methionine, tryptophan, and tyrosine residues, for this reason, monitoring oxidation is critical for mAb quality control during (114,115). By exposing mAbs to oxidation stress, it is examined how oxidation-sensitive residues affect the degradation pathway (61,115).

The location of the oxidation has a significant influence on the outcome of the oxidation and can lead to conformational changes causing the formation of insoluble and soluble aggregates (114). Oxidation in the CDR affects antibody binding to Fc receptors and antigens and affects mAb stability and half-life. Oxidation of Met residues can also cause an increase in immunogenicity (60,112,115).

3 MATERIALS AND METHODS

This thesis consists of two parts: stability study and forced degradation studies. In these studies, the samples were analyzed using the same analytical techniques to characterize the originator product and develop the biosimilar.

Size Exclusion Ultra High-Performance Liquid Chromatography (SE-UPLC), Imaged Capillary Isoelectric Focusing (icIEF), Reduced Capillary Electrophoresis-Sodium Dodecyl Sulfate (rCE-SDS), Non-Reduced Capillary Electrophoresis-Sodium Dodecyl Sulfate (nrCE-SDS) methods, and, when necessary, complement assay ELISA methods were used in both studies. These methods were developed and validated prior to the analysis of the samples.

3.1 Materials

For SE-UPLC analysis, sodium phosphate and sodium azide (Sigma Aldrich, Germany) and sodium chloride (Merck, Germany) were purchased. For CE-SDS analyses, iodoacetamide (Sigma Aldrich, Germany) and β-Mercaptoethanol (Merck, Germany) were purchased. For icIEF analysis, Carboxypeptidase-B (Sigma Aldrich, Germany), wide-range ampholytes (GE, USA) and narrow-range ampholytes (Bio-Rad, USA), isoelectric point (pI) markers 4.22 and 8.40 (Protein Simple, USA) were purchased.

Hydrogen peroxide and sodium hydroxide (Merck, Germany), citric acid monohydrate and sodium bicarbonate (Sigma Aldrich, Germany) materials were used for oxidation and acidic/basic pH stress applications. All chemicals and reagents used are of analytical grade.

Chromatograms and electropherograms were collected and processed with Empower 3 software. (Waters, USA). GraphPad Prism 9.1.3 (USA) software was used for statistical analysis.

3.2 Sample Descriptions

A biosimilar anti-C5 mAb was produced from Chinese hamster ovary (CHO) cell culture and purified as a drug substance (DS) using standard chromatographic methods. The biosimilar mAb sample used in the studies was aliquoted from the bulk DS and formulated in 10 mM Sodium Phosphate, 150 mM Sodium Chloride, 0.02% Polysorbate 80 pH 7.0, and a target protein concentration of 10 mg/mL. Aliquoted biosimilar mAb samples for stability studies were stored at three different storage conditions (≤-65°C, 5.0±3.0°C, and 25±2°C/60±5%RH) for the planned time.

In this thesis, three originator products with different lot numbers were used. Originator anti-C5 mAbs were produced from mouse myeloma cell (NS0). Due to the limited volume of originator, one lot was stored at 5.0±3.0°C and used in stability studies. The other two originator lots were used simultaneously in all forced degradation studies. Originator products were obtained from local pharmaceutical suppliers.

In forced degradation studies, formulation buffer (FB) without mAb was used as a blank, and the same stress conditions were applied as samples with mAb.

From this stage on, the biosimilar mAb sample was abbreviated as “BS” and the originator sample as “OR” for the simplicity of writing. The samples used in this thesis and their descriptions are given in Table 4.

Table 4: Sample descriptions

Sample Name	Abbreviation	The Study Used
Biosimilar mAb (Drug Substance)	BS	• Stability Study (for all storage conditions) • Forced Degradation Studies
Originator lot #1	OR	• Forced Degradation Studies
Originator lot #2		
Originator lot #3	OR	• Stability Study (for 5.0±3.0°C storage)
Formulation Buffer	FB	• Forced Degradation Studies

3.3 Stability Studies

The stability study was performed on three different storage conditions of the BS sample. The sample vials were stored in the controlled temperature reach-in stability chambers at ≤-65°C, 5.0±3.0°C, and 25±2°C/60±5%RH following the ICH guideline Q1A (R2) "Stability Test of New Drug Substances and Products". This study aims to determine the real-time and accelerated stability of BS.

For the purpose of the stability study, time zero is considered the day of staging. The samples were pulled from the stability chambers within seven days of the scheduled pull date and submitted for testing. All samples to be tested were stored at 5.0±3.0°C before and after the completion of testing. As additional data, the originator product stored at 5.0±3.0°C was also analyzed during the stability study. A description of the testing intervals is presented in Table 5. All testing was initiated within seven days of the pull date.

Table 5: Testing schedule

	Interval (Month)						
Storage Condition	**0**	**1**	**6**	**9**	**12**	**18**	**24**
5.0±3.0°C	x	x	x	x	x	x	x
25±2°C / 60±5%RH	x	x	x	x	x		
≤-65°C	x	x	x	x	x	x	x

The tests and test method references are described in Table 6 with their acceptance criteria. Each test was performed for each time point/condition. General, strength, and complement assay ELISA tests were carried out to provide additional information for the BS.

Table 6: Tests and their acceptance criteria

Test	Method	Acceptance Criteria
General	Visual Inspection	Clear to slightly opalescent Colorless to yellow liquid Free of visible particles
	pH Determination	6.7 – 7.3
	Osmolality Determination	Report results.
	Protein Content Determination	8.0-12.0 mg/mL
Purity	SE-UPLC	Monomer peak: ≥ 95.0% HMW: Report result (%)
	rCE-SDS	LC+HC: ≥ 90.0%
	nrCE-SDS	Total IgG: ≥ 90.0%
Charge Heterogeneity	icIEF	Main Variant: Report result (%) Acidic Variants: Report result (%) Basic Variants: Report result (%)
Potency	Complement Assay ELISA	Relative potency: 70-130%

3.4 Forced Degradation Studies

Samples were subjected to various types of stress to characterize the extent of degradation detected using a range of analytical methods. Forced degradation studies include thermal, agitation, pH (acid and base), freeze/thaw, and oxidation stress.

All stress conditions were applied to the biosimilar mAb (BS) and two originator product samples (OR). FB without mAb was used as blank, and the same stress conditions as samples with mAb were applied in every stress condition. All samples subjected to stress conditions are stored at 5.0±3°C until analysis. At the end of the incubation period, samples subjected to pH stress and oxidation stress were buffer exchanged back to FB.

3.4.1 Thermal stress

The thermal stress was performed by incubation of the samples at two different temperatures (37°C and 50°C). After 3, 7, and 14 days, the aliquots were pulled for testing. The stress conditions are detailed in Table 7.

Table 7: Thermal stress conditions

Conditions	Time Point 1	Time Point 2	Time Point 3
37°C	3 days	7 days	14 days
50°C	3 days	7 days	14 days

3.4.2 Agitation stress

For agitation stress, samples were placed in a shaker at 400 rpm at RT. Samples were pulled after 24 and 72 hours. The stress conditions are detailed in Table 8.

Table 8: Agitation stress conditions

Conditions	Time Point 1	Time Point 2
400 rpm at RT	24 hours	72 hours

3.4.3 pH stress

For acidic pH stress, the samples were titrated to pH 4.0 with 1N hydrochloric acid and placed at RT for 72 hours. For basic pH stress, the samples were titrated with 1M Tris to pH 9.0 and placed at RT for 72 hours. The stress conditions are detailed in Table 9.

Table 9: pH stress conditions

Condition	Time Point 1
Acidic pH Stress (pH 4.0) at RT	72 hours
Basic pH Stress (pH 9.0) at RT	72 hours

3.4.4 Freeze/thaw stress

For F/T studies, samples were cooled from 5.0±3.0°C to ≤-65ºC, held at ≤-65ºC for two hours, thawed to 5.0±3.0°C and held at 5.0±3.0°C for two hours during each cycle. At the end of repeated five F/T cycles, the samples were stored at 5.0±3.0°C until analysis. The stress conditions are detailed in Table 10.

Table 10: Freeze/thaw stress conditions

Condition	Time Point 1
Freeze (≤-65°C)	2 hours (Each cycle)
Thaw (5.0±3.0°C)	2 hours (Each cycle)

3.4.5 Oxidation stress

Samples were spiked with hydrogen peroxide to a final concentration of 0.5% (V/V) and then incubated at RT for 24 hours. The stress conditions are detailed in Table 11.

Table 11: Oxidation stress conditions

Condition	Time Point 1
Hydrogen Peroxide 0.5% (v/v) at RT	24 hours

3.5 Methods

3.5.1 General tests

General tests were performed only in stability studies for three storage conditions (≤-65°C, 5.0±3.0°C, and 25±2°C/60±5%RH) of the BS. General tests include visual inspection, pH determination, osmolality determination, and protein content determination.

3.5.1.1 Visual appearance

The visual appearance of the sample checks for any floating, settling, or visible particles and defines the visual color assessment and color determination of the BS. The test was carried out on the Bosch MIH LX Visual Inspection Device.

The sample containers were observed by checking the presence of settling or floating particulate on the white panel and then on the black panel for 5 seconds. Samples were compared against a white background with color reference standards (Sigma-Aldrich, Germany).

3.5.1.2 Protein concentration determination

UV/Vis spectrophotometry was used to analyze the concentration of BS using UV-Vis absorbance. The study was carried out on the NanoDrop One.

It calculates protein concentration using Beer-Lambert Law; Abs = ε.L.c (Abs = Absorbance; ε = molar absorptivity; L = light pathlength; c = sample concentration). 2 µl of the sample was used per reading.

3.5.1.3 pH determination

The study was carried out on the Mettler Toledo SevenExcellence pH meter. The samples were analyzed by measuring the pH with the temperature of the samples between 23°C and 27°C. 400 µl of the sample was used per reading.

3.5.1.4 Osmolality determination

The test measures the total solute concentration of the BS using cooling technology. The study was carried out on the Advanced Instruments Model 3320 Osmometer. 20 µl of the sample was used per reading.

3.5.2 Size exclusion ultra-performance liquid chromatography (SE-UPLC)

Size exclusion ultra-performance liquid chromatography (SE-UPLC) is a separations technique involving a column packed with a porous stationary phase. Analytes with small hydrodynamic radii experience longer residence times within the stationary phase, while analytes with larger hydrodynamic radii experience shorter residence times.

This difference leads to the partitioning of low molecular weight (LMW) and high molecular weight (HMW) species as they travel through the column. Elution is achieved by applying a constant flow of buffer, which displaces analytes from the pores over time. Samples possessing high molecular weights (or larger hydrodynamic radii) elute earlier than samples with relatively lower molecular weights (or smaller hydrodynamic radii).

The amount of monomer/aggregate/fragment in samples was determined by SE-UPLC. The study was carried out on an Acquity H-Class Bio UPLC® system with a UV detector which contains a titanium flow cell and Acquity UPLC® Protein BEH SEC200 column (200 Å, 1.7 μm, 4.6 mm x 300 mm).

The isocratic flow of the mobile phase, consisting of 20 mM sodium phosphate with 188 mM sodium chloride at pH 7.4, was used for separation at a flow rate of 0.250 mL/min.

The samples were diluted to 2.5 mg/mL with a mobile phase, and 2.5 μL was injected into the column. UV detection was done at 280 nm for a 20-minutes run time. Data acquisition, equipment control, and data processing were performed by Empower 3 software (Waters, Milford, USA).

3.5.3 Imaged capillary isoelectric focusing (icIEF)

Imaged capillary isoelectric focusing (icIEF) method was used to determine the charge heterogeneity of the samples, as well as the isoelectric point (pI). In icIEF, molecules migrate through a stable pH gradient until they reach a pH zone equal to their pIs, at which the net charge and mobility are zero.

The presence of lysine (Lys) amino acid on the C-terminal end of the heavy chain induces basic variants. The CpB enzyme is used to selectively cleave Lys residues at the C-terminal end of proteins to demonstrate that this variation is due to Lys at the C-terminal end.

The study was carried out on an iCE3 (Protein Simple) capillary electrophoresis instrument with fluorocarbon-coated capillary (50 μm i.d. × 20 cm). The samples were diluted to 3.9 mg/mL in water, treated with CpB, and heated to 37 °C for 1 hour. Then, 10 μL of the sample was mixed with 90 μL master mix, which consisted of 2 μL of Pharmalyte 3–10, 1 μL of Biolyte Ampholytes pH 4/6, 1 μL of Biolyte Ampholytes pH 6/8, 35 μL of 1% methylcellulose, 1 μL of each pI marker (4.22 and 8.40), and 2.5 μL of water. The mixed solution was injected into a capillary cartridge where the pre-focusing was performed at 1500 V for 2 minutes, followed by a hold at 3000 V for 10 minutes (focusing). The anolyte and catholyte electrolytic tanks at each end of the capillary cartridge were filled with 0.08 M phosphoric acid in 0.1% methylcellulose and 0.1 M sodium hydroxide in 0.1% methylcellulose, respectively.

All steps were conducted at RT, and the sample storage temperature was 10 °C. Data acquisition was done at 280 nm with iCE3 software, and the electropherograms were imported to Empower 3 software for data analysis.

The peak area percentages for species with pIs lower than the main peak were combined and reported as acidic variants. Similarly, the peak area percentages for species with pIs higher than the main peak were summed and reported as basic variants.

3.5.4 Capillary electrophoresis-sodium dodecyl sulfate (CE-SDS)

In capillary electrophoresis (CE), molecular species such as proteins and peptides are separated by differential migration in a buffer solution under the influence of an electric field within a small diameter capillary. Samples were denatured by dilution in sodium dodecyl sulfate (SDS). SDS evenly binds to the protein bonds and gives a uniform negative charge. Samples were run under reducing conditions using β-Mercaptoethanol (βME) or under non-reducing conditions, in which iodoacetamide was used to prevent disulfide bonds from forming. Analytes with LMW travel through the gel more rapidly than analytes with HMW. The molecular sizes of separated molecules can be approximated by comparison of the retention times to standards of known molecular weights. By CE-SDS, the purity/impurity levels of samples were determined. Free/heavy chain and light antibody fragments were determined by the nrCE-SDS method. By reducing the mAb, light and heavy chain ratios were determined by the rCE-SDS method.

The study was carried out in a Beckman Coulter PA 800 Plus system with a photodiode array (PDA) detector for both rCE-SDS and nrCE-SDS analyses. The bare-fused silica capillary (50 µm, 67 cm total length) with 100x200µm aperture and SDS-Mw gel buffer (pH 8, 0.2% SDS) was used for separation.

3.5.4.1 Reduced capillary electrophoresis-sodium dodecyl sulfate (rCE-SDS)

The samples at a concentration of 1.0 mg/mL were mixed with SDS sample buffer (100 mM Tris-HCl, pH 9.0, 1% SDS) and reduced with βME followed by heating to 70°C for 10 minutes. The total amount of protein in the samples was 100 µg. Samples were injected into the capillary at 5 kV in reverse polarity for 20 seconds. For reduced samples, the separation was carried out at 15 kV for 40 minutes. Data was collected at 220 nm with a reference channel set to 350±10 nm. The area % of components observed in reduced conditions were reported. Data were collected by 32 Karat software (Beckman Coulter) and processed using Empower 3.

3.5.4.2 Non-reduced capillary electrophoresis-sodium dodecyl sulfate

Non-reduced samples were prepared with 250mM iodoacetamide and SDS sample buffer. The samples at a concentration of 1.0 mg/mL were mixed with SDS sample buffer and heated to 70°C for 10 minutes. The total amount of protein in the samples was 100 µg. Samples were injected into the capillary at 5 kV in reverse polarity for 20 seconds. The separation was carried out at 15 kV for 40 minutes for non-reduced samples. Data was collected at 220 nm with a reference channel set to 350±10 nm. The TCA% of components observed in non-reduced were reported. Data were collected by 32 Karat software (Beckman Coulter) and processed using Empower 3 software.

3.5.5 Complement assay

The complement classical pathway enzyme-linked immunosorbent assay (ELISA) was used to determine the potency of samples relative to a reference standard. Samples were diluted and mixed with normal human serum, which exhibits the complement pathway under the immunoassay conditions. A dilution series of the samples were created and added to a plate that specifically activates the classical pathway. A labeled antibody specific to a neoepitope of the terminal complement complex was added. p-Nitrophenyl Phosphate (pNPP) substrate was added at the final step, which was converted to a colorimetric product based on the amount of bound labeled antibody. The concentration of this product was measured at 405 nm and used to determine the relative potency of the material.

4 RESULTS

The results obtained are summarized under two headings: stability studies and forced degradation studies.

4.1 Stability Study Results

In this stability study, biosimilar (BS) products of 3 different storage conditions (5.0±3.0°C and 25±2°C/60±5%RH, ≤-65°C) were analyzed. As additional data, the originator product (OR) was stored at 5.0±3.0°C and compared with the BS 5.0±3.0˚C product. As a result of SE-UPLC, icIEF, rCE-SDS, nrCE-SDS and complement assay analyses, no significant change was observed between the 5.0±3.0˚C condition of BS and OR in all analysis results considering $p < 0.05$. Stability result data of SE-UPLC, icIEF, rCE-SDS, nrCE-SDS and complement assay analyses and 5.0±3.0˚C condition graphs of BS and OR are given in the Appendix.

4.1.1 General tests

4.1.1.1 Visual appearance

All samples remained clear for the duration of the study, with no precipitates or particulate matter detected by the naked eye. No changes in color or turbidity were observed over test period. All visual appearance results are summarized in Table 12.

Table 12: Visual appearance results

Visual Appearance			
Month	**BS 5.0±3.0°C**	**BS 25±2°C/60±5%RH**	**BS ≤-65°C**
0	Clear, colorless. No visible particles.	Clear, colorless. No visible particles.	Clear, colorless. No visible particles.
1	Clear, colorless. No visible particles.	Clear, colorless. No visible particles.	Clear, colorless. No visible particles.
6	Clear, colorless. No visible particles.	Clear, colorless. No visible particles.	Clear, colorless. No visible particles.
9	Clear, colorless. No visible particles.	Clear, colorless. No visible particles.	Clear, colorless. No visible particles.
12	Clear, colorless. No visible particles.	Clear, colorless. No visible particles.	Clear, colorless. No visible particles.
18	Clear, colorless. No visible particles.	NT	Clear, colorless. No visible particles.
24	Clear, colorless. No visible particles.	NT	Clear, colorless. No visible particles.

NT: Not Tested

4.1.1.2 Protein concentration determination

For all samples, the expected concentration is between 8-12 mg/ml. The 5.0±3.0˚C and the ≤-65°C conditions showed similar concentration profiles and were in the range. For the 25±2°C/60±5%RH condition, measured concentrations tend to be higher than expected. All results are summarized in Table 13.

Table 13: Protein concentration results

Protein Concentration (mg/mL)			
Condition / Month	BS 5.0±3.0°C	BS 25±2°C/60±5%RH	BS ≤-65°C
0	11.0	11.0	11.0
1	11.3	11.5	11.4
6	11.5	12.5	11.4
9	11.1	12.5	10.8
12	11.1	13.2	10.6
18	11.3	NT	10.7
24	11.5	NT	10.7

NT: Not Tested

4.1.1.3 pH determination

The pH probe was immersed in a sample and measured between 23°C and 25°C for all samples. The pH values of the BS for all storage conditions are within the range. The results of pH measurements are given in Table 14.

Table 14: pH results

pH Determination			
Condition / Month	BS 5.0±3.0°C	BS 25±2°C 60±5%RH	BS ≤-65°C
0	7.0	7.0	7.0
1	7.0	7.0	7.0
6	7.0	7.0	7.0
9	7.0	6.9	6.9
12	7.0	6.9	6.9
18	7.0	NT	7.0
24	7.0	NT	6.8

NT: Not Tested

4.1.1.4 Osmolality determination

The BS osmolality results for 5.0±3.0˚C and ≤-65°C storage conditions are similar, but the osmolality results tend to increase for 25±2°C/60±5%RH storage conditions. The results of osmolality measurements are given in Table 15.

Table 15: Osmolality results

Osmolality (mOsm/kg)			
Condition / Month	BS 5.0±3.0°C	BS 25±2°C/60±5%RH	BS ≤-65°C
0	302	302	302
1	299	303	299
6	308	337	302
9	310	357	301
12	306	372	298
18	323	NT	306
24	327	NT	306

NT: Not Tested

4.1.2 Size exclusion ultra-performance liquid chromatography (SE-UPLC)

The BS was stored in separate aliquots at three different storage conditions and analyzed by SE-UPLC at predetermined intervals to obtain aggregate profiles. There was no significant change in the percentage of total aggregate (HMW) or the monomer for BS stored at 5.0±3.0˚C. In both 25±2°C/60±5%RH and ≤-65°C storage conditions, the percentage of monomer decreased while the percentage of aggregate increased. Results for all storage conditions are given in Figure 2.

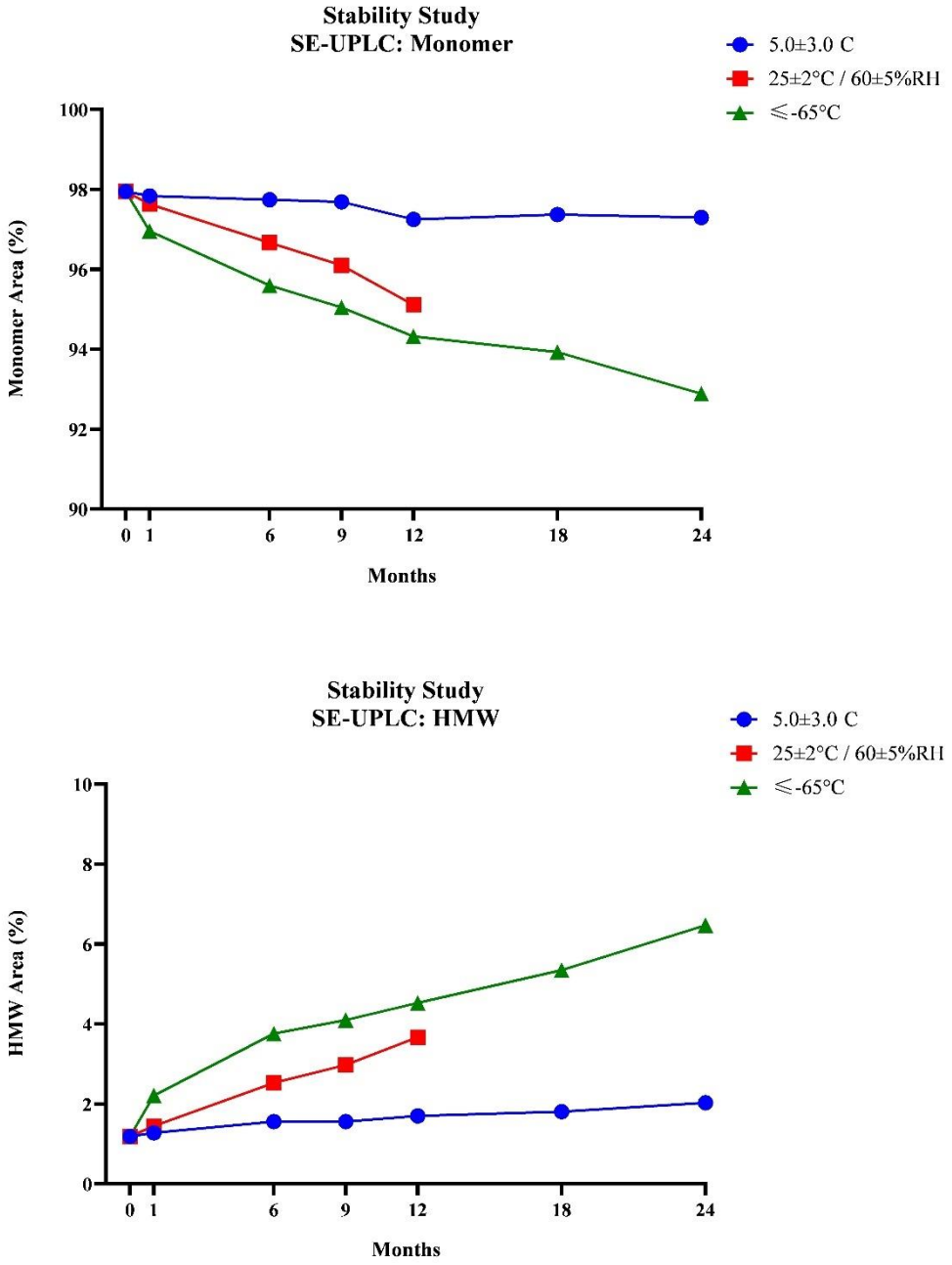

Figure 2: Stability Study, results of monomer area% (top) and HMW area % (bottom) obtained by SE-UPLC analysis.

Figure 3, Figure 4, and Figure 5, respectively, show overlapping chromatograms of the BS sample stored at 5.0±3.0˚C, 25±2°C/60±5%RH, and ≤-65°C, where SE-UPLC analysis was carried out at predetermined intervals.

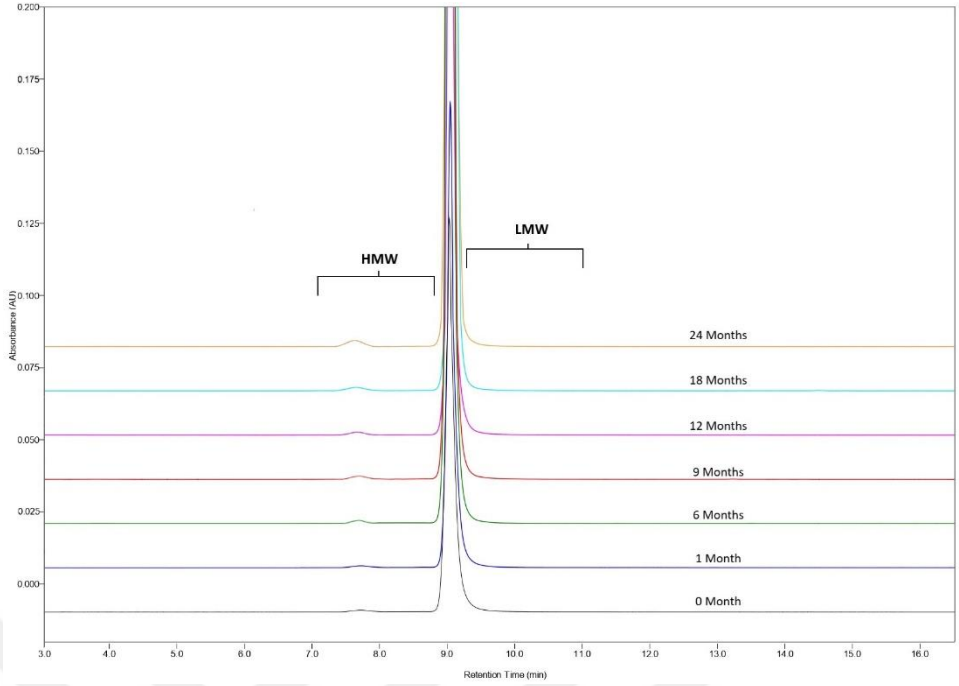

Figure 3: Overlapping SE-UPLC chromatograms of BS sample at 5.0±3.0˚C storage condition

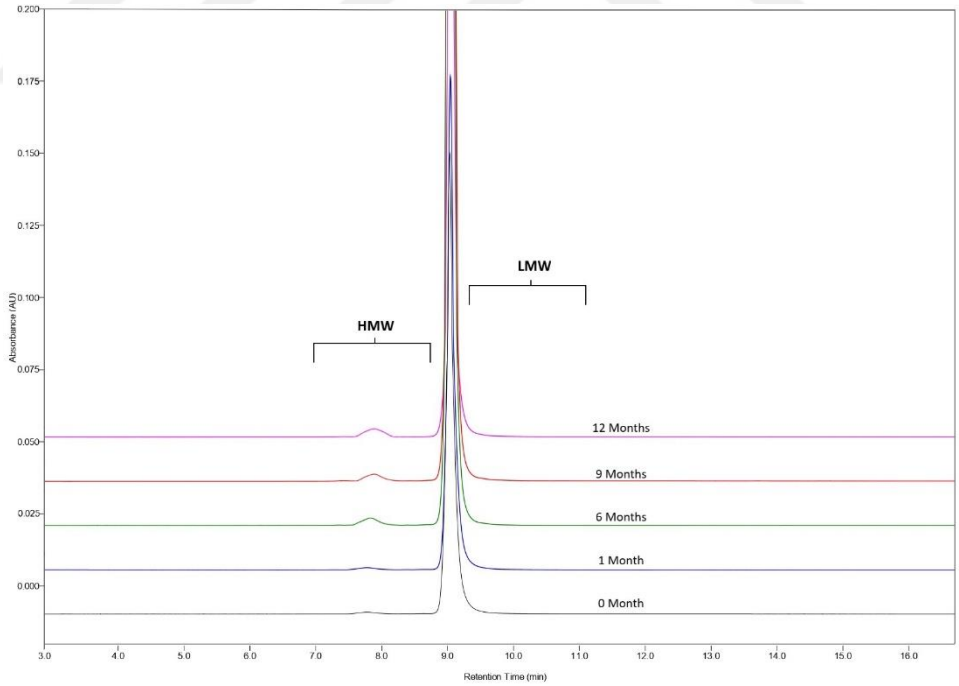

Figure 4: Overlapping SE-UPLC chromatograms of BS sample at 25±2°C/60±5%RH storage condition

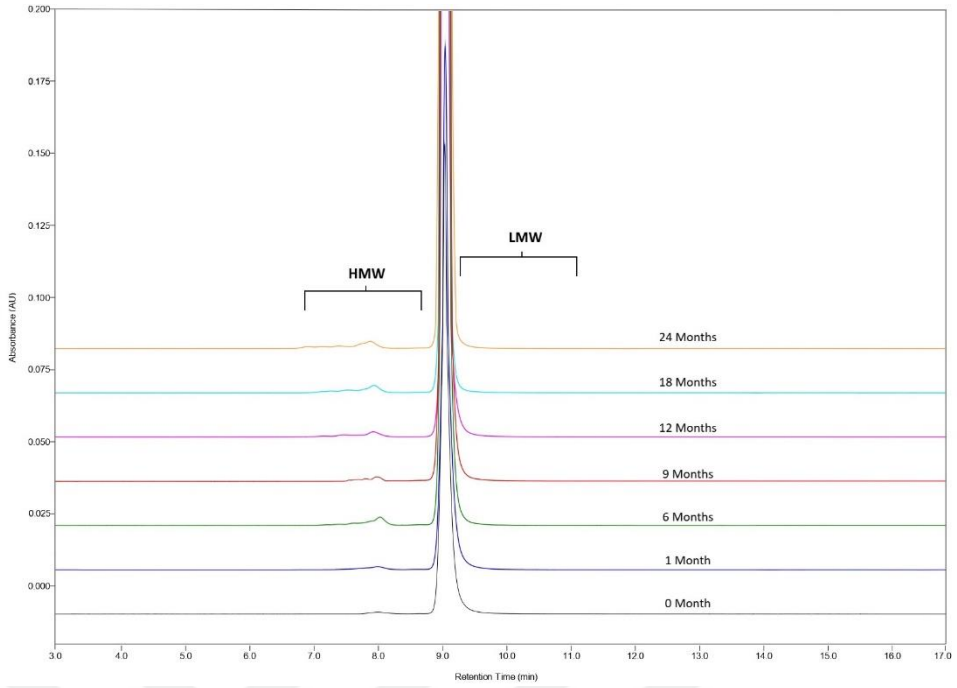

Figure 5: Overlapping SE-UPLC chromatograms of BS sample at ≤-65°C storage condition

4.1.3 Imaged capillary isoelectric focusing (icIEF)

The BS was stored in separate aliquots at three different storage conditions and analyzed by icIEF with and without CpB treatment at predetermined intervals to obtain charge variant profiles. There was no significant change in the percentage of all charge variants for BS stored at 5.0±3.0˚C and ≤-65°C storage conditions. In 25±2°C/60±5%RH storage conditions, the percentage of the main charge variants decreased while the percentage of the acidic charge variants increased. With and without CpB treatment, results for all storage conditions are given in Figure 6 and Figure 7, respectively.

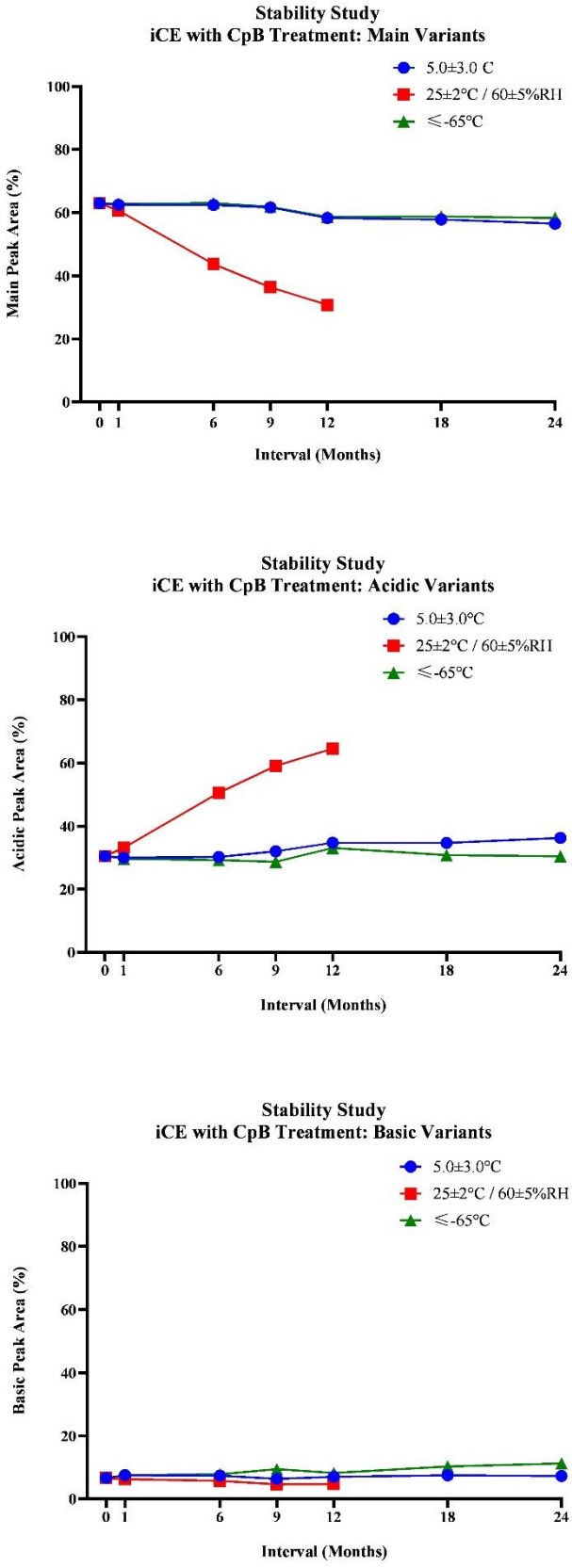

Figure 6: Stability Study, the main (top), acidic (middle), and basic (bottom) charge variants % area results with CpB treatment obtained by icIEF analysis.

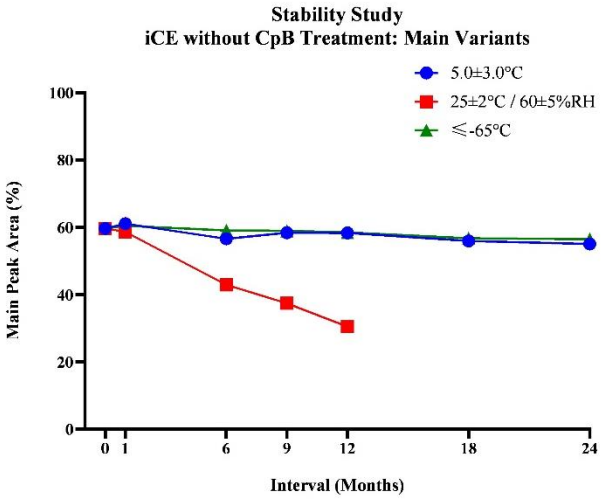

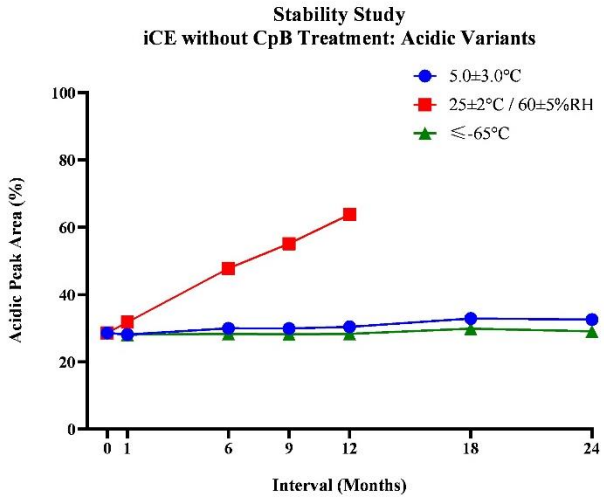

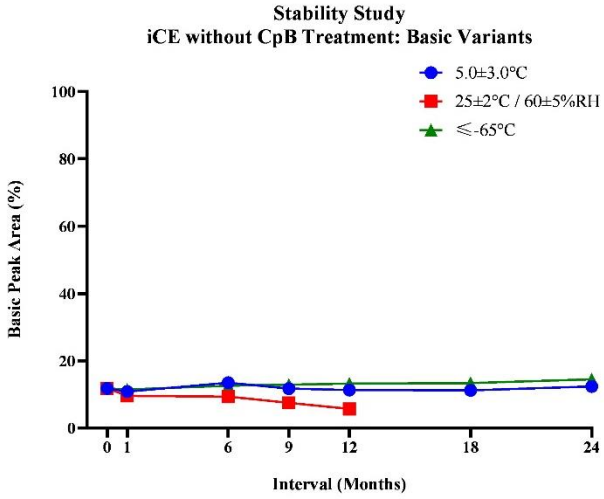

Figure 7: Stability Study, the main (top), acidic (middle), and basic (bottom) charge variants % area results without CpB treatment obtained by icIEF analysis.

Figure 8, Figure 9, and Figure 10, respectively, show overlaying electrograms of the BS sample stored at 5.0±3.0˚C, 25±2°C/60±5%RH, and ≤-65°C storage conditions, where icIEF analysis with CpB treatment was carried out at predetermined intervals.

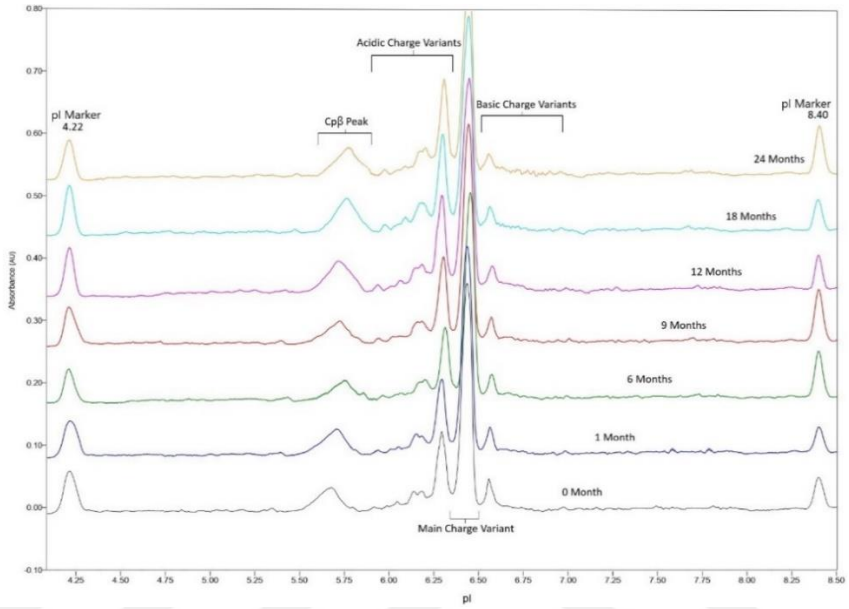

Figure 8: Overlaying icIEF electrograms of BS sample with CpB treatment at 5.0±3.0˚C storage condition

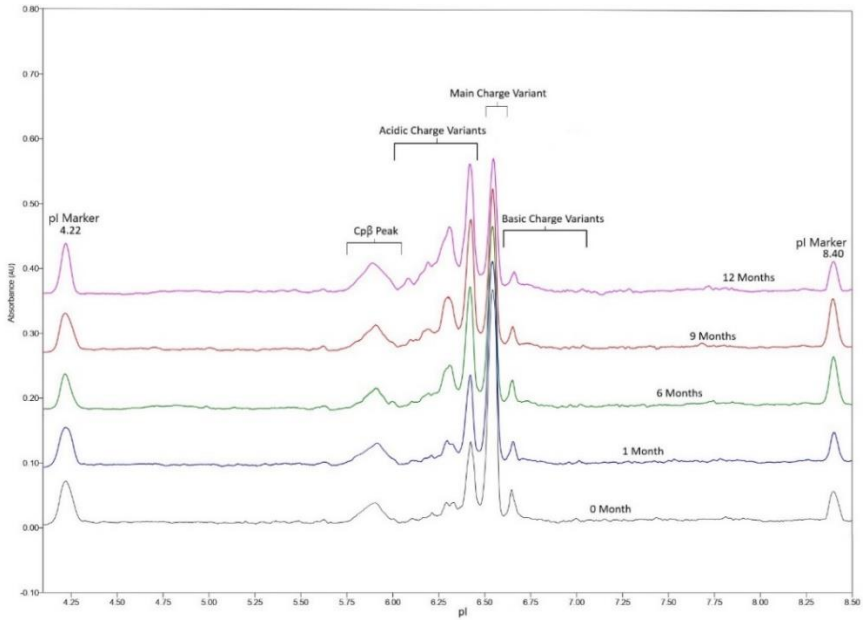

Figure 9: Overlaying icIEF electrograms of BS sample with CpB treatment at 25±2°C/60±5%RH storage condition

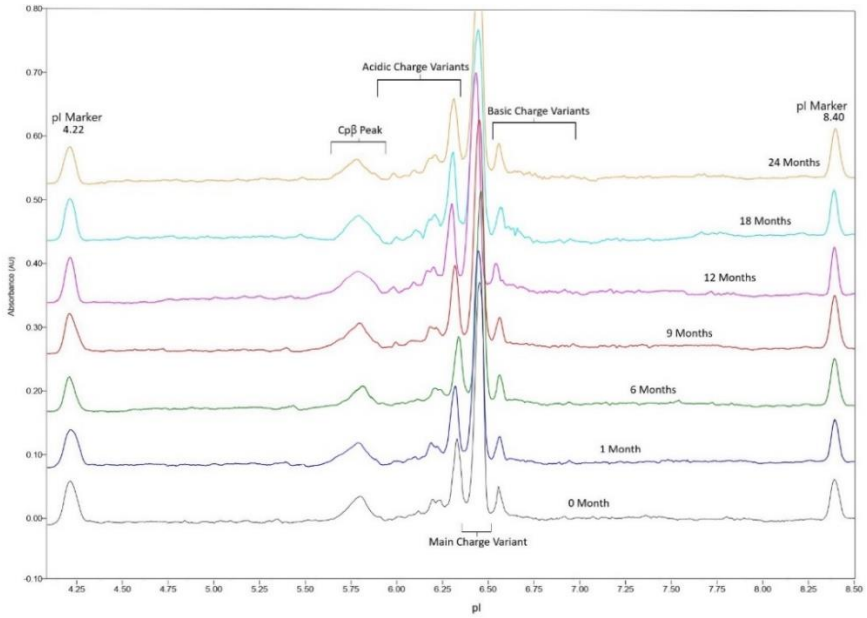

Figure 10: Overlaying icIEF electrograms of BS with CpB treatment at ≤-65°C storage condition

Figure 11, Figure 12, and Figure 13, respectively, respectively, show overlaying electrograms of the BS sample stored at 5.0±3.0˚C, 25±2°C/60±5%RH, and ≤-65°C storage conditions, where icIEF analysis without CpB treatment was carried out at predetermined intervals.

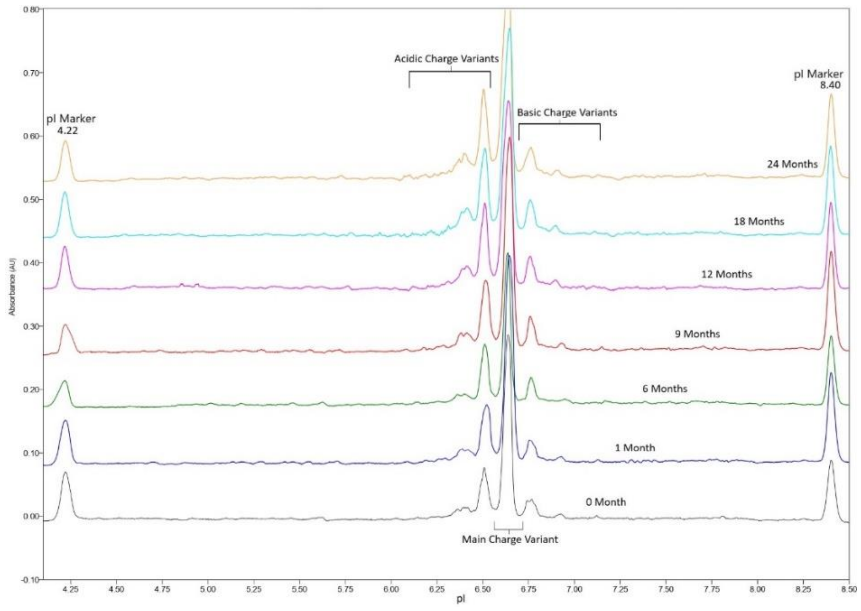

Figure 11: Overlaying icIEF electrograms of BS sample without CpB treatment at 5.0±3.0˚C storage condition

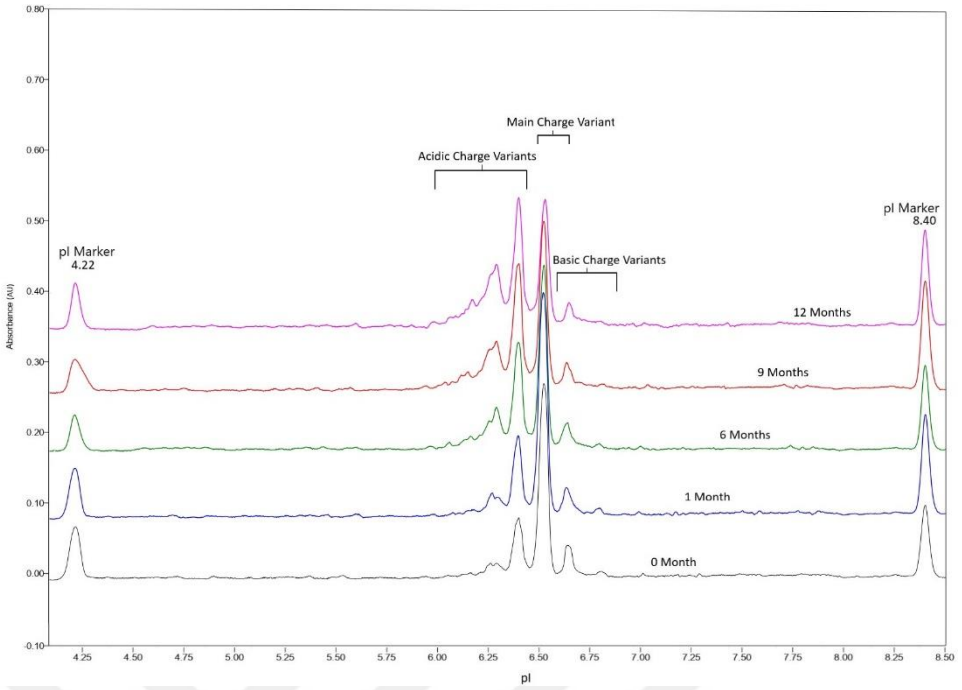

Figure 12: Overlaying icIEF electrograms of BS sample without CpB treatment at 25±2°C/60±5%RH storage condition

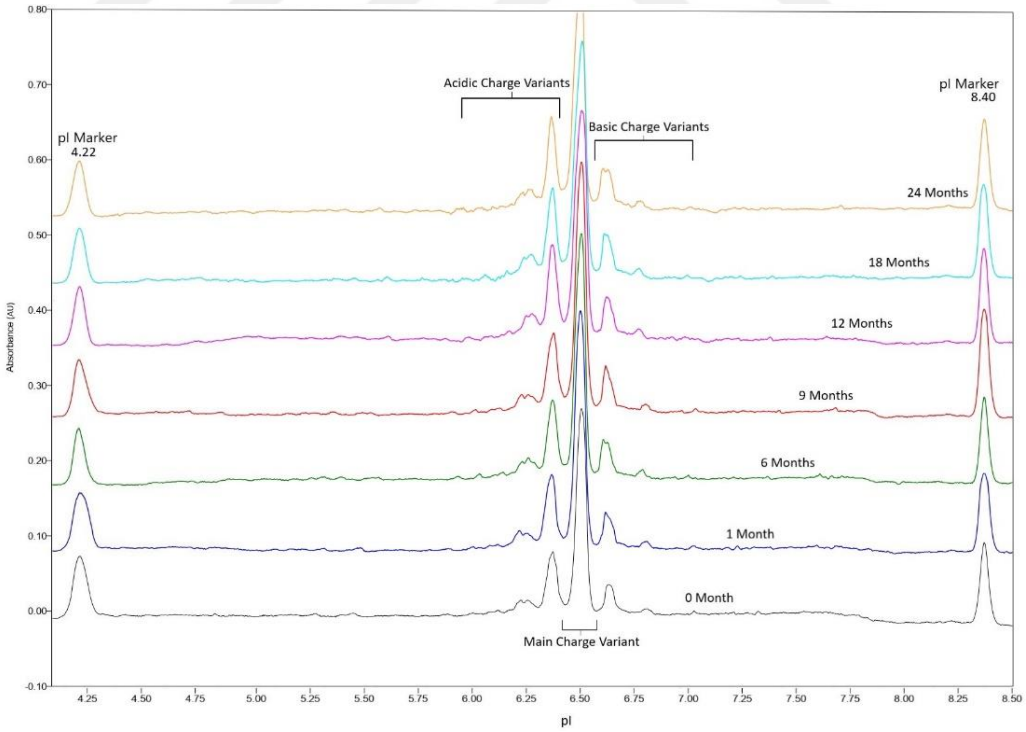

Figure 13: Overlaying icIEF electrograms of BS without CpB treatment at ≤-65°C storage condition

4.1.4 Capillary electrophoresis-sodium dodecyl sulfate (CE-SDS)

4.1.4.1 Reduced capillary electrophoresis-sodium dodecyl sulfate (rCE-SDS)

Under reducing conditions, the LC+HC value gives the purity level, and the remaining values give the impurity level. There was no significant change in the percentage of purity level for BS stored at 5.0±3.0˚C and ≤-65°C storage conditions. In 25±2°C/60±5%RH storage condition, the percentage of purity level started to decrease after six months. Results for all storage conditions are given in Figure 14.

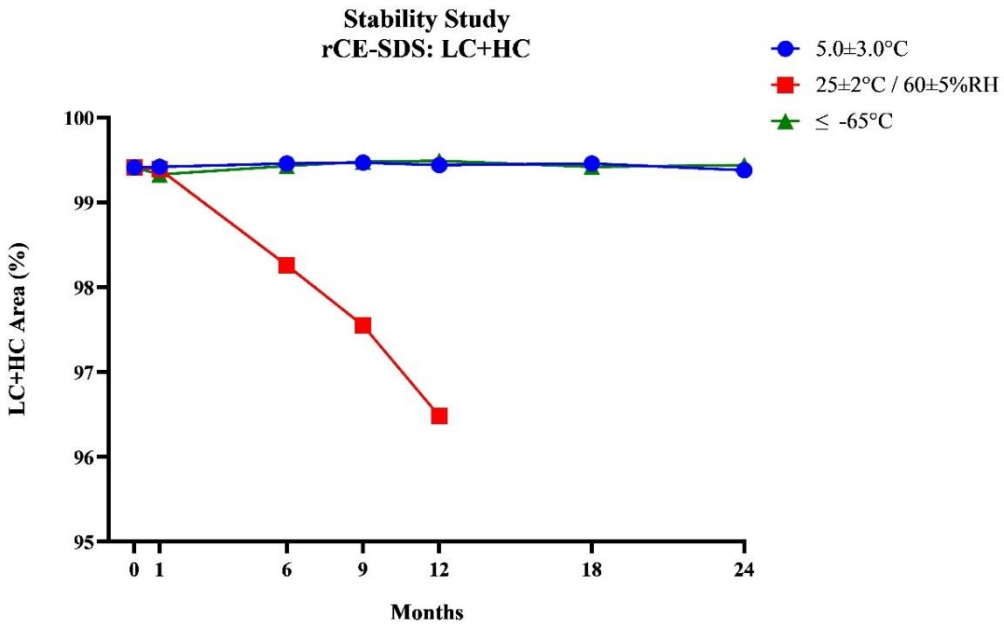

Figure 14: Stability Study, results of LC+HC % area obtained by rCE-SDS analysis.

Figure 15, Figure 16, and Figure 17, respectively, show overlapping electrograms of the BS sample stored at 5.0±3.0˚C, 25±2°C/60±5%RH, and ≤-65°C, where rCE-SDS analysis was carried out at predetermined intervals.

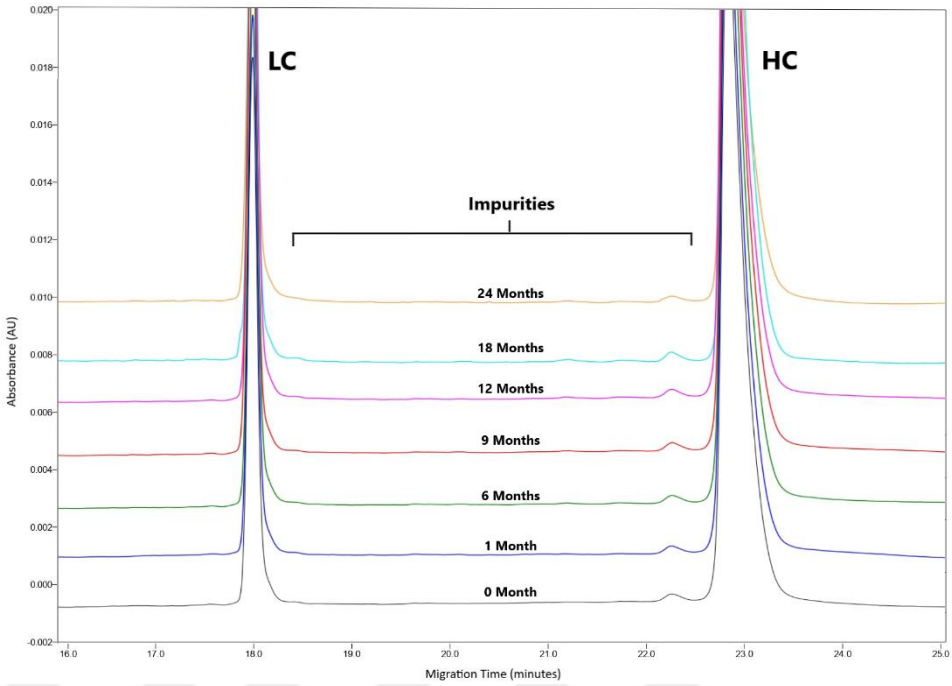

Figure 15: Overlaying rCE-SDS electrograms of BS sample at 5.0±3.0˚C storage condition

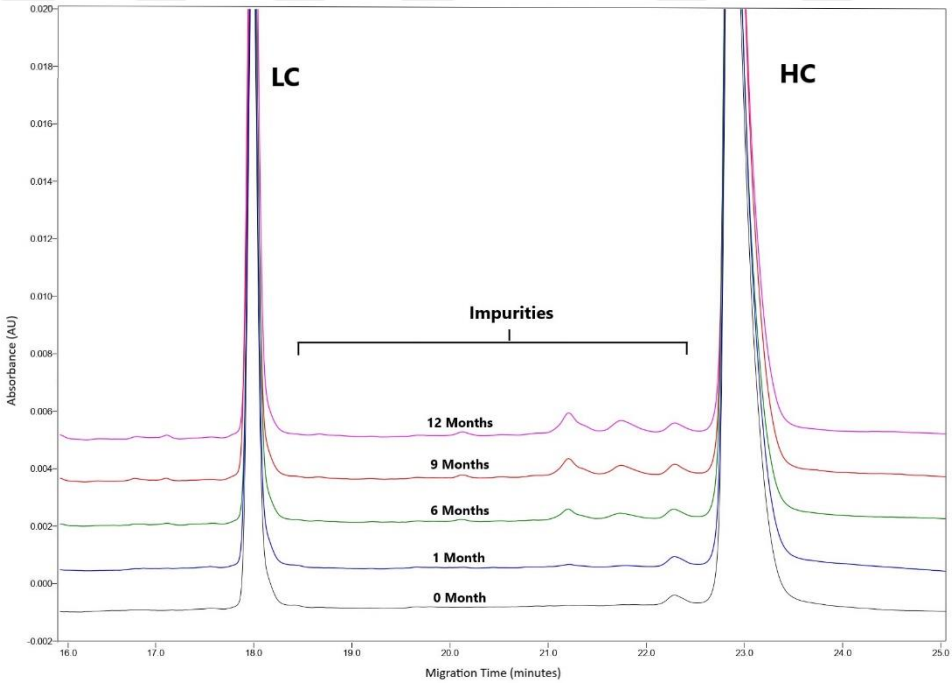

Figure 16: Overlaying rCE-SDS electrograms of BS sample at 25±2°C/60±5%RH storage condition

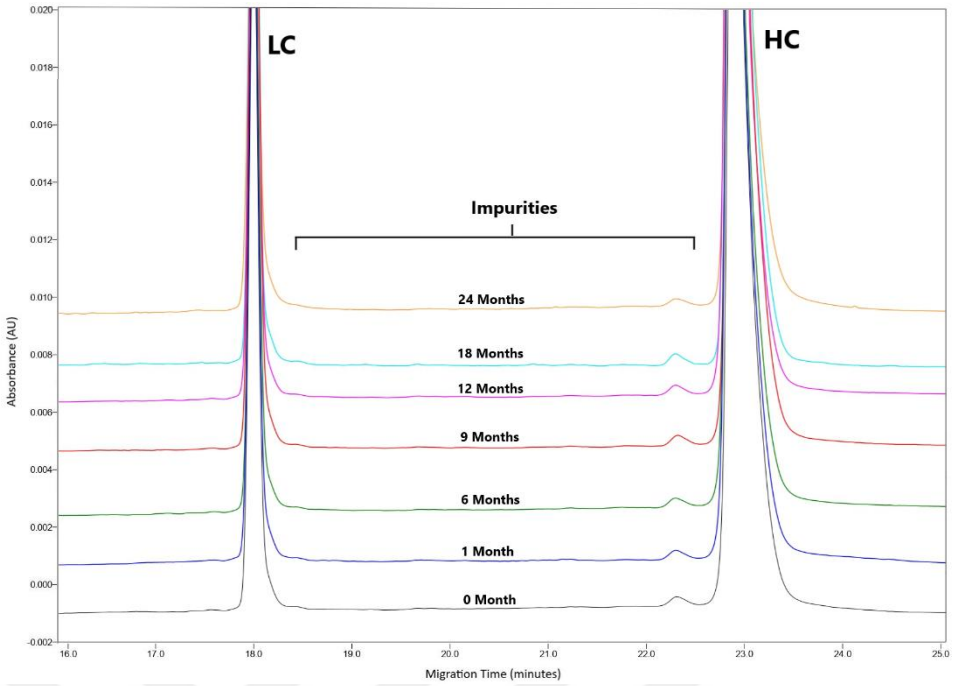

Figure 17: Overlaying rCE-SDS electrograms of BS sample at ≤-65°C storage condition

4.1.4.2 Non-reduced capillary electrophoresis-sodium dodecyl sulfate (nrCE-SDS)

The total main (IgG) value is important for non-reducing conditions. There was no significant change in the percentage of total main for BS stored at 5.0±3.0˚C and ≤-65°C storage conditions until 18 months. In 25±2°C/60±5%RH storage condition, the percentage of purity level started to decrease after nine months. Results for all storage conditions are given in Figure 18.

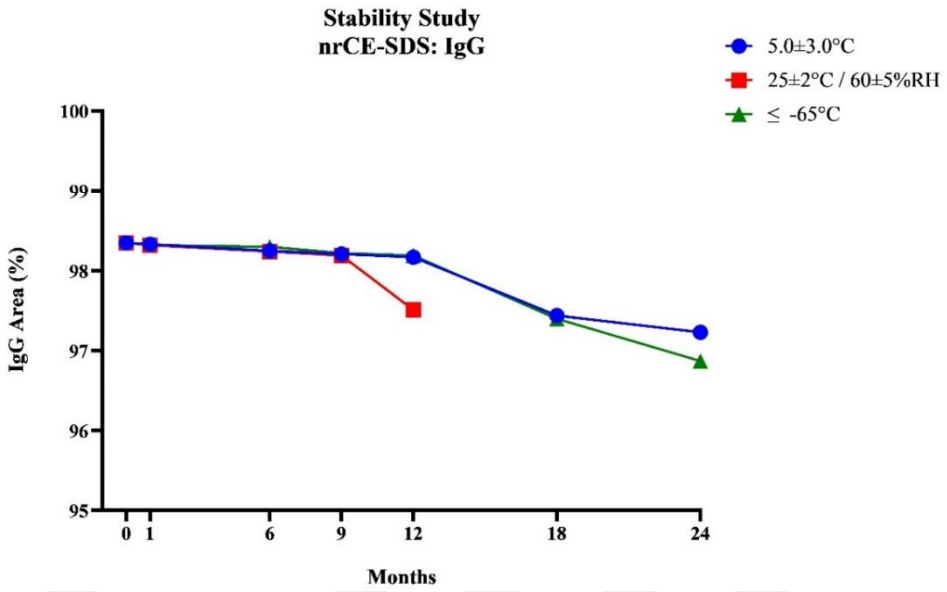

Figure 18: Stability Study, results of IgG % area obtained by nrCE-SDS analysis.

Figure 19, Figure 20, and Figure 21, respectively, show overlapping electrograms of the BS sample stored at 5.0±3.0˚C, 25±2°C/60±5%RH, and ≤-65°C, where nrCE-SDS analysis was carried out at predetermined intervals.

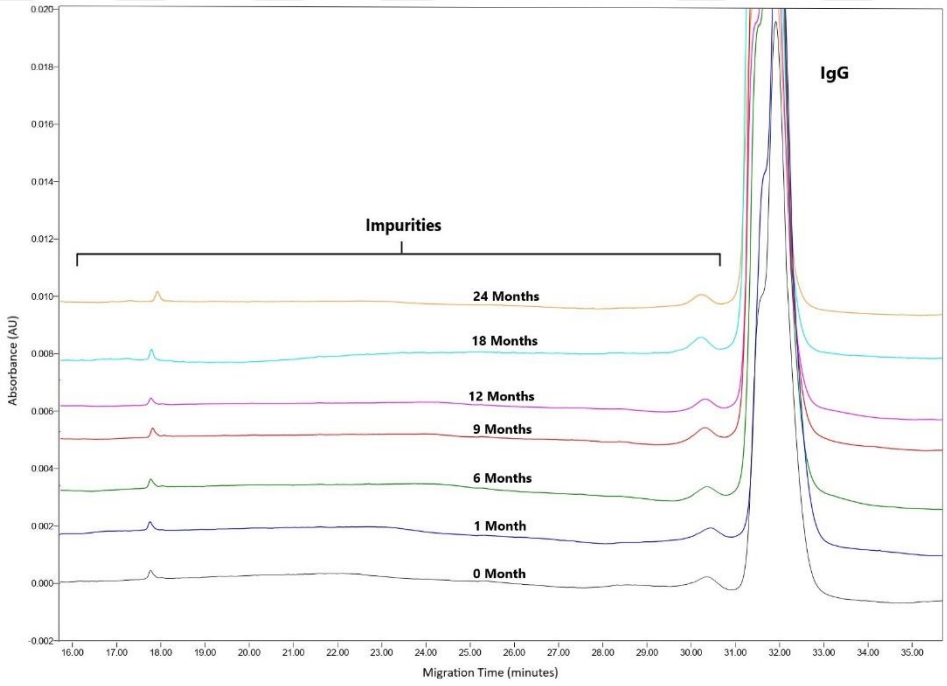

Figure 19: Overlaying nrCE-SDS electrograms of BS sample at 5.0±3.0˚C storage condition

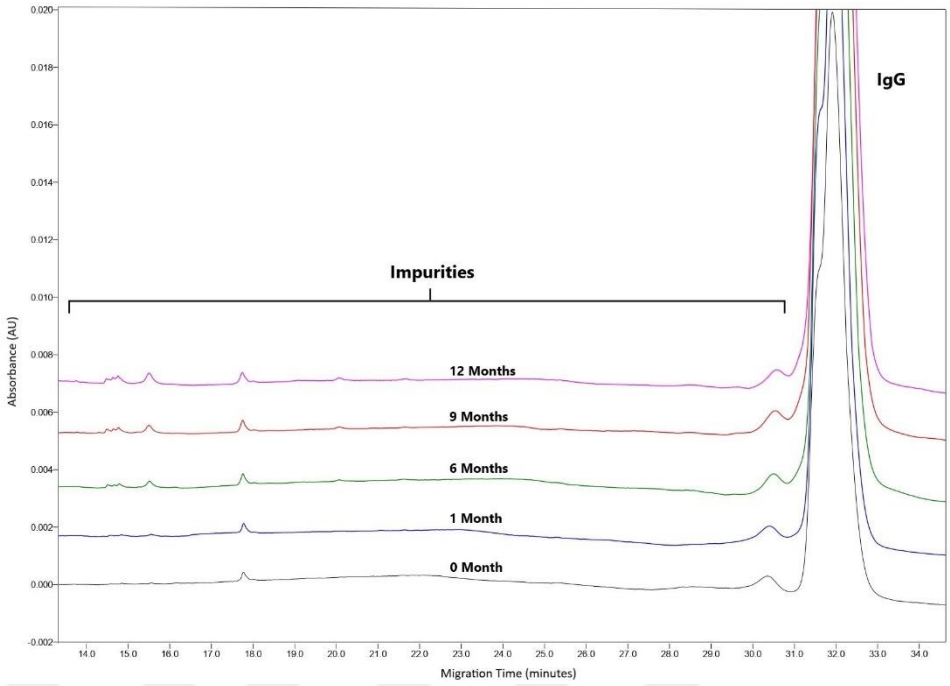

Figure 20: Overlaying nrCE-SDS electrograms of BS sample at 25±2°C/60±5%RH storage condition

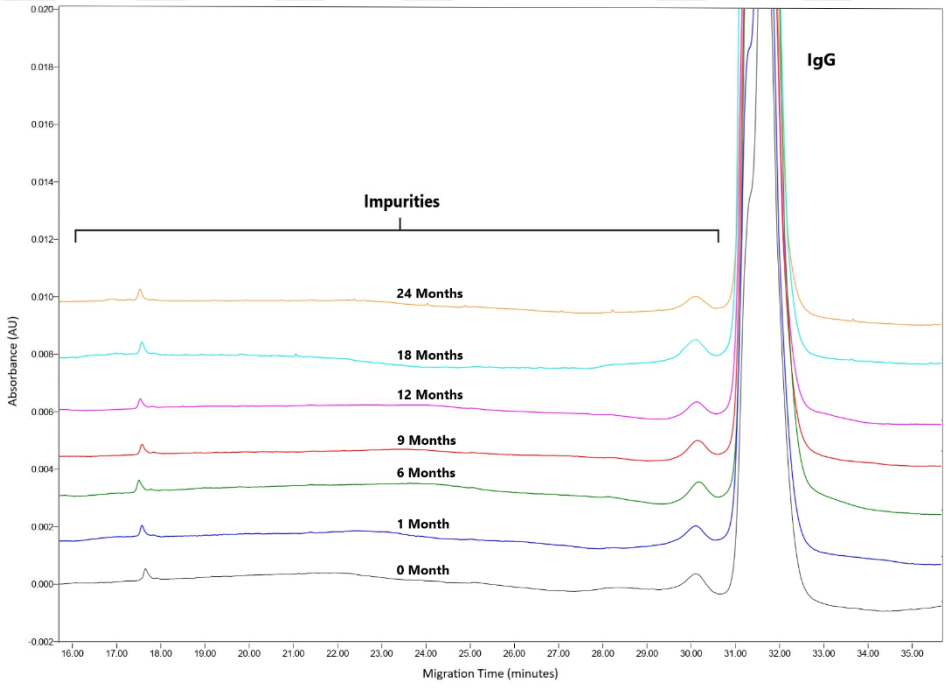

Figure 21: Overlaying nrCE-SDS electrograms of BS sample at ≤-65°C storage condition

4.1.5 Complement assay

Relative potencies were evaluated by the complement assay (ELISA), which quantitates the amount of neoantigen (C5b-C9) in the presence of human serum. The BS samples at three different storage conditions were analyzed.

Percent of the relative potency of BS samples at three different storage condition were calculated against the unstressed BS sample as an interim reference standard.

Complement assay results for all storage conditions of the BS sample are very close to each other at all time points. The results of all samples in the analysis performed at all time points are within the specification range. Results for all storage conditions are given in Figure 22.

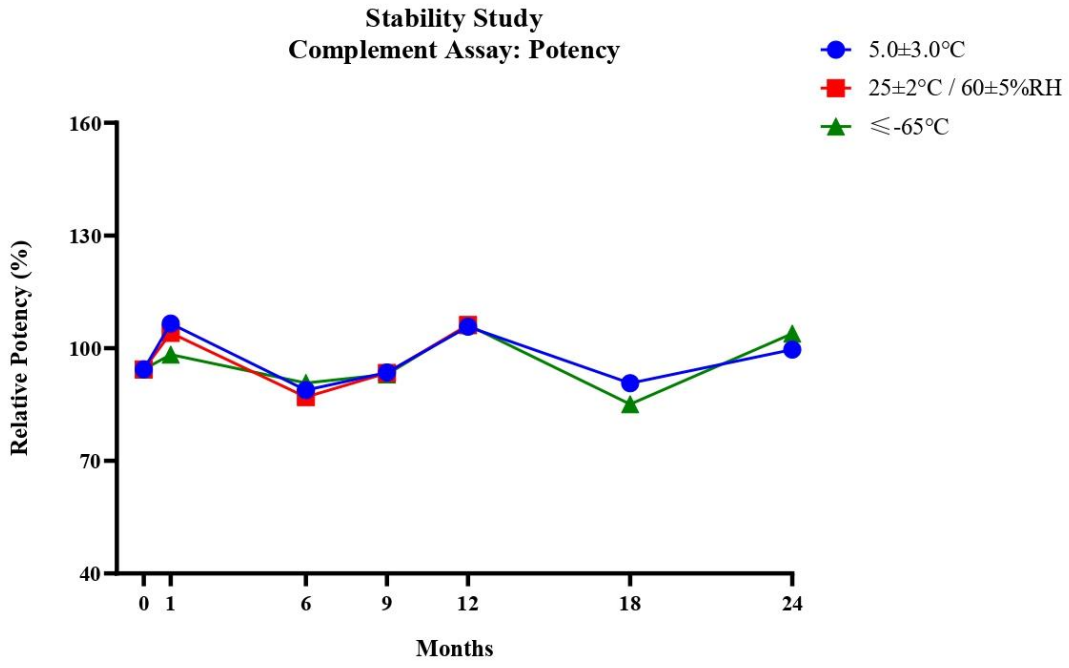

Figure 22: Stability Study, results of potency % obtained by complement assay

4.2 Forced Degradation Study Results

One-way analysis of variance (ANOVA) Dunn's multiple comparisons test was used to compare the difference between BS and OR samples. Results are observed as a mean ± SD, where p-value < 0.05 was considered a statistically significant difference. The software used for the performed statistical analysis was GraphPad Prism Software 9.0.

4.2.1 Thermal stress

The thermal stress was performed by incubation of the samples at two different temperatures (37°C and 50°C). The samples were pulled for testing after three days, seven days, and 14 days. The pulled samples were stored at 2-8˚C until analysis. SE-UPLC, rCE-SDS, nrCES-SDS, and icIEF analyzes were performed. The complement assay analysis provided additional information for the thermal stress. A summary of the results of the performed analyses is given in Table 16, for samples incubated at 37°C and Table 17 for samples incubated at 50°C.

Table 16: Thermal stress (37°C) % area results for BS and OR samples. Percentages are given as mean ± SD.

Thermal stress (37°C)		BS							OR						
		Control	37°C, 3 days	p-value	37°C, 7 days	p-value	37°C, 14 days	p-value	Control	37°C, 3 days	p-value	37°C, 7 days	p-value	37°C, 14 days	p-value
SE-UPLC	Monomer	97.94 ±0.01	97.10 ±0.01	>0.9999	96.95 ±0.01	0.2169	96.62 ±0.01	0.0100*	98.05 ±0.02	97.27 ±0.01	0.8308	97.08 ±0.01	0.0183*	96.85 ±0.01	<0.0001*
	HMW	1.19 ±0.01	2.04 ±0.01	0.4862	2.18 ±0.01	0.2177	2.38 ±0.01	0.0101*	1.03 ±0.02	1.82 ±0.02	0.8325	1.93 ±0.01	0.0817	2.25 ±0.04	<0.0001*
CE-SDS	rCE-SDS LC+HC	99.37 ±0.04	98.30 ±0.00	0.9760	97.85 ±0.05	0.4857	97.18 ±0.04	0.0149*	98.52 ±0.02	97.97 ±0.62	>0.9999	97.29 ±0.09	0.0366*	96.65 ±0.06	0.0002*
	nrCE-SDS IgG	97.77 ±0.20	97.62 ±0.04	>0.9999	97.54 ±0.02	>0.9999	96.42 ±0.02	0.3605	98.55 ±0.03	98.47 ±0.14	>0.9999	97.81 ±0.10	0.4904	97.47 ±0.14	0.0013*
icIEF	Main Variants	59.63 ±0.24	58.10 ±0.02	>0.9999	55.58 ±0.11	>0.9999	49.80 ±0.18	0.2863	52.76 ±0.21	51.18 ±0.11	>0.9999	49.26 ±0.13	0.2730	43.51 ±0.25	0.0307*
	Acidic Variants	28.59 ±0.30	30.78 ±0.05	>0.9999	33.82 ±0.01	>0.9999	40.09 ±0.03	0.0655	34.57 ±0.29	36.58 ±0.16	>0.9999	39.21 ±0.08	0.6576	45.41 ±0.28	0.0307*
	Basic Variants	11.79 ±0.53	11.13 ±0.07	>0.9999	10.61 ±0.11	0.7701	10.11 ±0.16	0.4578	12.67 ±0.23	12.25 ±0.11	>0.9999	11.54 ±0.09	0.4076	11.08 ±0.08	0.0137*

*Statistically meaningful

At the end of the stress incubation applied to the BS and OR samples at 37°C for three days, no significant differences were observed for both sample groups compared to the control samples. After seven days of stress incubation at 37°C, no significant differences were observed in the BS compared to the control; significant differences were observed in the results of only monomer (p=0.0183) and LC+HC (p=0.0366) of the OR compared to the control. After 14 days of incubation at 37°C, significant differences were observed in the results of monomer (p=0.0100), HMW (p=0.0101), and LC+HC (p=0.0149) of the BS. At the end of 14 days, significant differences were observed in the results of the OR compared to the control.

Table 17: Thermal stress (50°C) % area results for BS and OR samples. Percentages are given as mean ± SD.

Thermal stress (50°C)		BS							OR						
		Control	50°C, 3 days	p-value	50°C, 7 days	p-value	50°C, 14 days	p-value	Control	50°C, 3 days	p-value	50°C, 7 days	p-value	50°C, 14 days	p-value
SE-UPLC	Monomer	97.94 ±0.01	94.56 ±0.01	>0.9999	92.72 ±0.01	0.9755	89.59 ±0.02	0.0872	98.05 ±0.02	94.43 ±0.01	0.2892	92.05 ±0.01	0.0033*	86.44 ±0.01	<0.0001*
	HMW	1.19 ±0.01	4.44 ±0.01	>0.9999	6.21 ±0.01	0.9764	8.97 ±0.02	0.0874	1.03 ±0.02	4.55 ±0.02	0.2902	6.89 ±0.02	0.0033*	12.19 ±0.01	<0.0001*
CE-SDS	rCE-SDS LC+HC	99.37 ±0.04	97.21 ±0.16	>0.9999	96.24 ±0.07	0.3770	92.16 ±0.50	0.0102*	98.52 ±0.02	96.32 ±0.20	0.6007	94.20 ±0.08	0.0185*	90.62 ±0.21	<0.0001*
	nrCE-SDS IgG	97.77 ±0.20	97.62 ±0.03	>0.9999	97.00 ±0.04	>0.9999	96.43 ±0.06	0.1204	98.55 ±0.03	98.05 ±0.13	>0.9999	97.38 ±0.17	0.0211*	96.83 ±0.07	<0.0001*
icIEF	Main Variants	59.63 ±0.24	49.09 ±0.04	>0.9999	37.58 ±0.26	0.5381	25.09 ±0.01	0.0655	52.76 ±0.21	43.62 ±0.56	>0.9999	32.44 ±0.31	0.0984	19.62 ±0.15	0.0019*
	Acidic Variants	28.59 ±0.30	41.41 ±0.14	>0.9999	53.81 ±0.12	0.5381	67.55 ±0.28	0.0655	34.57 ±0.29	44.98 ±0.43	>0.9999	58.53 ±0.44	0.0984	73.29 ±0.14	0.0019*
	Basic Variants	11.79 ±0.53	9.50 ±0.18	>0.9999	8.62 ±0.14	0.6233	7.37 ±0.29	0.3374	12.67 ±0.23	11.41 ±0.27	>0.9999	9.03 ±0.16	0.0984	7.09 ±0.04	0.0004*

*Statistically meaningful

At the end of the three and seven days of stress incubation applied to the BS samples at 50°C, no significant differences were observed compared to the control sample. At the end of 14 days, significant differences were observed in the LC+HC results (p=0.0102). At the end of the stress incubation applied to the OR samples at 50°C for three days, no significant differences were observed compared to the control sample. At the end of seven days of incubation of OR samples at 50°C, significant differences were observed except for the charge variant results. At the end of 14 days, significant differences were observed in the results of the OR samples compared to the control.

4.2.1.1 Size exclusion ultra-performance liquid chromatography (SE-UPLC)

Triplicate results of the BS sample (n=3) and triplicate results of OR samples (n=6) were grouped and compared for the 37°C and 50°C stress conditions.

The differences in mean monomer % area values between BS and OR samples exposed to 37°C thermal stress for three days and their controls were determined as 0.84% and 0.78%, respectively. After at 37°C for seven days, the differences between samples and controls were observed as 0.99% for BS and 0.97% for OR. After 14 days of incubation, the differences between samples and controls were 1.32% for BS and 1.20% for OR. For the 37°C thermal stress, linear curves of the monomer % area values of the BS and OR samples were compared and are given in Figure 23. The differences between the slopes are not significant (p=0.6555).

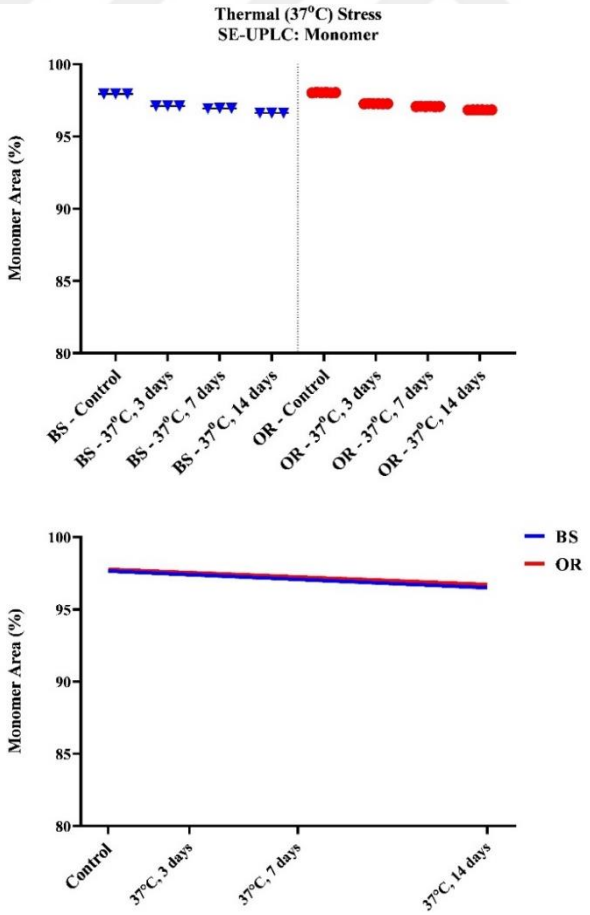

Figure 23: Thermal stress (37°C), monomer area % results obtained by SE-UPLC. The results are grouped as mean ± SD (top) and linear curves (bottom).

The differences in mean HMW % area values between BS and OR samples exposed to 37°C thermal stress for three days and their controls were determined as 0.85% and 0.79%, respectively. After seven days of incubation at 37°C, the differences were 0.99% for BS and 0.90% for OR. After 14 days of incubation, the differences between samples and controls were 1.19% for BS and 1.22% for OR. For the 37°C thermal stress, linear curves of the HMW % area values of the BS and OR samples were generated and compared. The differences between the slopes are not significant (p=0.8760). The results and linear curves are given in Figure 24.

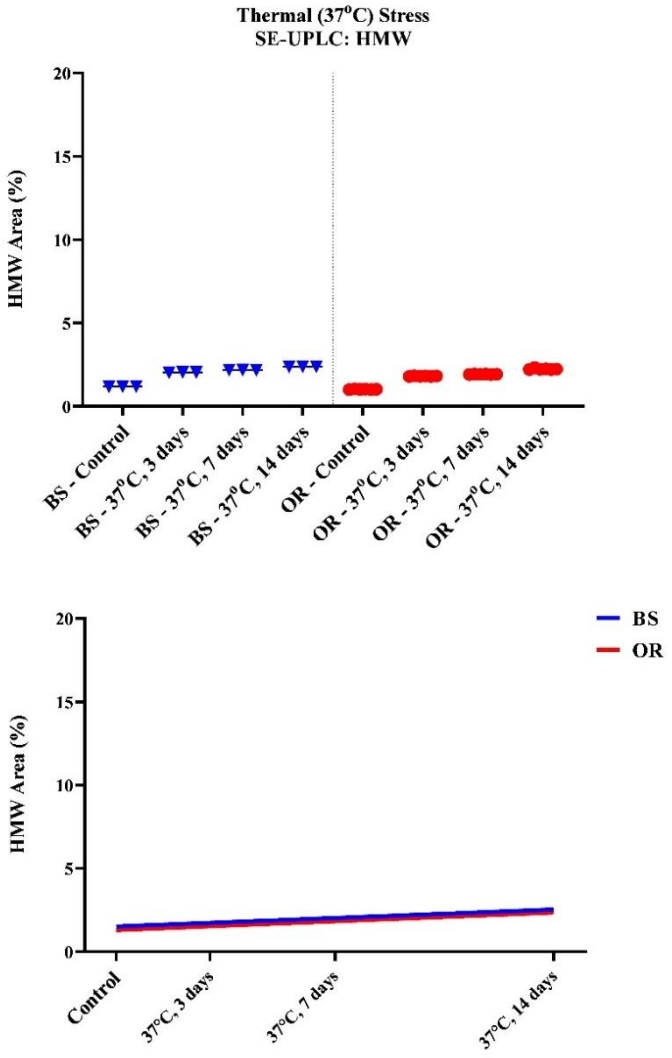

Figure 24: Thermal stress (37°C), HMW area % results obtained by SE-UPLC analysis. The results are grouped as mean ± SD (top) and linear curves (bottom).

The differences in mean monomer % area values between BS and OR samples exposed to 50°C thermal stress for three days and their controls were determined as 3.38% and 3.62%, respectively. After the same group of samples was incubated at 50°C for seven days, the differences between samples and controls were observed as 5.22% for BS and 6.00% for OR. After 14 days of incubation, the differences between samples and controls were 8.35% for BS and 11.61% for OR. For the 50°C thermal stress, linear curves of the monomer % area values of the BS and OR were compared are given in Figure 25. A significant difference was observed ($p<0.0001$) between the linear curves, where the degradation was more obvious.

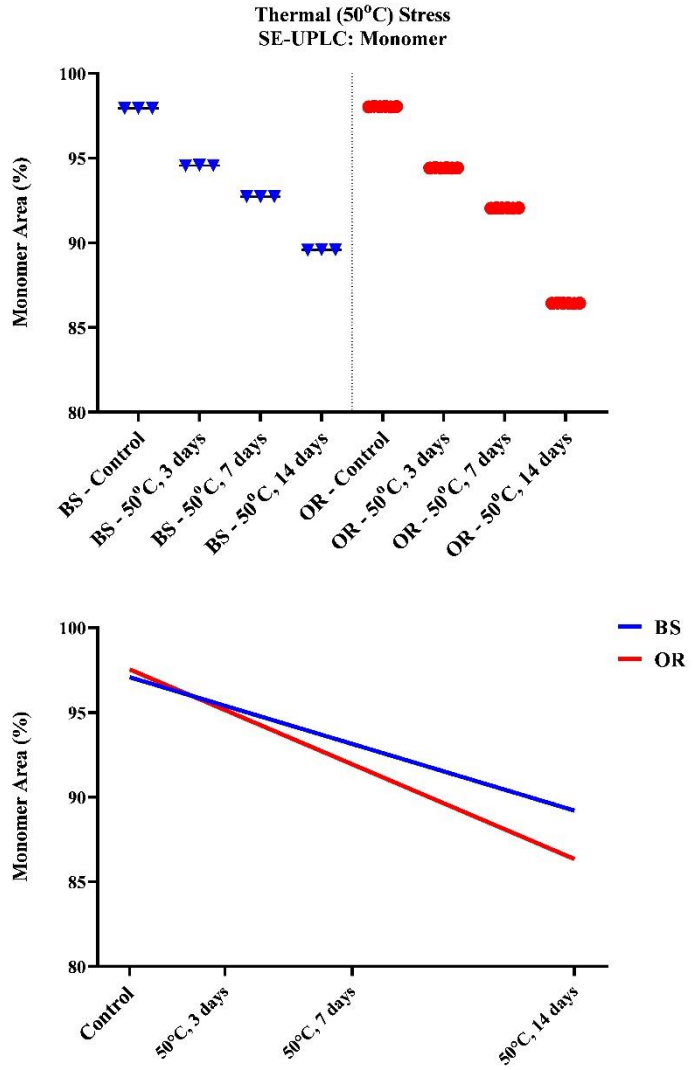

Figure 25: Thermal stress (50°C), monomer area % results obtained by SE-UPLC. The results are grouped as mean ± SD (top) and linear curves (bottom).

The differences in mean HMW % area values between BS and OR samples exposed to 50°C thermal stress for three days and their controls were determined as 3.25% and 3.52%, respectively. After seven days of incubation at 50°C, the differences were 5.02% for BS and 5.86% for OR. After 14 days of incubation, the differences between samples and controls were 7.78% for BS and 11.16% for OR. For the 50°C thermal stress, linear curves of the HMW % area values of the BS and OR samples were compared and are given in Figure 26. A significant difference was observed ($p<0.0001$) between the linear curves.

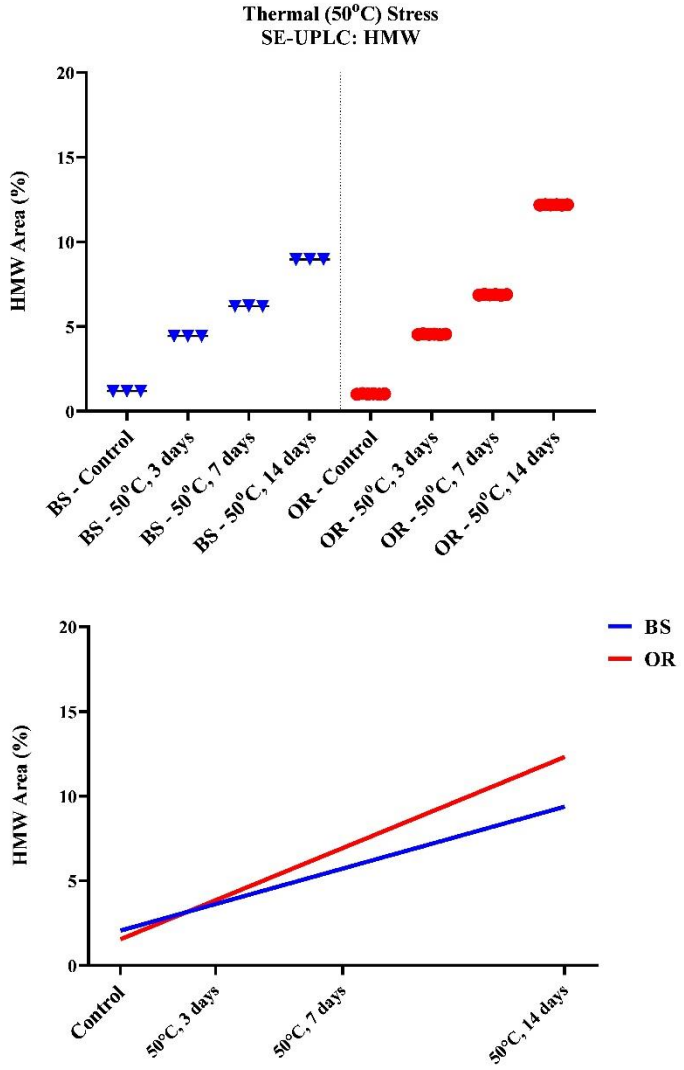

Figure 26: Thermal stress (50°C), HMW area % results obtained by SE-UPLC. The results are grouped as mean ± SD (top) and linear curves (bottom).

Overlaying SE-UPLC chromatograms of thermal stressed BS and OR samples, stressed FB and unstressed BS and OR samples are given in Figure 27. In BS and OR samples, it is observed that the amount of HMW and LMW increases in direct proportion to the thermal stress application temperature and time.

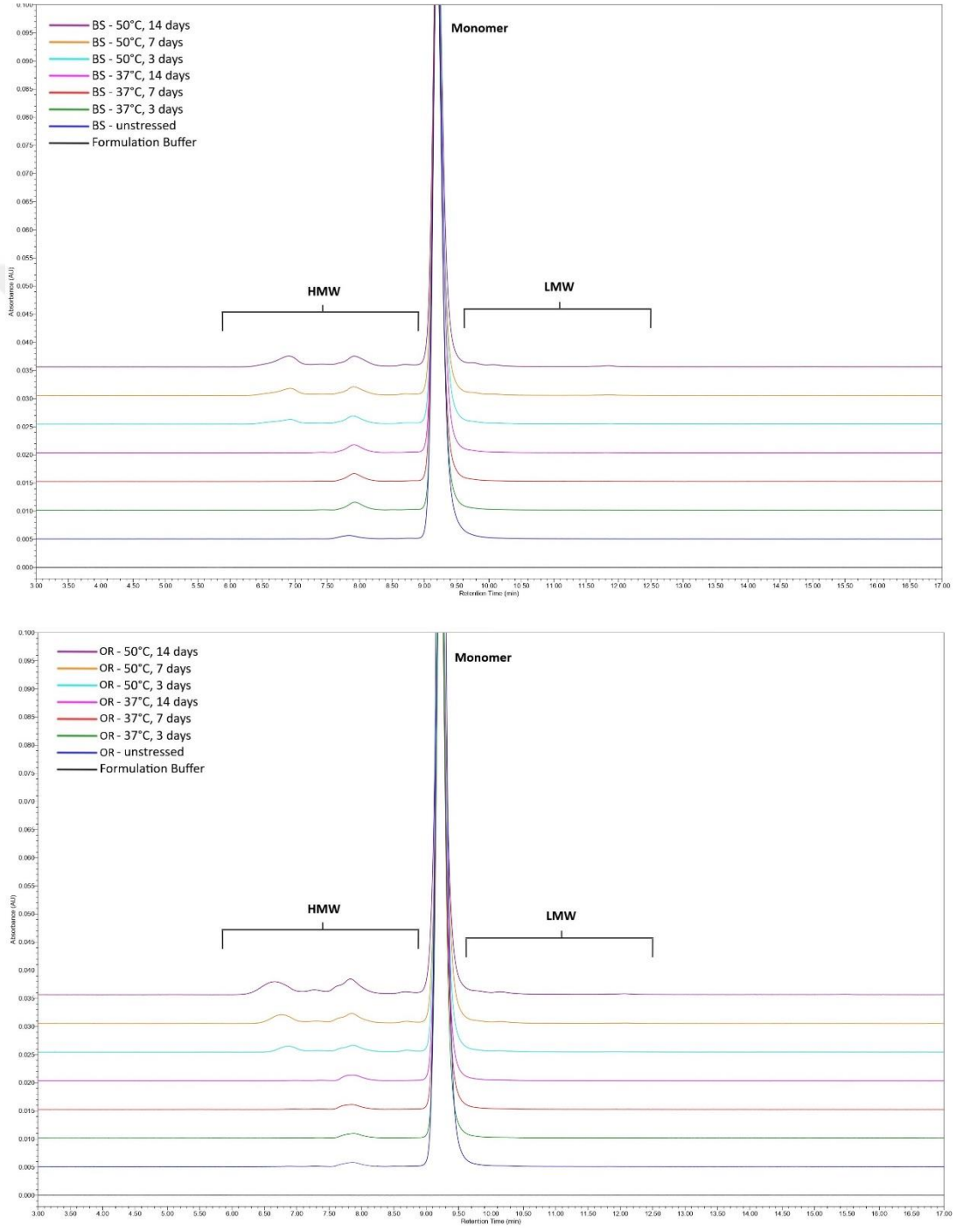

Figure 27: SE-UPLC chromatograms of BS (top) and OR (bottom) subjected to thermal stress

4.2.1.2 Imaged capillary isoelectric focusing (icIEF)

Duplicate results of the BS sample (n=2) and duplicate results of two different OR samples (n=4) were grouped and compared separately for 37°C and 50°C.

The differences in mean main charge variant % area values between BS and OR samples exposed to 37°C thermal stress for three days and their controls were determined as 1.53% and 1.58%, respectively. After incubation at 37°C for seven days, the differences were observed as 4.05% for BS and 3.50% for OR. The differences between samples and controls were 9.83% for BS and 9.25% for OR after 14 days of incubation at 37°C. For the 37°C thermal stress, linear curves of the main charge variant % area values of the BS and OR were compared and are given in Figure 28. The differences between the slopes are not significant (p=0.2550).

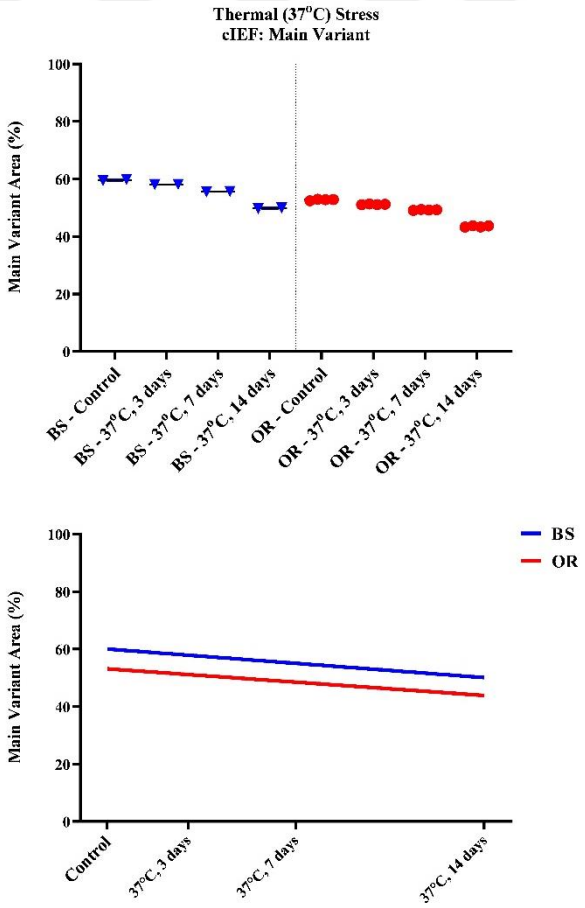

Figure 28: Thermal stress (37°C), main variant area % results obtained by icIEF. The results are grouped as mean ± SD (top) and linear curves (bottom).

The differences in mean acidic charge variant % area values between BS and OR samples exposed to 37°C thermal stress for three days and their controls were determined as 2.19% and 2.01%, respectively. After incubation at 37°C for seven days, the differences between samples and controls were observed as 5.23% for BS and 4.64% for OR. The differences between samples and controls were 11.50% for BS and 10.84% for OR after 14 days of incubation at 37°C. For the 37°C thermal stress, linear curves of the acidic charge variant % area values of the BS and OR samples were generated and compared. The differences between the slopes are not significant (p=0.1292). The results and linear curves are given in Figure 29.

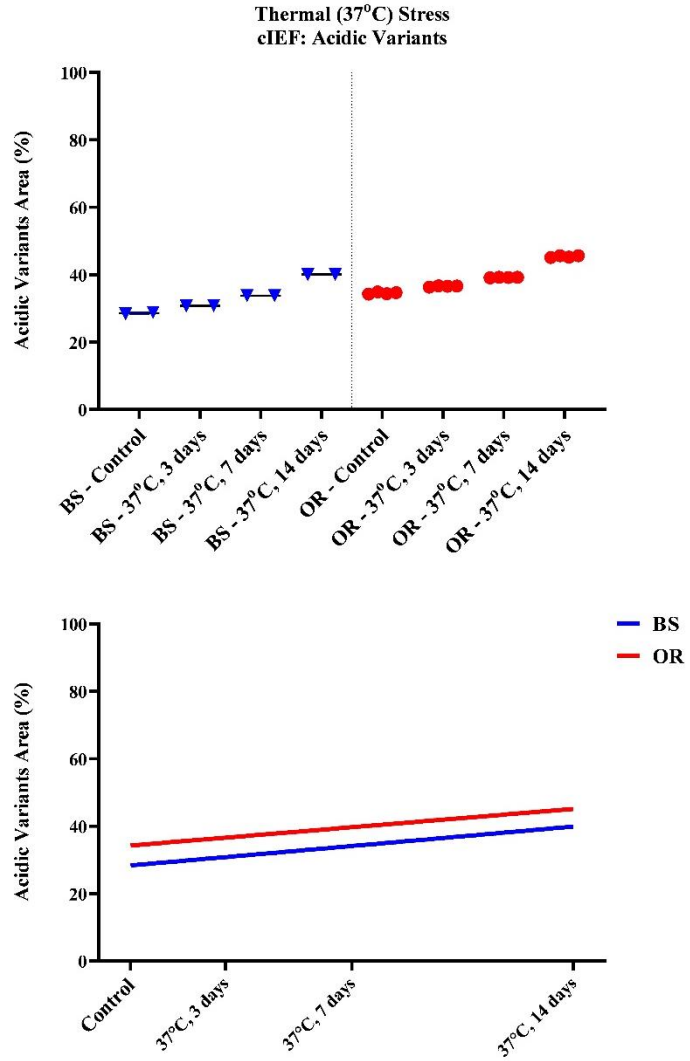

Figure 29: Thermal stress (37°C), acidic variants area % results obtained by icIEF. The results are grouped as mean ± SD (top) and linear curves (bottom).

The differences in mean basic charge variant % area values between BS and OR samples exposed to 37°C thermal stress for three days and their controls were determined as 0.66% and 0.42%, respectively. After incubation at 37°C for seven days, the differences between samples and controls were observed as 1.18% for BS and 1.13% for OR. The differences between samples and controls were 1.68% for BS and 1.59% for OR after 14 days of incubation at 37°C. For the 37°C thermal stress, linear curves of the basic charge variant % area values of the BS and OR samples were generated and compared. The differences between the slopes are not significant (p=0.9934). The results and linear curves are given in Figure 30.

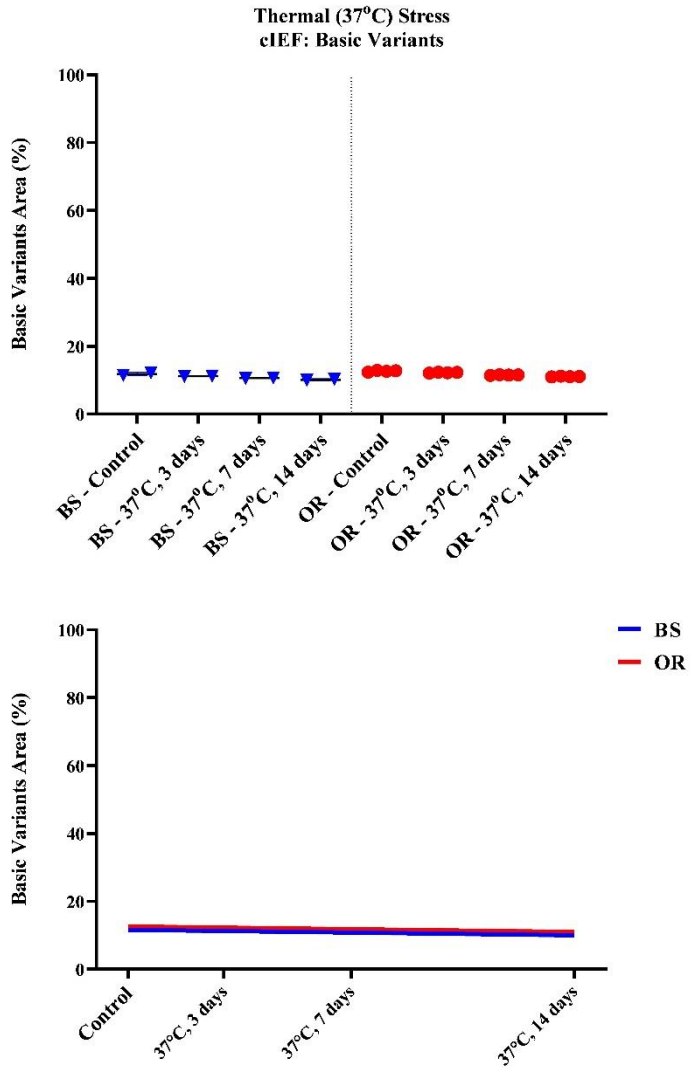

Figure 30: Thermal stress (37°C), basic variants area % results obtained by icIEF. The results are grouped as mean ± SD (top) and linear curves (bottom).

The differences in mean main charge variant % area values between BS and OR samples exposed to 50°C thermal stress for three days and their controls were determined as 10.54% and 9.14%, respectively. After incubation at 50°C for seven days, the differences between samples and controls were observed as 22.05% for BS and 20.32% for OR. The differences between samples and controls were 34.54% for BS and 33.14% for OR after 14 days of incubation at 50°C. For the 50°C thermal stress, linear curves of the main charge variant % area values of the BS and OR samples were generated and compared. The differences between the slopes are not significant (p=0.6220). The results and linear curves are given in Figure 31.

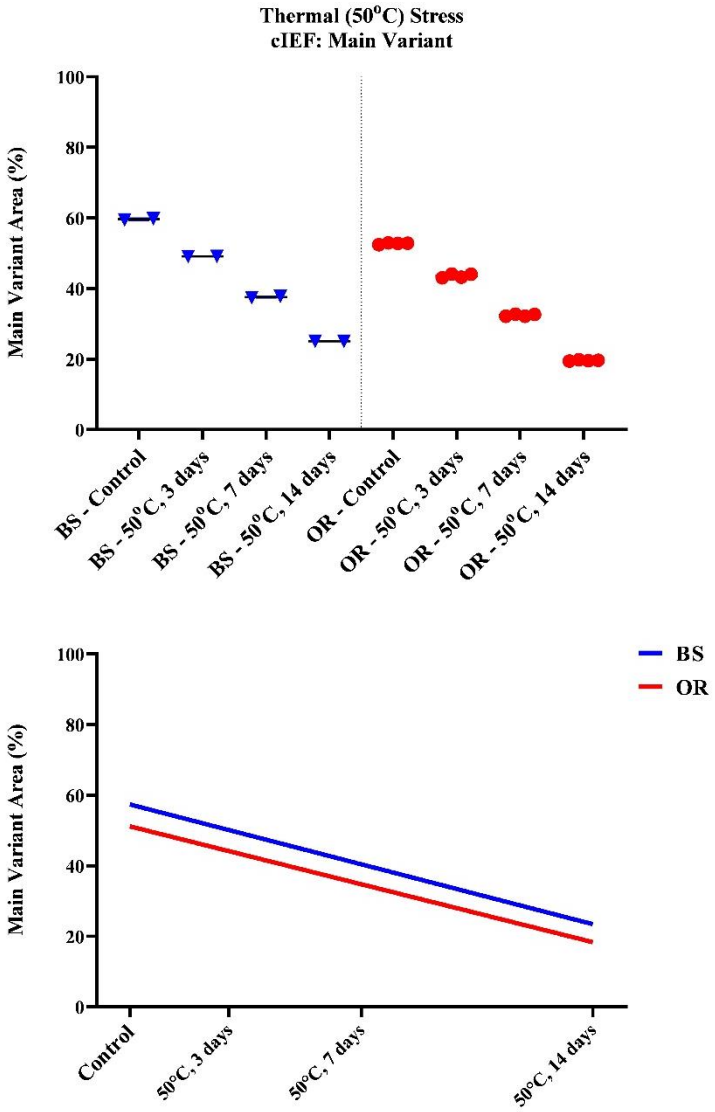

Figure 31: Thermal stress (50°C), main variant area % results obtained by icIEF. The results are grouped as mean ± SD (top) and linear curves (bottom).

The differences in mean acidic charge variant % area values between BS and OR samples exposed to 50°C thermal stress for three days and their controls were determined as 12.82% and 10.23%, respectively. After the same group of samples was incubated at 50°C for seven days, the differences between samples and controls were observed as 25.22% for BS and 23.96% for OR. The differences between samples and controls were 38.96% for BS and 38.72% for OR after 14 days of incubation at 50°C. For the 50°C thermal stress, linear curves of the acidic charge variant % area values of the BS and OR samples were and compared and are given in Figure 32. The differences between the slopes are not significant (p=0.8515).

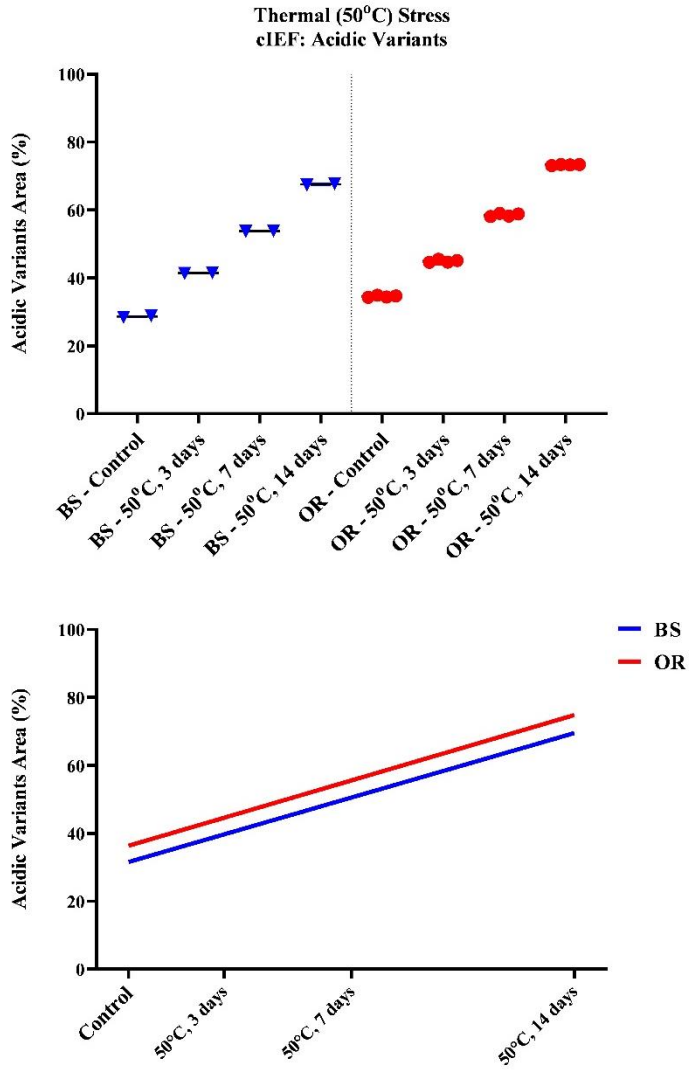

Figure 32: Thermal stress (50°C), acidic variants area % results obtained by icIEF. The results are grouped as mean ± SD (top) and linear curves (bottom).

The differences in mean basic charge variant % area values between BS and OR samples exposed to 50°C thermal stress for three days and their controls were determined as 2.29% and 1.26%, respectively. After incubation at 50°C for seven days, the differences between samples and controls were observed as 3.17% for BS and 3.64% for OR. The differences between samples and controls were 4.42% for BS and 5.58% for OR after 14 days of incubation at 50°C. For the 50°C thermal stress, linear curves of the basic charge variant % area values of the BS and OR samples were generated and compared. The differences between the slopes are significant (p=0.0143). The results and linear curves are given in Figure 33.

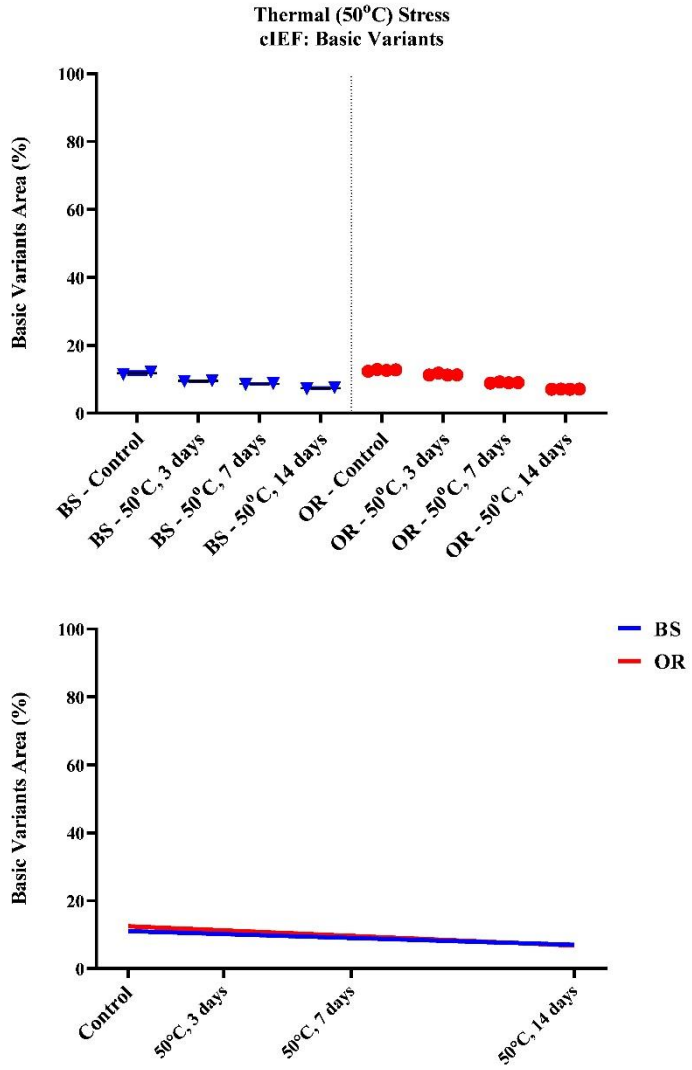

Figure 33: Thermal stress (50°C), basic variants area % results obtained by icIEF. The results are grouped as mean ± SD (top) and linear curves (bottom).

Overlaying icIEF electrograms of thermal stressed BS and OR samples, stressed FB and unstressed BS and OR samples are given in Figure 34. In BS and OR samples, it is observed that the amount of acidic charge variants increased in direct proportion to time and temperature.

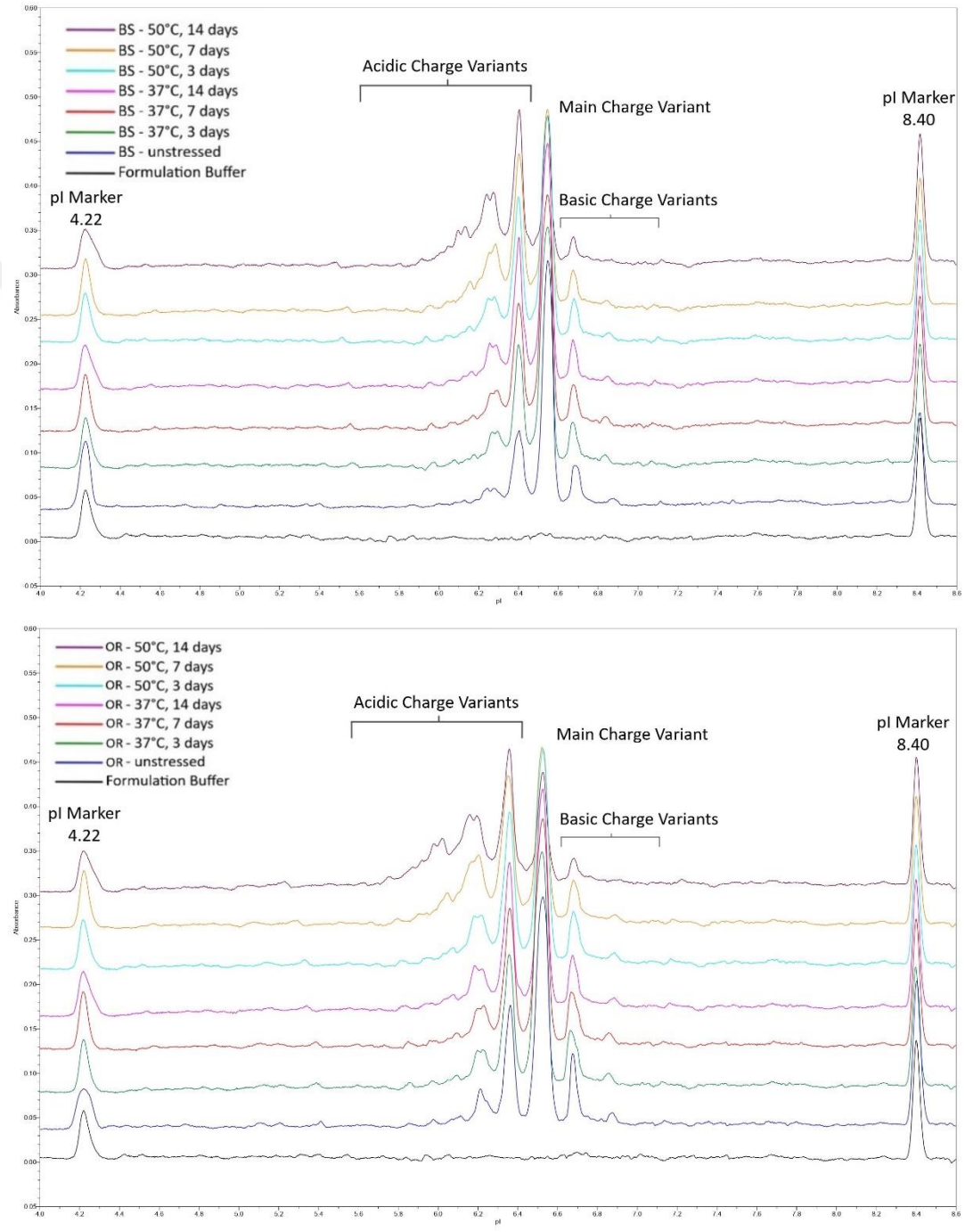

Figure 34: icIEF electrograms of BS (top) and OR (bottom) for thermal stress

4.2.1.3 Capillary electrophoresis-sodium dodecyl sulfate (CE-SDS)

4.2.1.3.1 Reduced CE-SDS

Triplicate results of the BS sample (n=3) and triplicate results of two different OR samples (n=6) were grouped and compared separately for 37°C and 50°C.

The differences in mean LC+HC % area values between BS and OR exposed to 37°C thermal stress for three days and their controls were determined as 1.07% and 0.55%, respectively. After incubation at 37°C for seven days, the differences were observed as 1.52% for BS and 1.23% for OR. After 14 days of incubation, the differences were 2.19% for BS and 1.87% for OR. For the 37°C thermal stress, linear curves of the LC+HC % area values of the BS and OR were compared and are given in Figure 35. The differences between the slopes are not significant (p=0.5733).

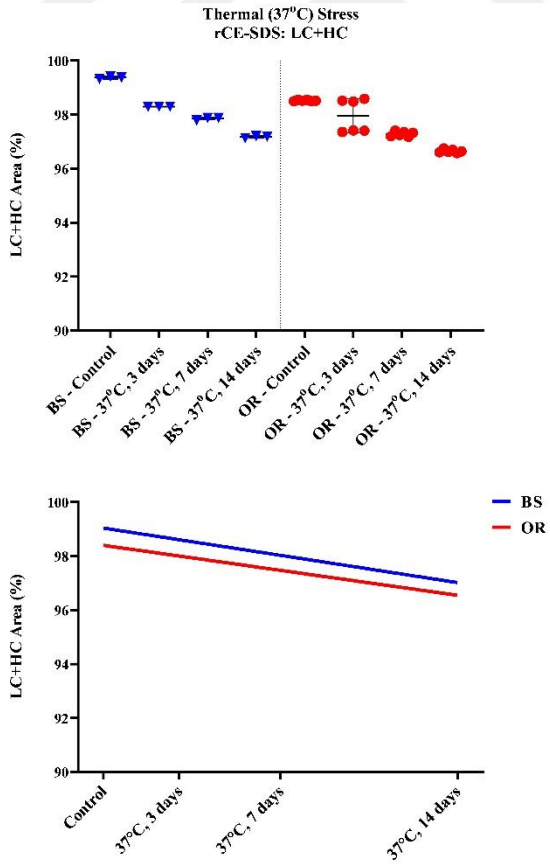

Figure 35: Thermal stress (37°C), LC+HC area % results obtained by rCE-SDS. The results are grouped as mean ± SD (top) and linear curves (bottom).

The differences in mean LC+HC % area values between BS and OR samples exposed to 50°C thermal stress for three days and their controls were determined as 2.16% and 2.20%, respectively. After the same group of samples was incubated at 50°C for seven days, the differences between samples and controls were observed as 3.13% for BS and 4.32% for OR. After 14 days of incubation, the differences between samples and controls were 7.21% for BS and 7.90% for OR. For the 50°C thermal stress, linear curves of the LC+HC % area values of the BS and OR samples were compared, and are given in Figure 36. The differences between the slopes are significant (p=0.0158).

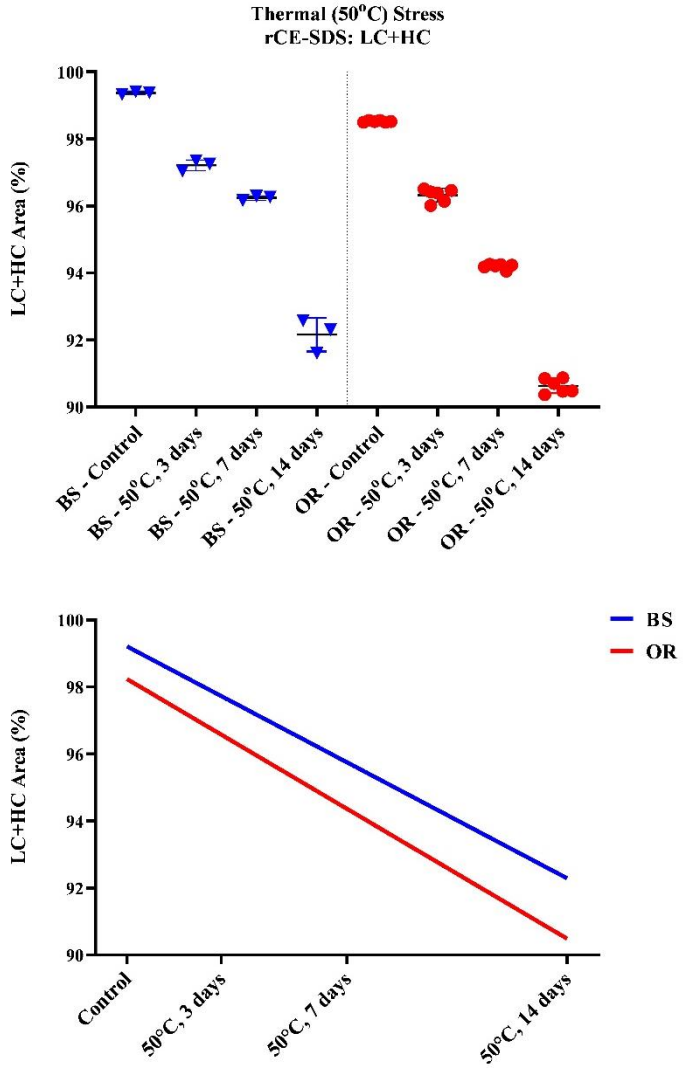

Figure 36: Thermal stress (50°C), LC+HC area % results obtained by rCE-SDS. The results are grouped as mean ± SD (top) and linear curves (bottom).

Overlaying rCE-SDS electrograms of thermal stressed BS and OR, stressed FB and unstressed BS and OR are given in Figure 37. It observed that the amount of LC+HC decreased, and impurities increased in direct proportion to time in samples.

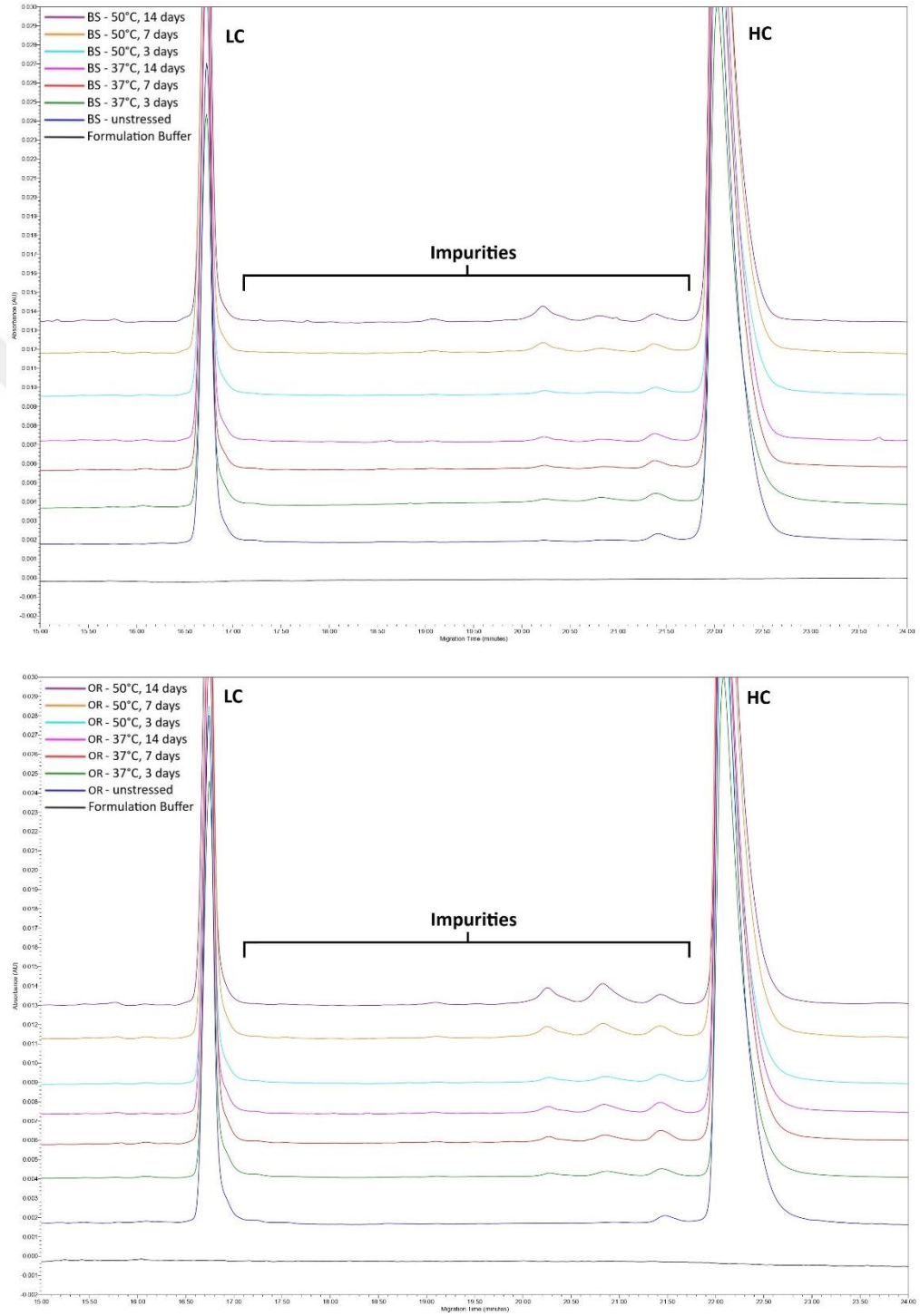

Figure 37: rCE-SDS electrograms of BS (top) and OR (bottom) for thermal stress

4.2.1.3.2 Non-reduced CE-SDS

Triplicate results of the BS sample (n=3) and triplicate results of two different OR samples (n=6) were grouped and compared separately for the 37°C and 50°C.

The differences in mean IgG % area values between BS and OR exposed to 37°C thermal stress for three days and their controls were determined as 0.15% and 0.08%, respectively. After incubation at 37°C for seven days, the differences were observed as 0.23% for BS and 0.74% for OR. After 14 days of incubation, the differences were 1.35% for BS and 1.08% for OR. For the 37°C thermal stress, linear curves of the IgG % area values of the BS and OR were compared, and are given in Figure 38. The differences between the slopes are not significant (p=0.2921).

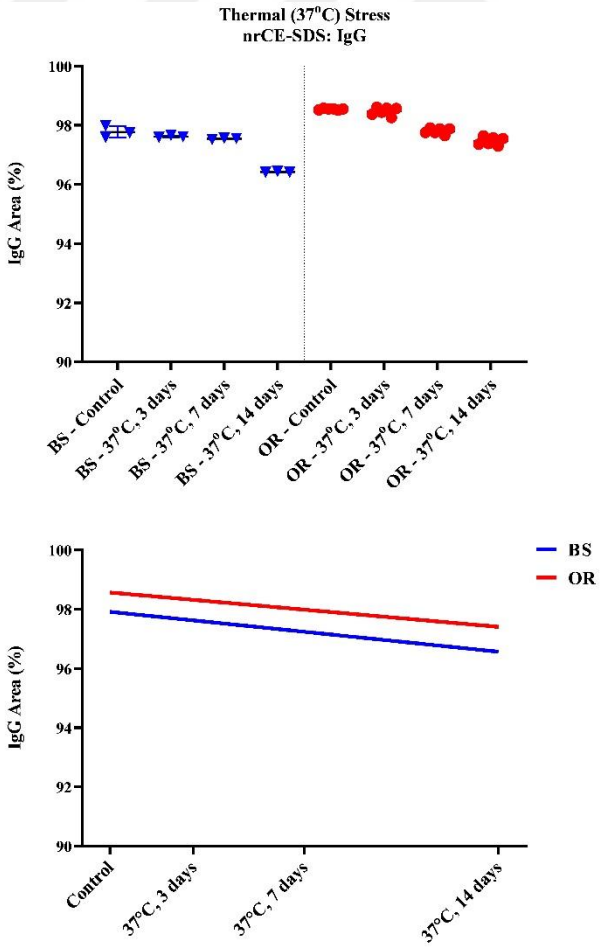

Figure 38: Thermal stress (37°C), IgG area % results obtained by nrCE-SDS. The results are grouped as mean ± SD (top) and linear curves (bottom).

The differences in mean IgG % area values between BS and OR samples exposed to 50°C thermal stress for three days and their controls were determined as 0.15% and 0.50%, respectively. After the same group of samples was incubated at 50°C for seven days, the differences between samples and controls were observed as 0.77% for BS and 1.17% for OR. After 14 days of incubation, the differences between samples and controls were 1.34% for BS and 1.72% for OR. For the 50°C thermal stress, linear curves of the IgG % area values of the BS and OR samples were generated and compared. The differences between the slopes are not quite significant (p=0.0644). The results and linear curves are given in Figure 39.

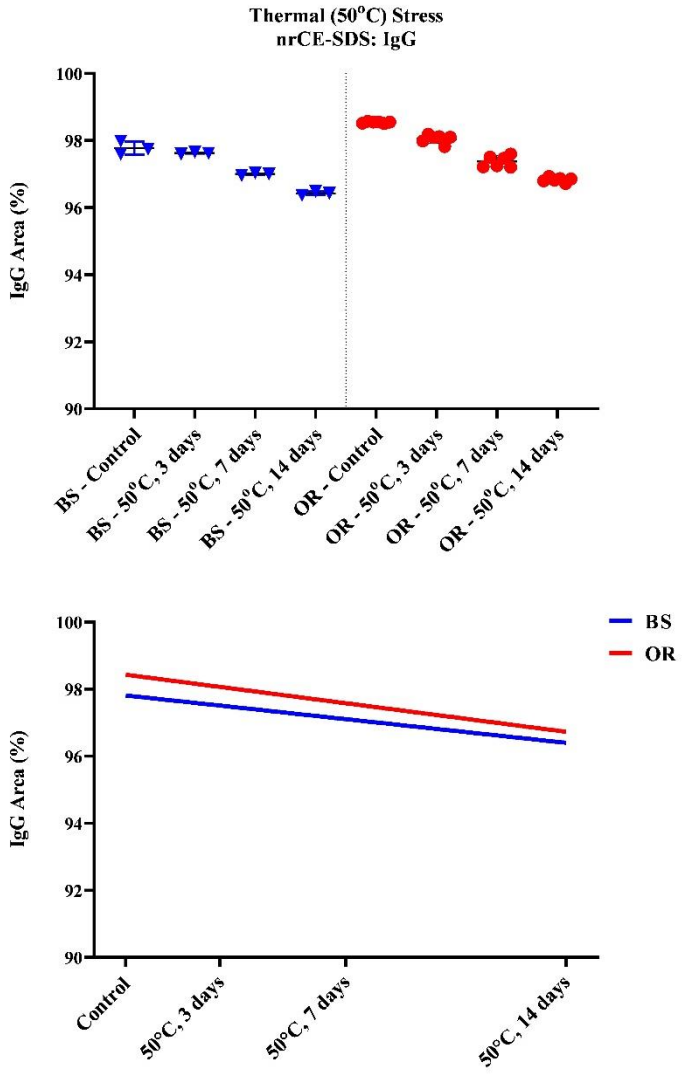

Figure 39: Thermal stress (50°C), IgG area % results obtained by nrCE-SDS. The results are grouped as mean ± SD (top) and linear curves (bottom).

Overlaying nrCE-SDS electrograms of thermal stressed BS and OR, stressed FB and unstressed BS and OR samples are given in Figure 40. It is observed that the amount of impurities increased in direct proportion to time in BS and OR samples.

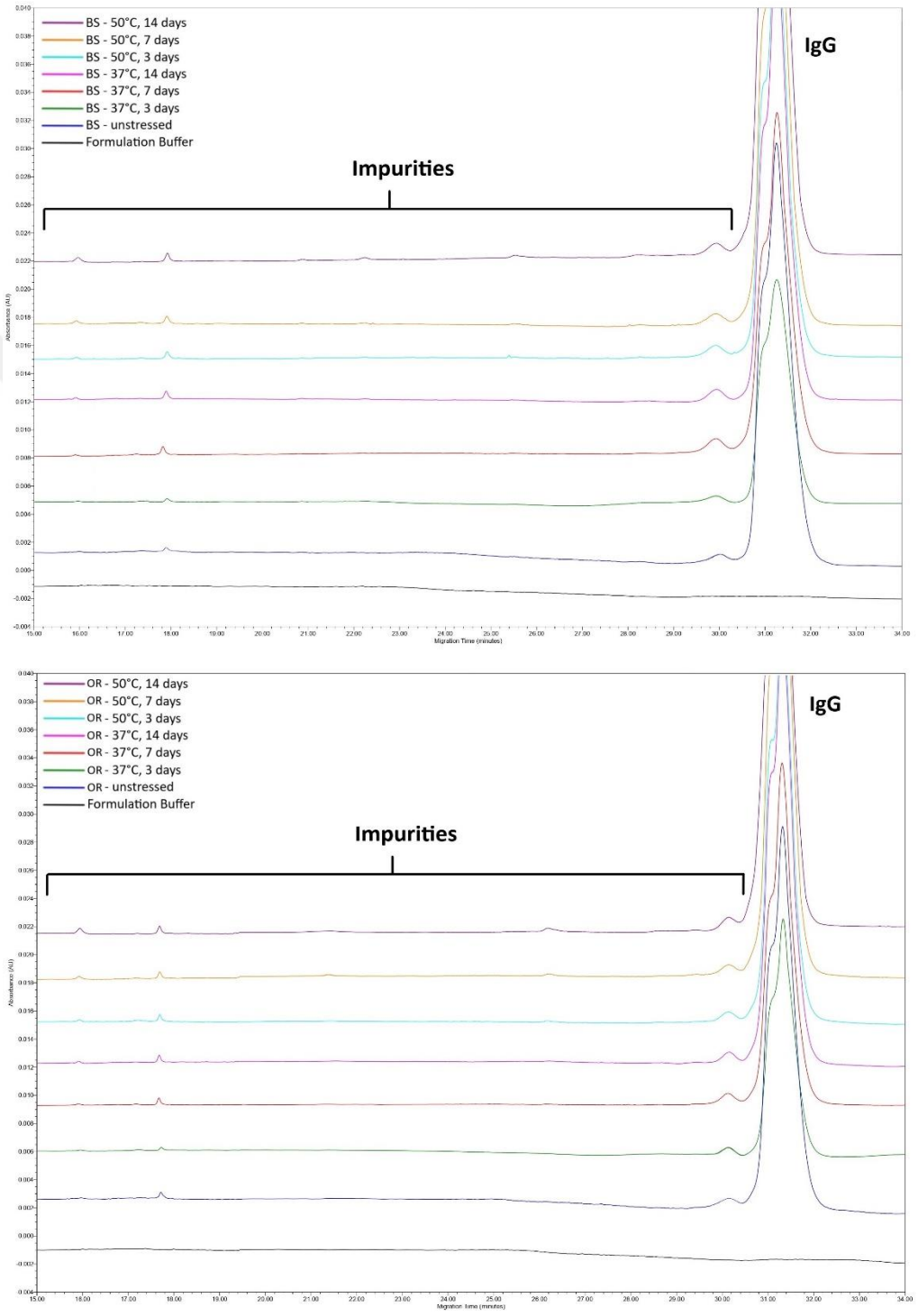

Figure 40: nrCE-SDS electrograms of BS (top) and OR (bottom) subjected to thermal stress

4.2.1.4 Complement assay

Relative potencies were evaluated by the complement assay (ELISA), which quantitates the amount of neoantigen (C5b-C9) in the presence of human serum. As it was the harshest condition, only the 14 days incubation at 37°C and 50°C samples were analyzed. Percent of the relative potency of the thermal stressed BS and OR was calculated against the unstressed BS as an interim reference standard.

Relative potency results for the BS and OR samples show similar results to each other in the same temperature conditions. In the temperature condition of 50°C, a significant decrease in the relative potency of the samples is observed. The results are given in Table 18.

Table 18: Thermal stress (14 days incubation at 37°C and 50°C) % relative potency results for BS and OR samples.

Sample Name	**% Relative Potency**	**Average % Relative Potency**
BS (unstressed)	NA	
BS - 37°C, 14 days	85.78%	
OR lot #1 - 37°C, 14 days	83.92%	OR - 37°C, 14 days 84.02%
OR lot #2 - 37°C, 14 days	84.12%	
BS - 50°C, 14 days	80.42%	
OR lot #1 - 50°C, 14 days	76.89%	OR - 50°C, 14 days 77.67%
OR lot #2 - 50°C, 14 days	78.45%	

4.2.2 Agitation stress

For agitation studies, aliquoted samples were placed in a plate shaker at 400 rpm at room temperature. Samples were pulled after 24 and 72 hours of shaking. The pulled samples were stored at 2-8˚C until analysis. SE-UPLC, r-CE-SDS, nr-CES-SDS and icIEF analyzes were performed. A summary of the analyzes performed is given in Table 19.

Table 19: Agitation stress % area results for BS and OR samples. Percentages are given as mean ± SD.

Agitation Stress		**BS**					**OR**				
		Control	400 rpm, 24 hours	p-value	400 rpm, 72 hours	p-value	Control	400 rpm, 24 hours	p-value	400 rpm, 72 hours	p-value
SE-UPLC	Monomer	97.94±0.01	97.31±0.01	0.0765	97.28±0.02	0.0235*	98.05±0.02	97.57±0.01	0.1888	97.53±0.01	0.0045*
	HMW	1.19±0.01	1.88±0.01	0.0817	1.90±0.01	0.0216*	1.03±0.02	1.54±0.02	0.1448	1.56±0.01	0.0065*
CE-SDS	rCE-SDS LC+HC	99.37±0.04	98.36±0.03	0.4906	98.32±0.09	0.3576	98.52±0.02	97.58±0.31	0.0070*	97.46±0.34	0.0025*
	nrCE-SDS IgG	97.77±0.20	97.43±0.07	>0.9999	97.22±0.02	0.5420	98.55±0.03	97.99±0.05	0.6021	97.76±0.07	0.0152*
icIEF	Main Variants	59.63±0.24	57.23±0.16	>0.9999	55.98±0.21	>0.9999	52.76±0.21	50.39±0.04	>0.9999	48.60±0.20	0.1363
	Acidic Variants	28.59±0.30	30.44±0.02	>0.9999	31.32±0.30	>0.9999	34.57±0.29	36.29±0.08	>0.9999	37.71±0.04	0.1359
	Basic Variants	11.79±0.53	12.34±0.13	>0.9999	12.70±0.09	>0.9999	12.67±0.23	13.32±0.06	0.6572	13.69±0.23	0.0571

*Statistically meaningful

At the end of the 24 hours of agitation stress, except for LC+HC results for the OR sample (p=0.070, no significant differences were observed for both sample groups compared to the control samples. After 72 hours of agitation stress, significant differences were observed in the results of monomer (p=0.0235 for BS, p=0.0216 for OR) and HMW (p=0.0045 for BS, p=0.0065 for OR) for both sample groups compared to the control samples. Also, significant differences were observed in the LC+HC (p=0.0025), and IgG (0.0152) results for the OR sample compared to the control.

4.2.2.1 Size exclusion ultra-performance liquid chromatography (SE-UPLC)

Triplicate results of the BS sample (n=3) and triplicate results of OR samples (n=6) were grouped and compared.

The differences between the mean monomer % area values of the BS and OR samples, which were subjected to 400 rpm agitation stress for 24 hours, from their control mean monomer % area value, were determined as 0.63% and 0.48%, respectively. At the end of 72 hours, the differences were observed as 0.66% for BS and 0.52% for OR. For the agitation stress, linear curves of the monomer % area values of the BS and OR samples were compared and are given in Figure 41. The differences between the slopes are not significant (p=0.4758).

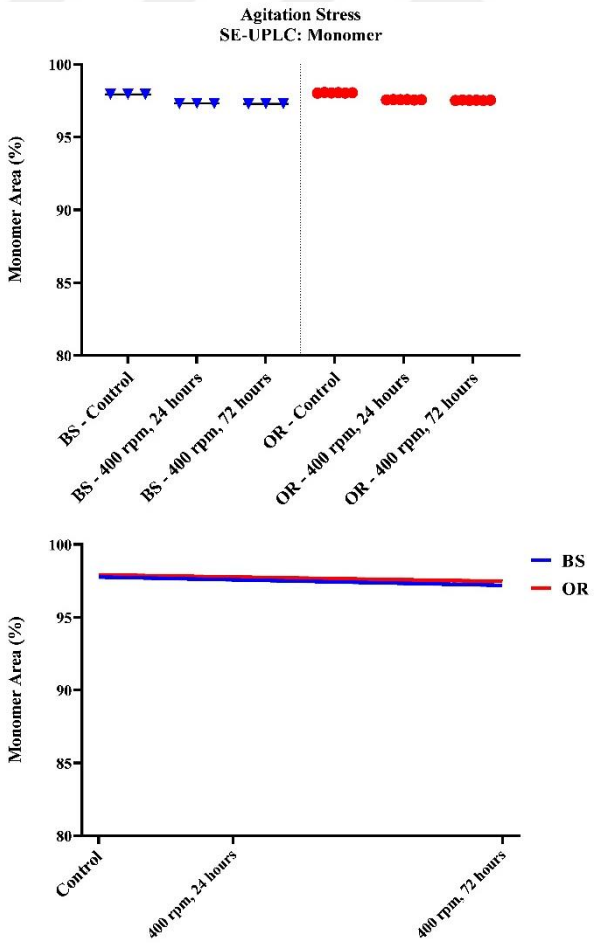

Figure 41: Agitation stress, monomer area % results obtained by SE-UPLC. The results are grouped as mean ± SD (top) and linear curves (bottom).

The differences in mean HMW % area values between BS and OR samples exposed to 400 rpm agitation stress for 24 hours and their controls were determined as 0.69% and 0.51%, respectively. At the end of 72 hours, the differences were observed as 0.71% for BS and 0.53% for OR.

The slopes of the linear curves of the HMW % area values of the samples subjected to agitation stress were compared. The linear curves did not differ from each other (p=0.4261). Curves are given in Figure 42.

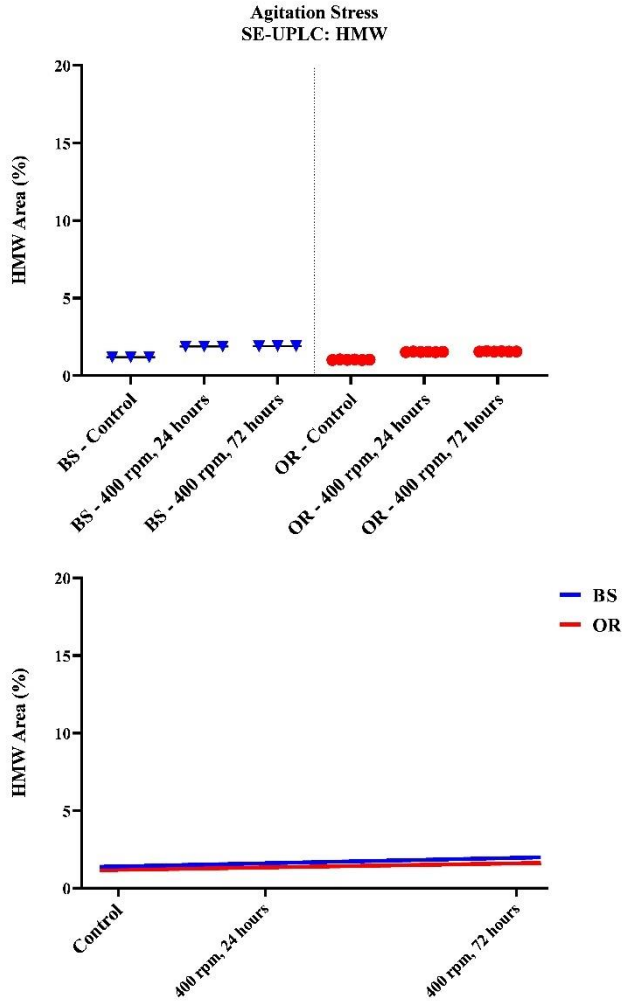

Figure 42: Agitation stress, HMW area % results obtained by SE-UPLC. The results are grouped as mean ± SD (top) and linear curves (bottom).

Overlaying SE-UPLC chromatograms of agitation stressed BS and OR samples, stressed FB and unstressed BS and OR are given in Figure 43. In BS and OR samples, it is observed that the amount of HMW is slightly increased.

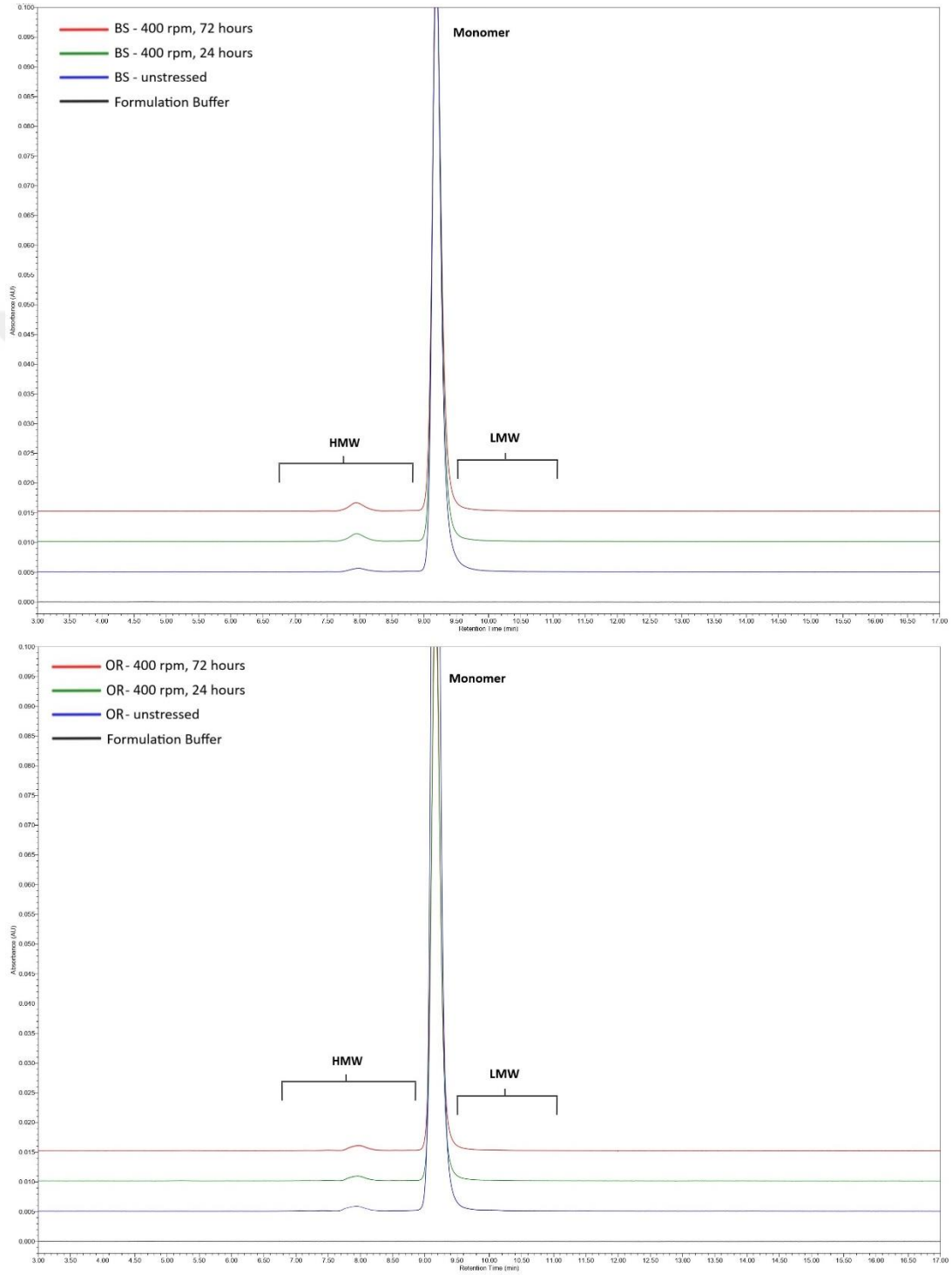

Figure 43: SE-UPLC chromatograms of BS (top) and OR (bottom) subjected to agitation stress

4.2.2.2 Imaged capillary isoelectric focusing (cIEF)

Duplicate results of the BS sample (n=2) and duplicate results of two different OR samples (n=4) were grouped and compared separately.

The differences in mean main charge variant % area values between BS and OR samples exposed to 400 rpm agitation stress for 24 hours and their controls were determined as 2.40% and 2.37%, respectively. At the end of 72 hours, the differences were observed as 3.65% for BS and 4.16% for OR. Linear curves of the main charge variant % area values of the BS and OR samples were compared and are given in Figure 44. The differences between the slopes are not significant (p=0.4393).

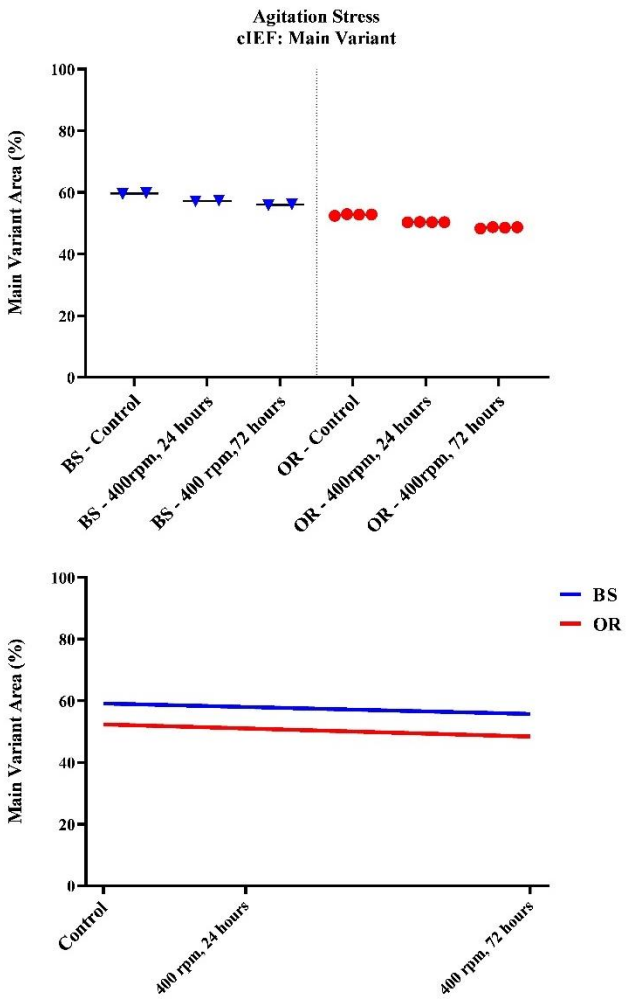

Figure 44: Agitation stress, main variant area % results obtained by icIEF. The results are grouped as mean ± SD (top) and linear curves (bottom).

The differences in mean acidic charge variant % area values between BS and OR samples exposed to 400 rpm agitation stress for 24 hours and their controls were determined as 1.95% and 1.72%, respectively. At the end of 72 hours, the differences between the samples and controls were observed as 2.73% for BS and 3.14% for OR. For the 400 rpm agitation stress, linear curves of the acidic charge variant % area values of the BS and OR samples were generated and compared. The differences between the slopes are not significant (p=0.3927). The results and linear curves are given in Figure 45.

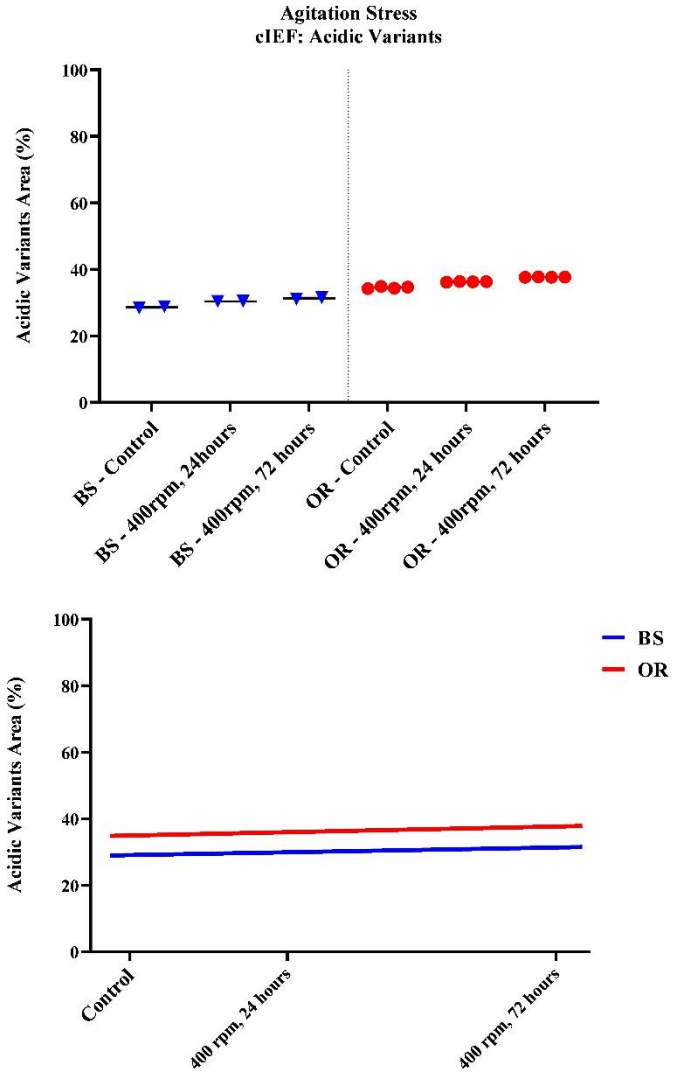

Figure 45: Agitation stress, acidic charge variants area % results obtained by icIEF. The results are grouped as mean ± SD (top) and linear curves (bottom).

The differences in mean basic charge variant % area values between BS and OR samples exposed to 400 rpm agitation stress for 24 hours and their controls were determined as 0.55% and 0.65%, respectively. At the end of 72 hours, the differences between the samples and controls were observed as 0.91% for BS and 1.02% for OR. For the 400 rpm agitation stress, linear curves of the basic charge variant % area values of the BS and OR samples were generated and compared. The differences between the slopes are not significant (p=0.7826). The results and linear curves are given in Figure 46.

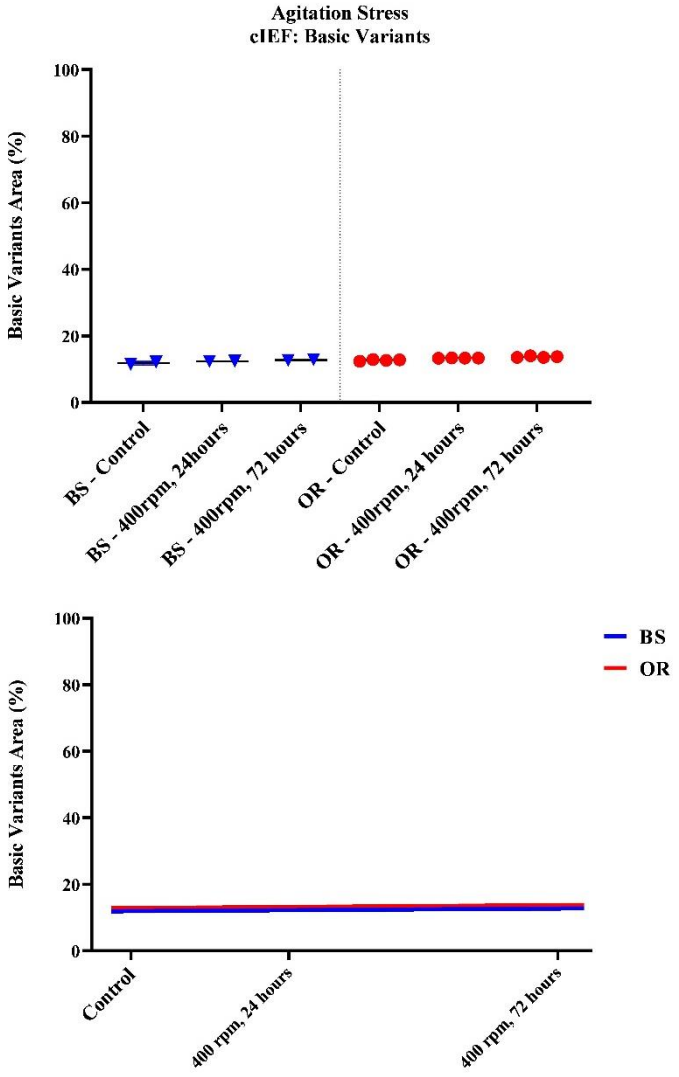

Figure 46: Agitation stress, basic charge variants area % results obtained by icIEF. The results are grouped as mean ± SD (top) and linear curves (bottom).

Overlaying icIEF electrograms of agitation stressed BS and OR samples, stressed FB and unstressed BS and OR samples are given in Figure 47. In BS and OR samples, it is observed that the amount of acidic variants slightly increased in direct proportion to time.

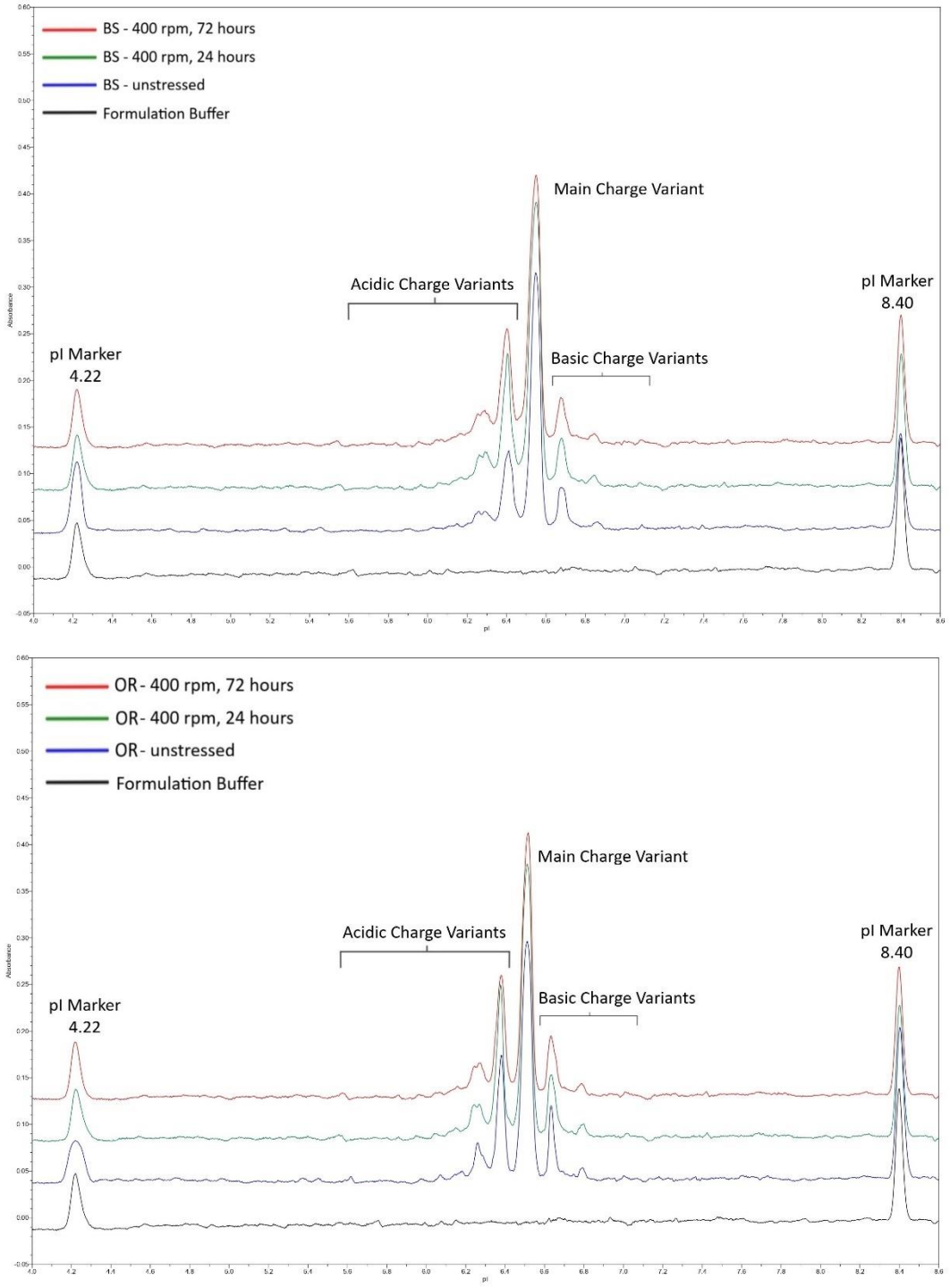

Figure 47: icIEF electrograms of BS (top) and OR (bottom) for agitation stress

4.2.2.3 Capillary electrophoresis-sodium dodecyl sulfate (CE-SDS)

4.2.2.3.1 Reduced CE-SDS

Triplicate results of the BS sample (n=3) and triplicate results of two different OR samples (n=6) were grouped and compared.

The differences in mean LC+HC % area values between BS and OR exposed to 400 rpm agitation stress for 24 hours and their controls were determined as 1.01% and 0.94%, respectively. At the end of 72 hours, the differences were observed as 1.05% for BS and 1.06% for OR. The slopes of the obtained BS and OR linear curves were compared and are given in Figure 48. The differences between the slopes are not significant (p=0.9437).

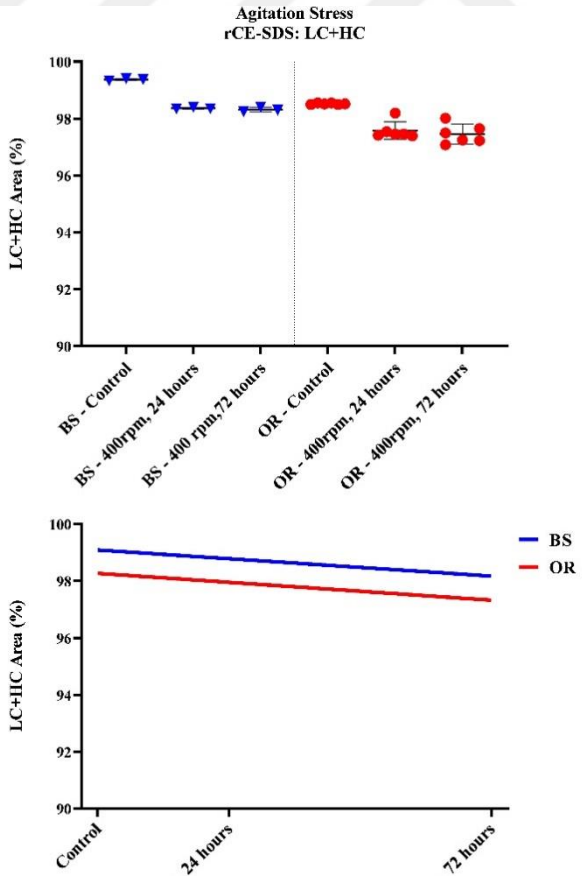

Figure 48: Agitation stress, LC+HC area % results obtained by rCE-SDS. The results are grouped as mean ± SD (top) and linear curves (bottom).

Overlaying rCE-SDS electrograms of agitation stressed BS and OR samples, stressed FB, and unstressed BS and OR samples are given in Figure 49. The amount of impurities slightly increased in direct proportion to time in BS and OR samples.

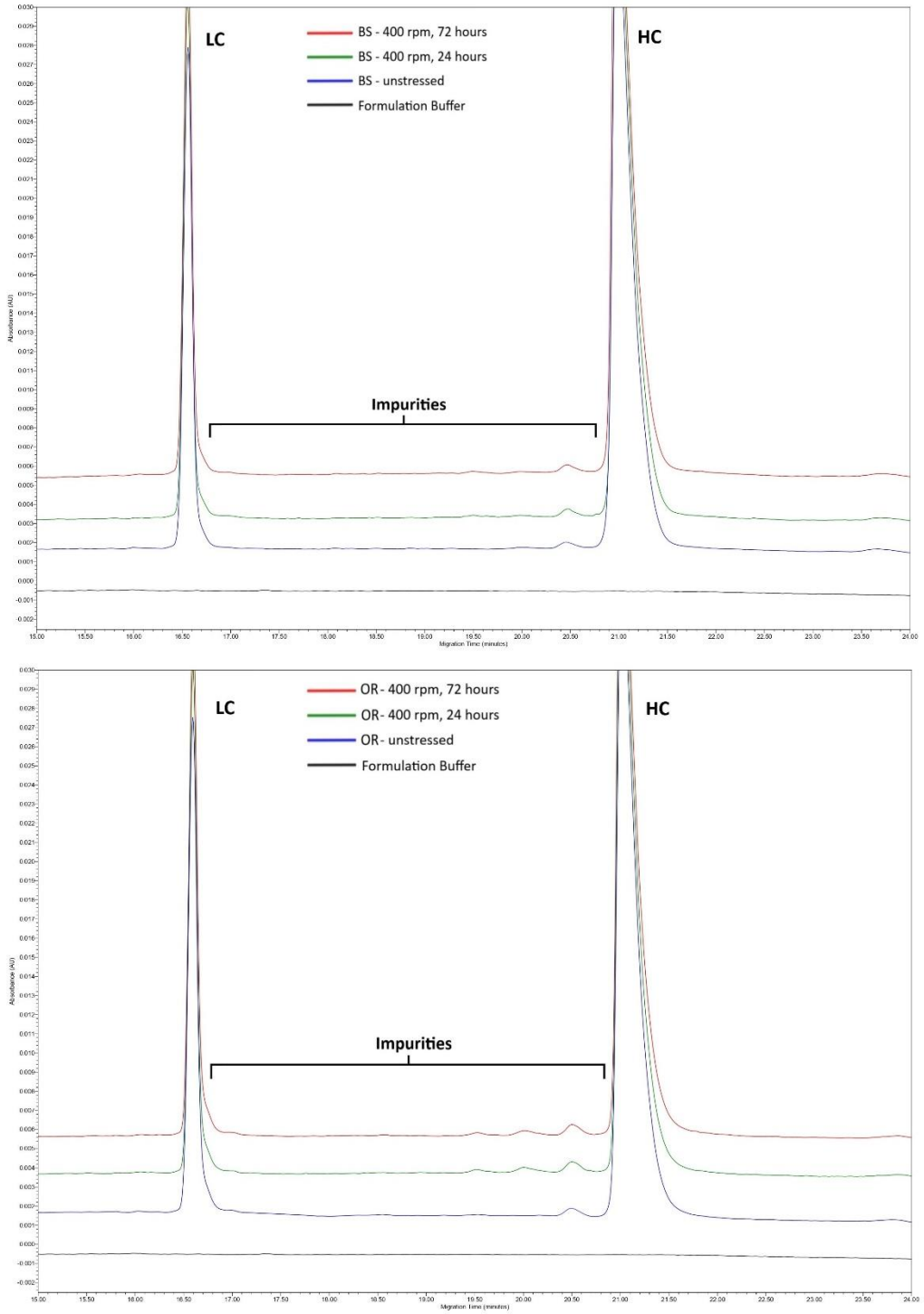

Figure 49: rCE-SDS electrograms of BS (top) and OR (bottom) for agitation stress

4.2.2.3.2 Non-reduced CE-SDS

Triplicate results of the BS sample (n=3) and triplicate results of two different OR samples (n=6) were grouped and compared.

The differences in mean IgG % area values between BS and OR exposed to 400 rpm agitation stress for 24 hours and their controls were determined as 0.34% and 0.56%, respectively. At the end of 72 hours, the differences were observed as 0.55% for BS and 0.79% for OR. Linear curves of the IgG % area values of the agitation stress applied samples were compared and are given in Figure 50. The differences between the slopes are not significant (p=0.1732).

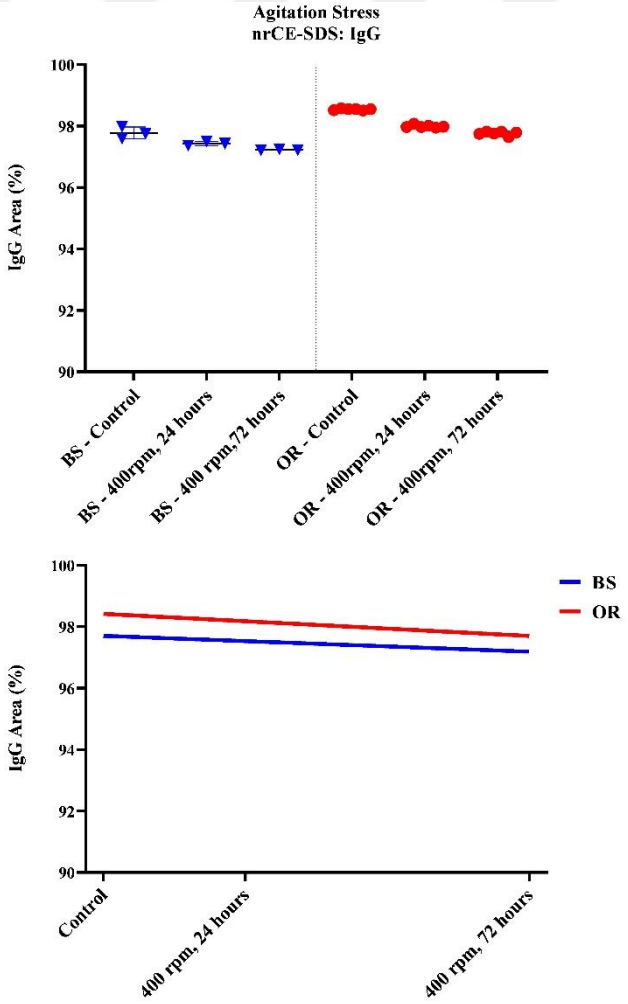

Figure 50: Agitation stress, IgG area % results obtained by nrCE-SDS. The results are grouped as mean ± SD (top) and linear curves (bottom).

Overlaying nrCE-SDS electrograms of agitation stressed BS and OR samples, stressed FB, and unstressed BS and OR samples are given in Figure 51. It is observed that the amount of impurities slightly increased in direct proportion to time.

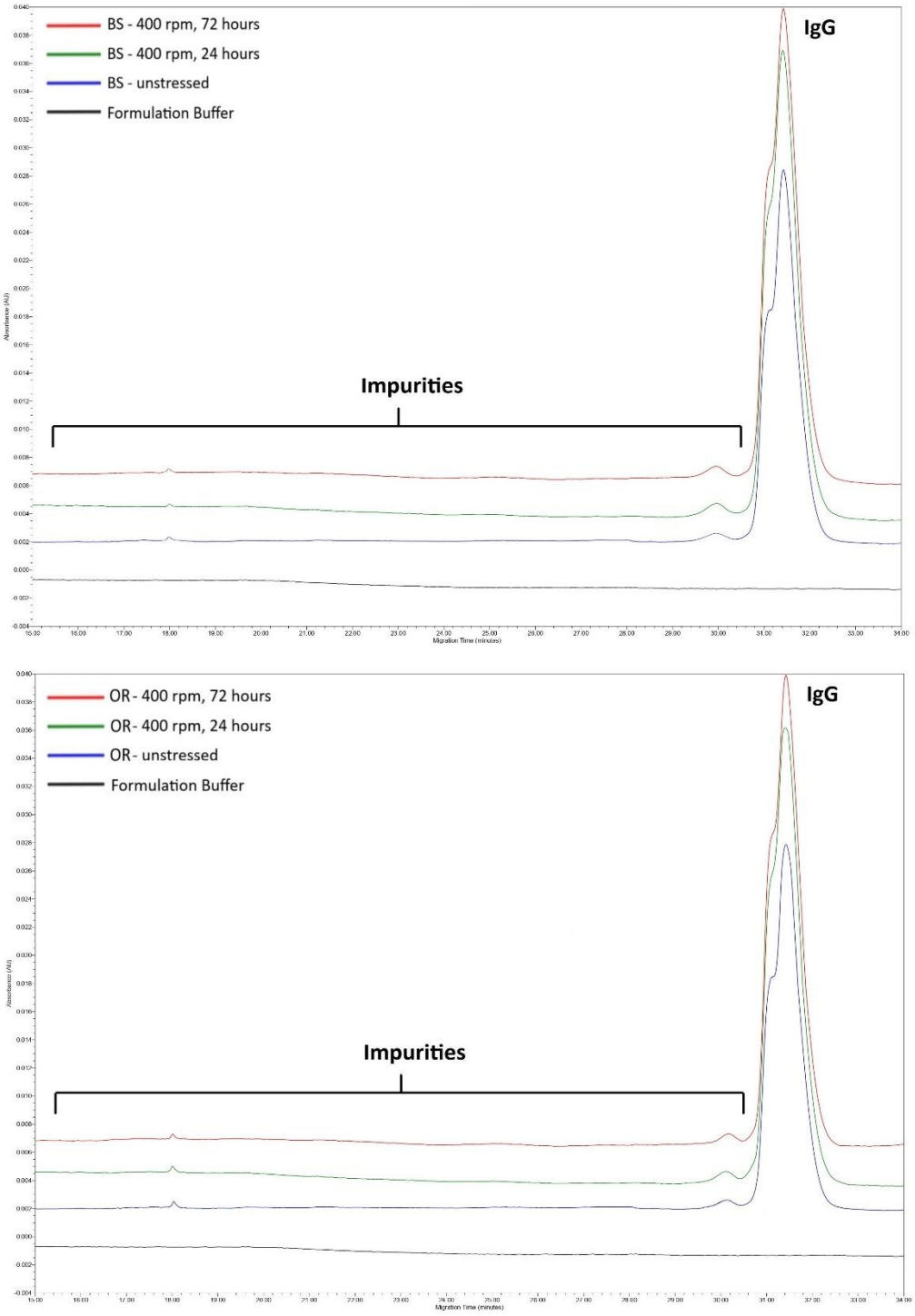

Figure 51: nrCE-SDS electrograms of BS (top) and OR (bottom) subjected to thermal stress

4.2.3 pH stress

The pH stress was performed by titration of the samples to acidic and basic pH values (pH 4 for acidic pH stress and pH 9 for basic pH stress). The samples were pulled for testing after 72 hours. The pulled samples were buffer exchanged back into formulation buffer and stored at 2-8˚C until analysis. SE-UPLC, r-CE-SDS, nr-CES-SDS and icIEF analyzes were performed. The complement assay analysis provided additional information for the pH stress. A summary of the analyzes performed is given in Table 20.

Table 20: pH stress % area results for BS and OR samples. Percentages are given as mean ± SD.

pH Stress		**BS**					**OR**				
		Control	pH 4, 72 hours	p-value	pH 9, 72 hours	p-value	Control	pH 4, 72 hours	p-value	pH 9, 72 hours	p-value
SE-UPLC	Monomer	97.94±0.01	53.55±0.02	0.9808	96.90±0.04	0.0767	98.05±0.02	30.25±0.02	0.0002*	97.01±0.01	0.0068*
	HMW	1.19±0.01	45.58±0.03	0.9799	2.16±0.02	0.0771	1.03±0.02	68.81±0.01	0.0002*	1.98±0.01	0.0069*
CE-SDS	rCE-SDS LC+HC	99.37±0.04	97.07±0.08	0.0773	97.70±0.12	0.0773	98.52±0.02	96.30±0.06	0.0069*	96.56±0.28	0.0069*
	nrCE-SDS IgG	97.77±0.20	96.79±0.04	0.0775	97.17±0.02	0.4126	98.55±0.03	97.39±0.09	0.0069*	97.78±0.05	0.0370*
icIEF	Main Variants	59.63±0.24	51.55±0.15	0.1922	55.91±0.08	>0.9999	52.76±0.21	46.16±0.13	0.0372*	48.73±0.14	0.2333
	Acidic Variants	28.59±0.30	26.22±0.04	0.5345	32.48±0.51	>0.9999	34.57±0.29	26.22±0.18	0.0121*	38.69±0.18	0.2333
	Basic Variants	11.79±0.53	22.24±0.18	0.1922	11.62±0.43	>0.9999	12.67±0.23	27.62±0.07	0.0372*	12.59±0.13	>0.9999

No significant differences were observed for BS sample compared to the control sample for both pH 4 acidic stress and pH 9 basic stress. Significant differences were observed in all analyzes compared to the control except the pH 9 basic stress icIEF results of the OR sample.

4.2.3.1 Size exclusion ultra-performance liquid chromatography (SE-UPLC)

Triplicate results of the BS sample (n=3) and triplicate results of two different OR samples (n=6) were grouped and compared.

The differences between the mean monomer % area of the BS and OR samples exposed to pH 4 acidic stress for 72 hours from the control samples were determined as 44.39% and 67.80%, respectively. The differences in mean HMW % area values between BS and OR samples and their controls were determined as 44.39% and 67.78%, respectively.

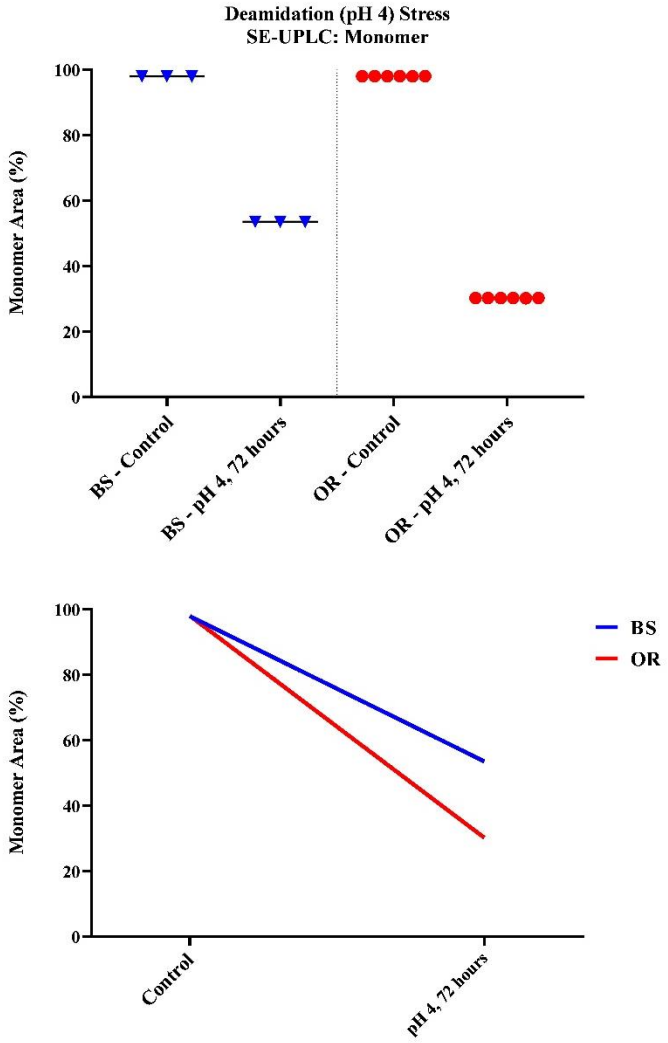

Figure 52: pH 4 acidic stress, monomer area % results obtained by SE-UPLC. The results are grouped as mean ± SD (top) and linear curves (bottom).

Linear curves of the % area values of the samples subjected to pH 4 acidic stress were generated, and the slopes of the obtained BS and OR linear curves were compared. Significant differences were observed between all linear curves for pH 4 acidic stress ($p<0.0001$). Curves are given in Figure 52 for monomer and Figure 53 for HMW.

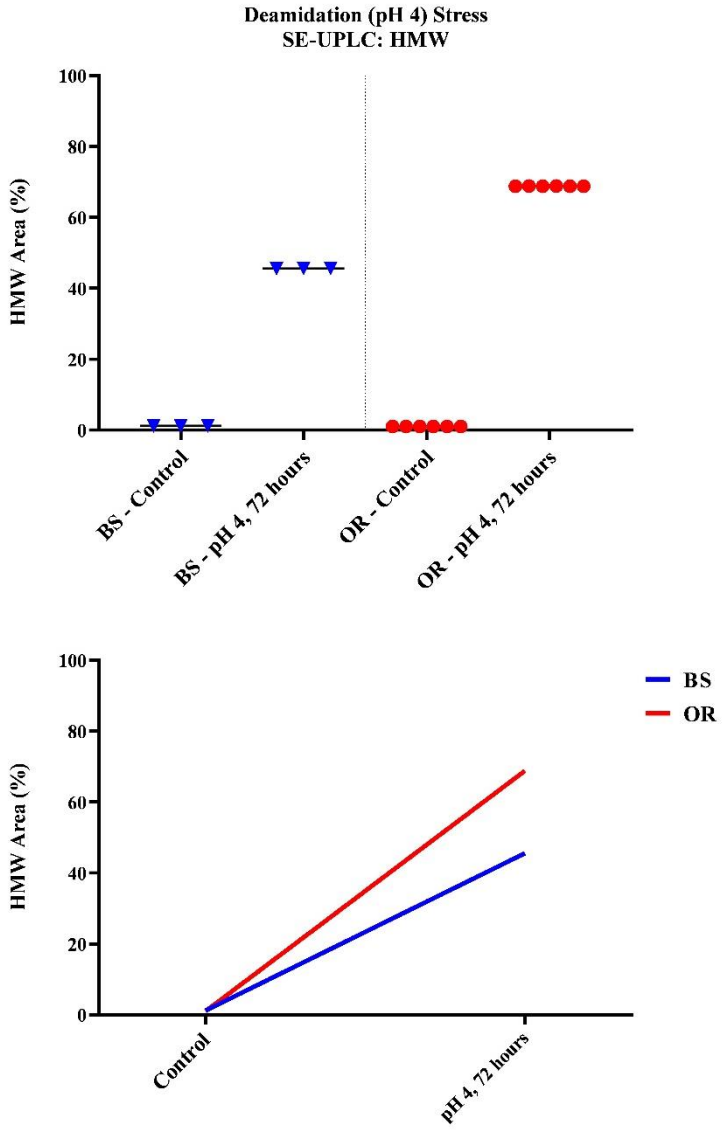

Figure 53: pH 4 acidic stress, HMW area % results obtained by SE-UPLC. The results are grouped as mean ± SD (top) and linear curves (bottom).

Overlaying SE-UPLC chromatograms of pH 4 acidic stressed BS and OR samples, stressed FB and unstressed BS and OR samples are given in Figure 54. In BS and OR samples, it is observed that the amount of HMW increases extremely with the application of pH stress.

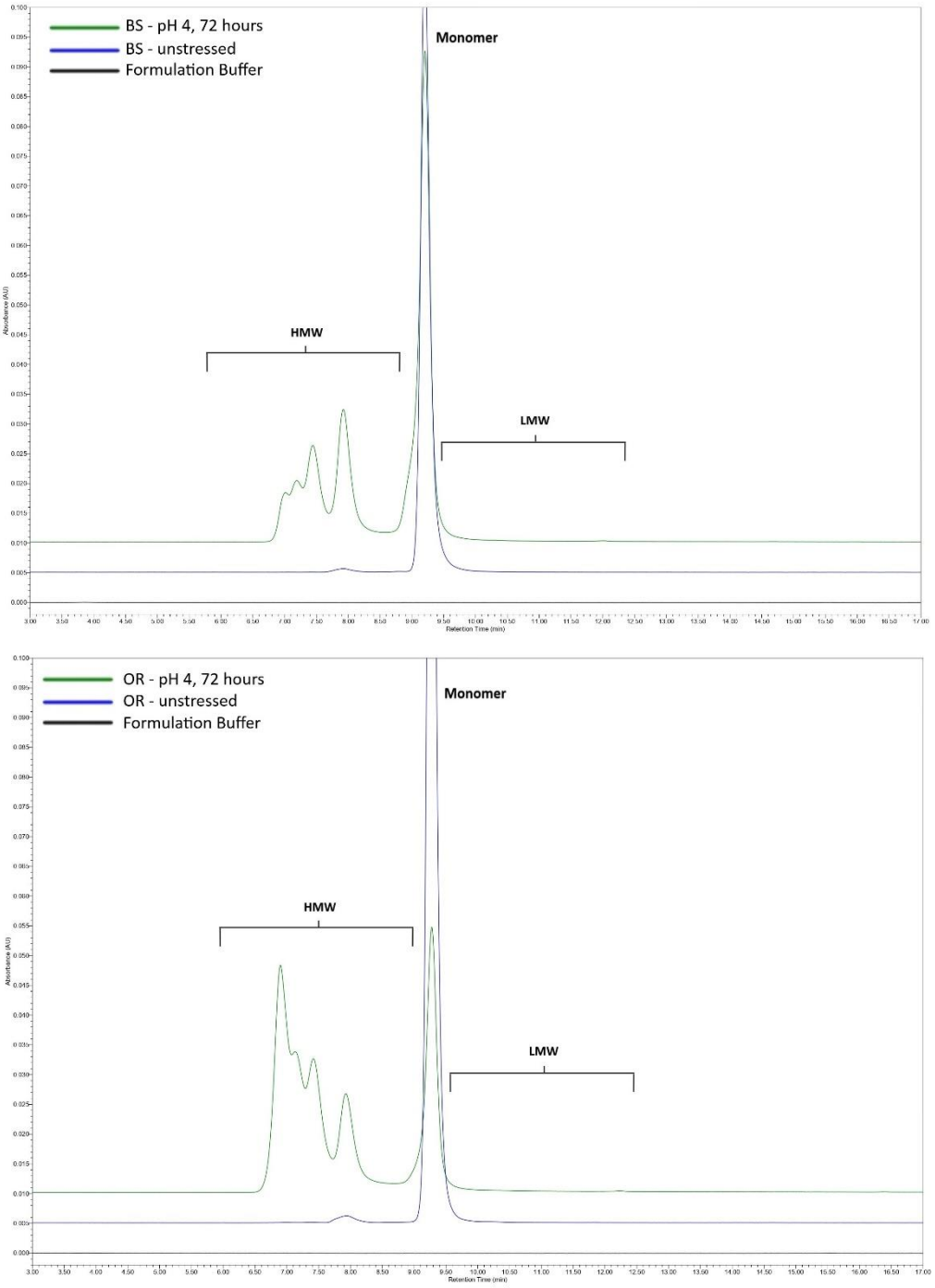

Figure 54: SE-UPLC chromatograms of BS (top) and OR (bottom) subjected to pH 4 acidic stress

The differences between the mean monomer % area of the BS and OR samples exposed to pH 9 basic stress for 72 hours from the control samples were determined as 1.04% for both. The differences in mean HMW % area values between BS and OR samples and their control samples were determined as 0.97% and 0.95%, respectively.

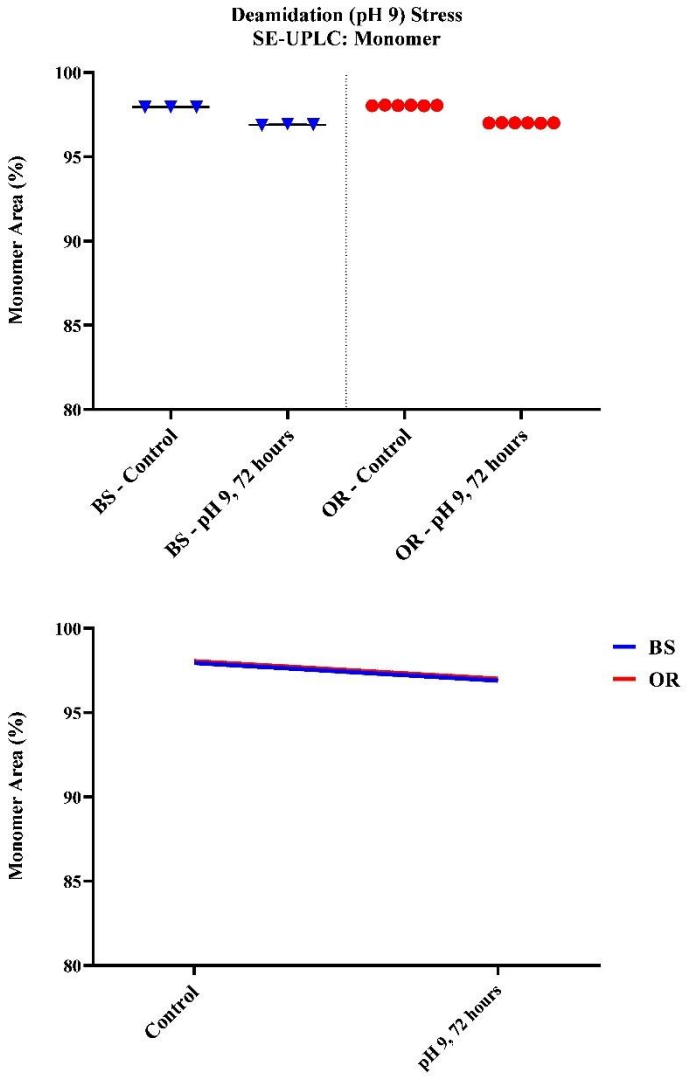

Figure 55: pH 9 basic stress, monomer area % results obtained by SE-UPLC. The results are grouped as mean ± SD (top) and linear curves (bottom).

Linear curves of the % area values of the samples subjected to pH 9 basic stress were formed, and the slopes of the obtained BS and OR linear curves were compared. The differences between monomer % area slopes and HMW % area slopes are not significant (p=0.7125 and p=0.1178, respectively.) Curves are given in Figure 55 for monomer and Figure 56 for HMW.

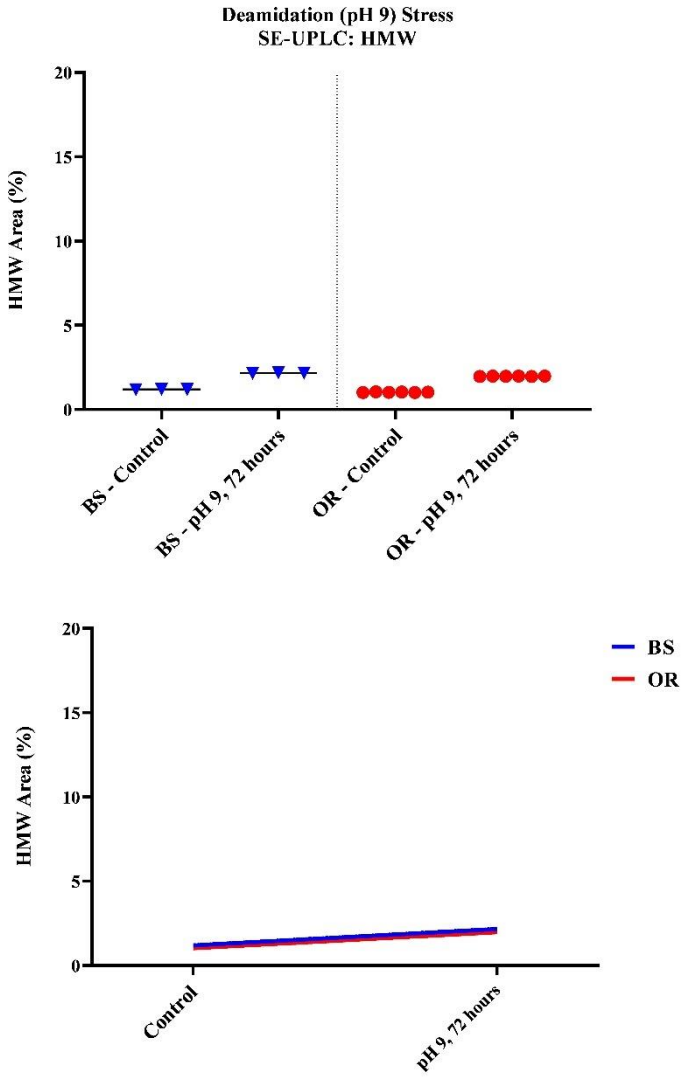

Figure 56: pH 9 basic stress, HMW area % results obtained by SE-UPLC. The results are grouped as mean ± SD (top) and linear curves (bottom).

Overlaying SE-UPLC chromatograms of pH 9 basic stressed BS and OR samples, stressed FB and unstressed BS and OR samples are given in Figure 57. No significant changes were observed in the chromatograms of the BS and OR samples.

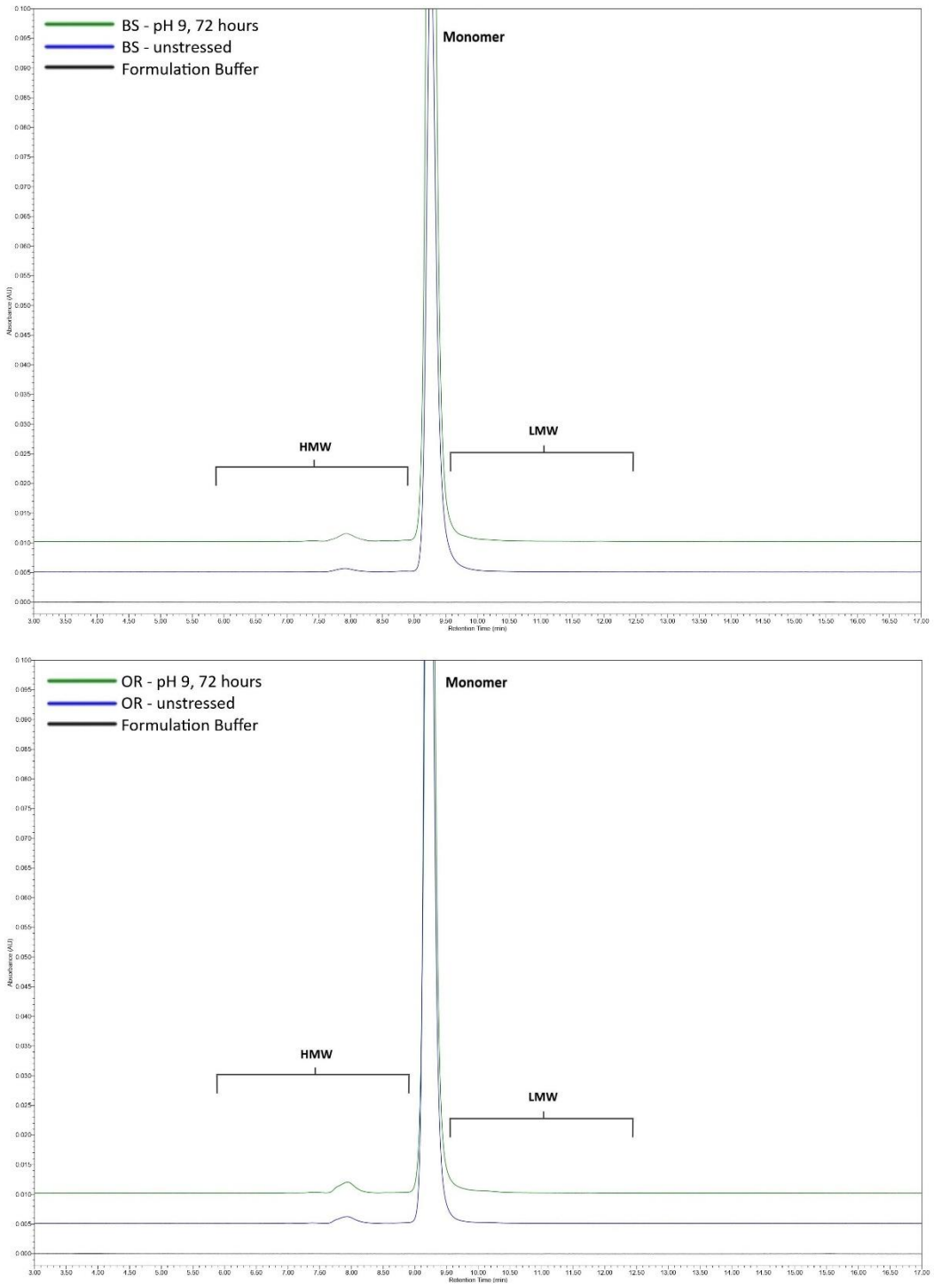

Figure 57: SE-UPLC chromatograms of BS (top) and OR (bottom) subjected to pH 9 basic stress

4.2.3.2 Imaged capillary isoelectric focusing (icIEF)

Duplicate results of the BS sample (n=2) and duplicate results of two different OR samples (n=4) were grouped and compared separately for the two pH conditions.

For BS and OR samples exposed to pH 4 acidic stress for 72 hours, the differences in mean main charge variant % area values and their controls were determined as 8.08% and 6.60%, respectively. The differences in mean acidic charge variant % area values between BS and OR samples and their controls were determined as 2.37% and 8.35%, respectively. The differences between the samples and controls were observed for the basic charge variant as 10.45% for BS and 14.95% for OR.

For the pH 4 acidic stress, linear curves of the BS and OR samples were generated and compared. The differences between the slopes are extremely significant for all charge variants ($p=0.002$ for the main charge variant, $p<0.0001$ for the acidic and the basic charge variants). The results and linear curves are given in Figure 58.

For BS and OR samples exposed to pH 9 basic stress for 72 hours, the differences in mean main charge variant % area values and their controls were determined as 3.72% and 4.03%, respectively. The differences in mean acidic charge variant % area values between BS and OR samples and their controls were determined as 3.89% and 4.12%, respectively. The differences between the samples and controls were observed for the basic charge variant as 0.17% for BS and 0.08% for OR.

For the pH 9 basic stress, linear curves of the charge variant % area values of the BS and OR samples were generated and compared. The differences between the slopes are not significant ($p=0.1937$ for the main charge variant, $p=0.5409$ for the acidic charge variant, and for the basic charge variant $p=0.8175$). The results and linear curves are given in Figure 59.

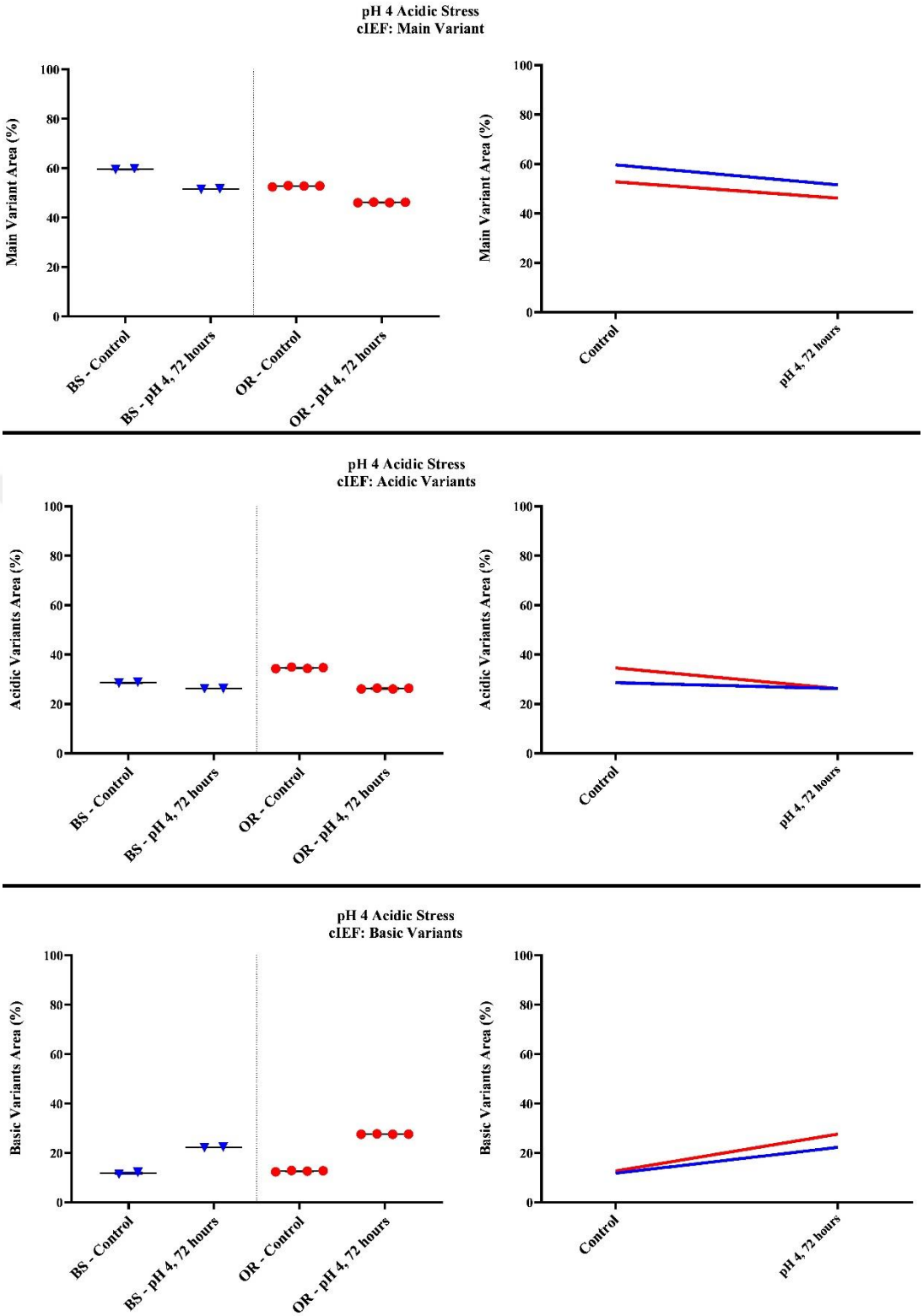

Figure 58: pH 4 acidic stress, charge variant area % results obtained by icIEF. The results are grouped as mean ± SD (left) and linear curves (right).

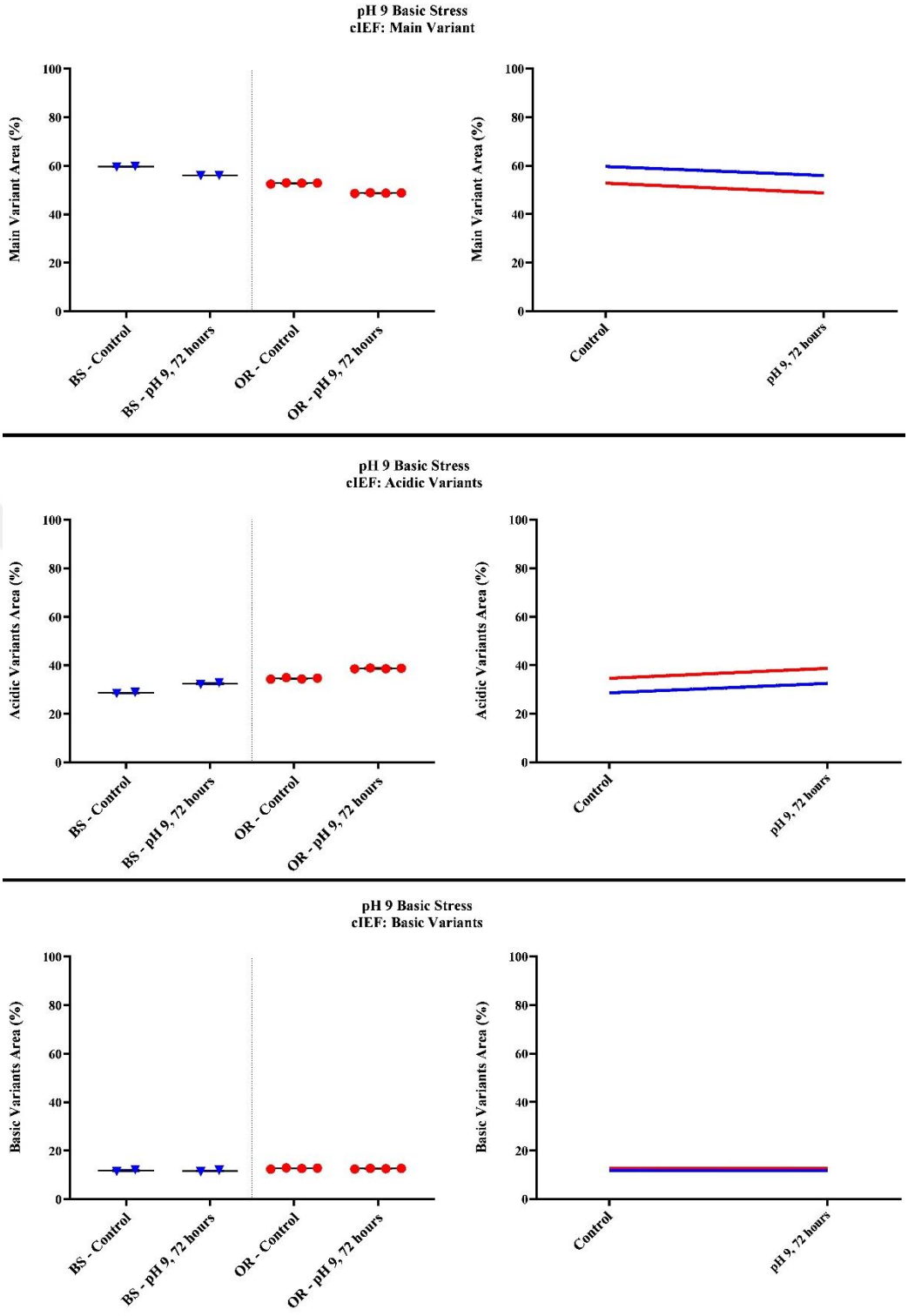

Figure 59: pH 9 basic stress, charge variant area % results obtained by icIEF. The results are grouped as mean ± SD (left) and linear curves (right).

Overlaying icIEF electrograms of pH 4 acidic stressed BS and OR samples, stressed FB and unstressed BS and OR samples are given in Figure 60. It is observed that the amount of basic charge variants increased while the main and acidic charge variants decreased in stressed BS and OR samples compared to the controls.

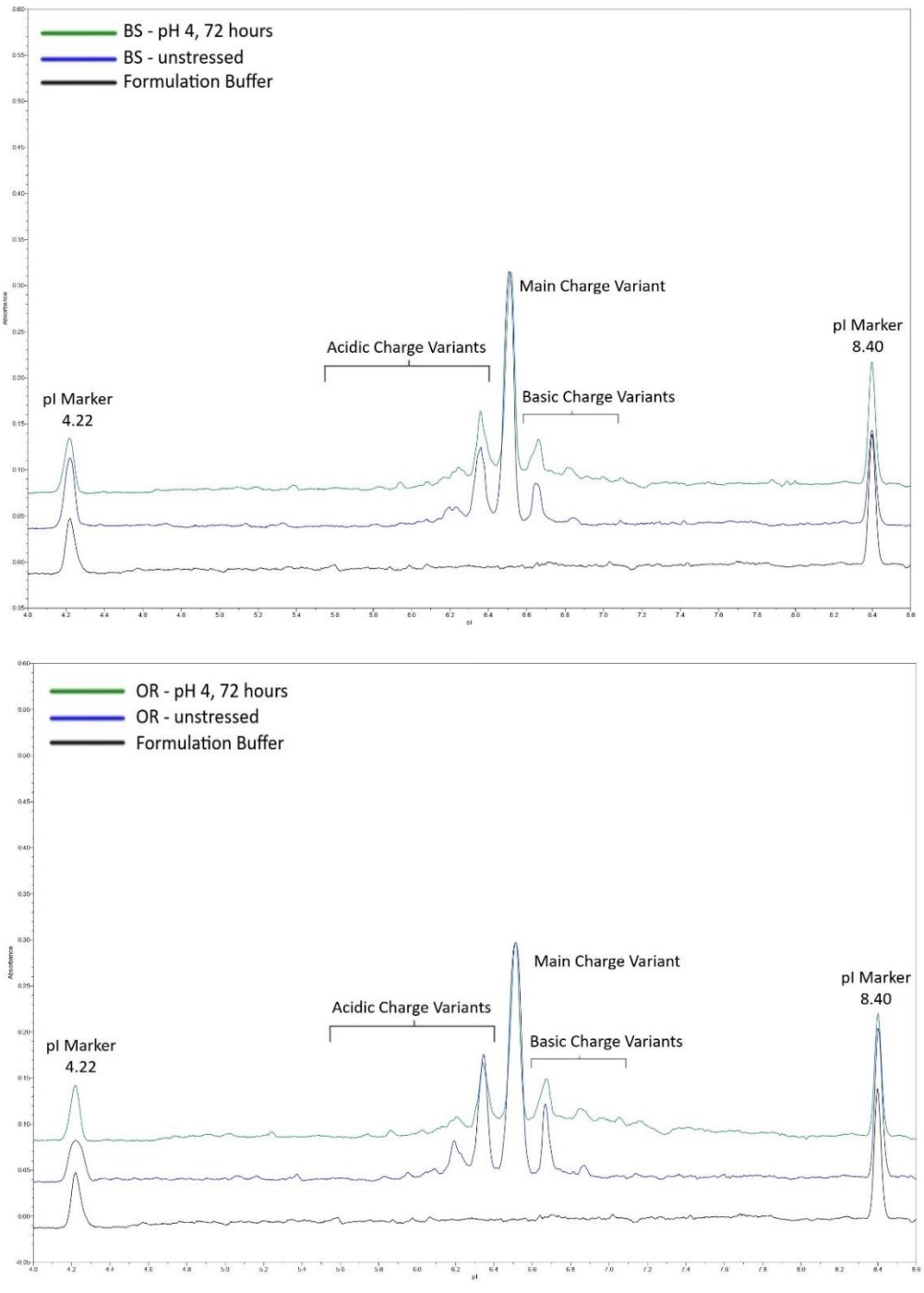

Figure 60: icIEF electrograms of BS (top) and OR (bottom) for pH 4 acidic stress

Overlaying icIEF electrograms of pH 9 basic stressed BS and OR samples, stressed FB and unstressed BS and OR samples are given in Figure 61. It is observed that the amount of acidic variant increased, and the amount of main charge variant decreased in BS and OR samples after pH 9 stress application.

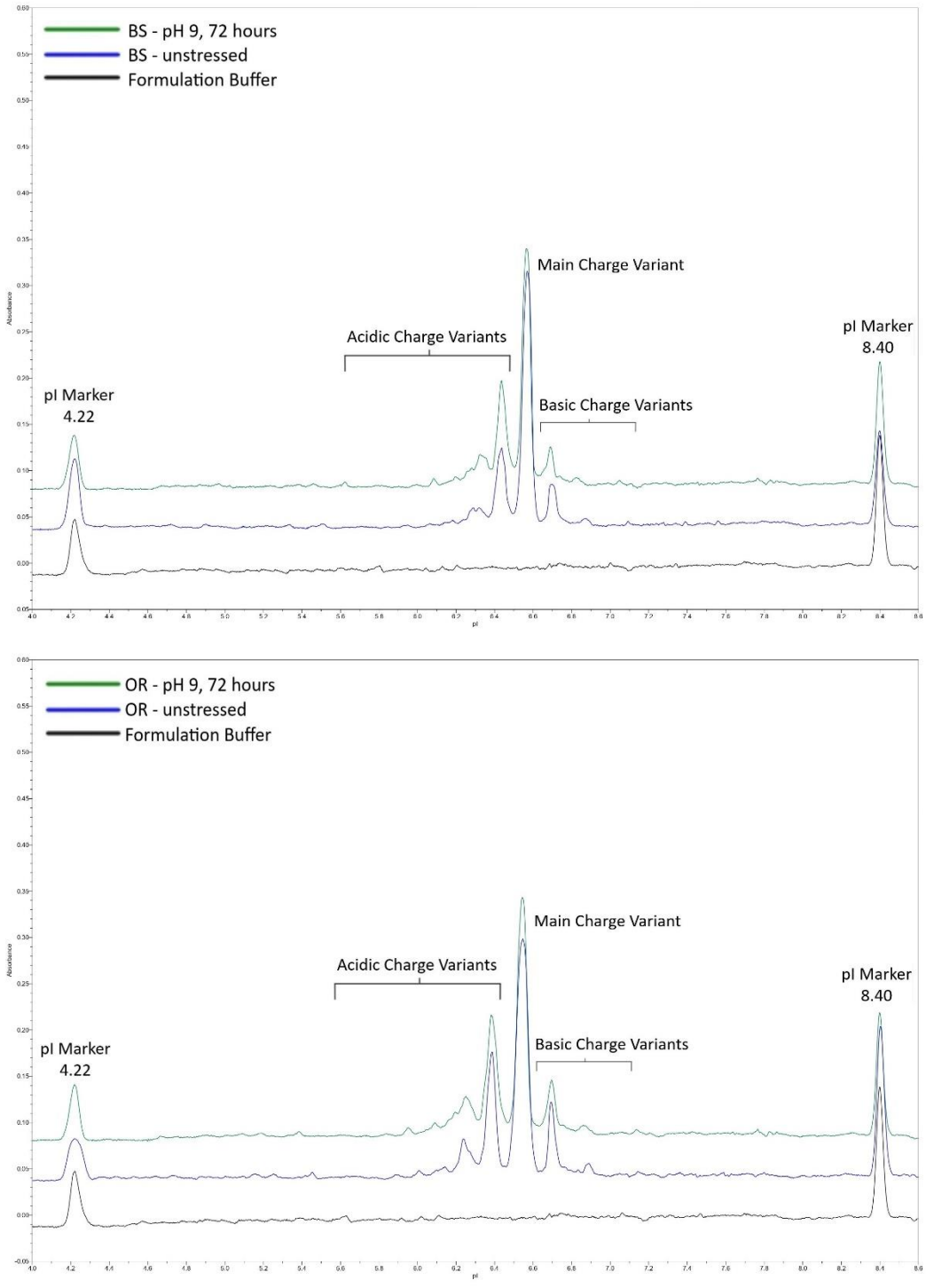

Figure 61: icIEF electrograms of BS (top) and OR (bottom) for pH 9 basic stress

4.2.3.3 Capillary Electrophoresis-Sodium Dodecyl Sulfate (CE-SDS)

4.2.3.3.1 Reduced CE-SDS

Triplicate results of the BS sample (n=3) and triplicate results of two different OR samples (n=6) were grouped and compared.

The differences in LC+HC % area values between BS and OR exposed to pH 4 acidic stress and their controls were determined as 2.30% and 2.22%, respectively. The slopes of the obtained BS and OR linear curves were compared and are given in Figure 62. The differences between the slopes are not significant (p=0.1636).

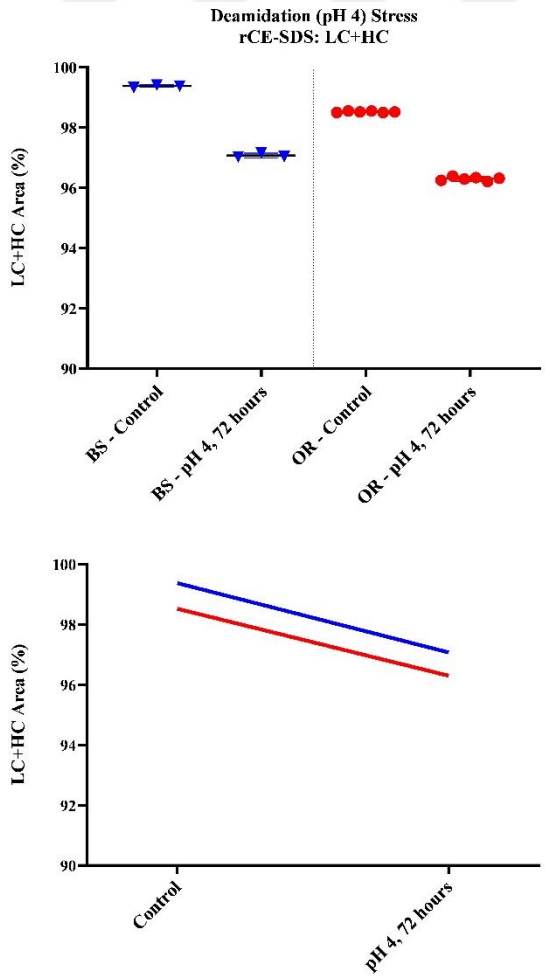

Figure 62: pH 4 acidic stress, LC+HC area % results obtained by rCE-SDS. The results are grouped as mean ± SD (top) and linear curves (bottom).

Overlaying rCE-SDS electrograms of pH 4 acidic stressed BS and OR samples, stressed FB, and unstressed BS and OR samples are given in Figure 63. It is seen that the amount of LC+HC decreased, and the level of impurities increased in BS and OR samples.

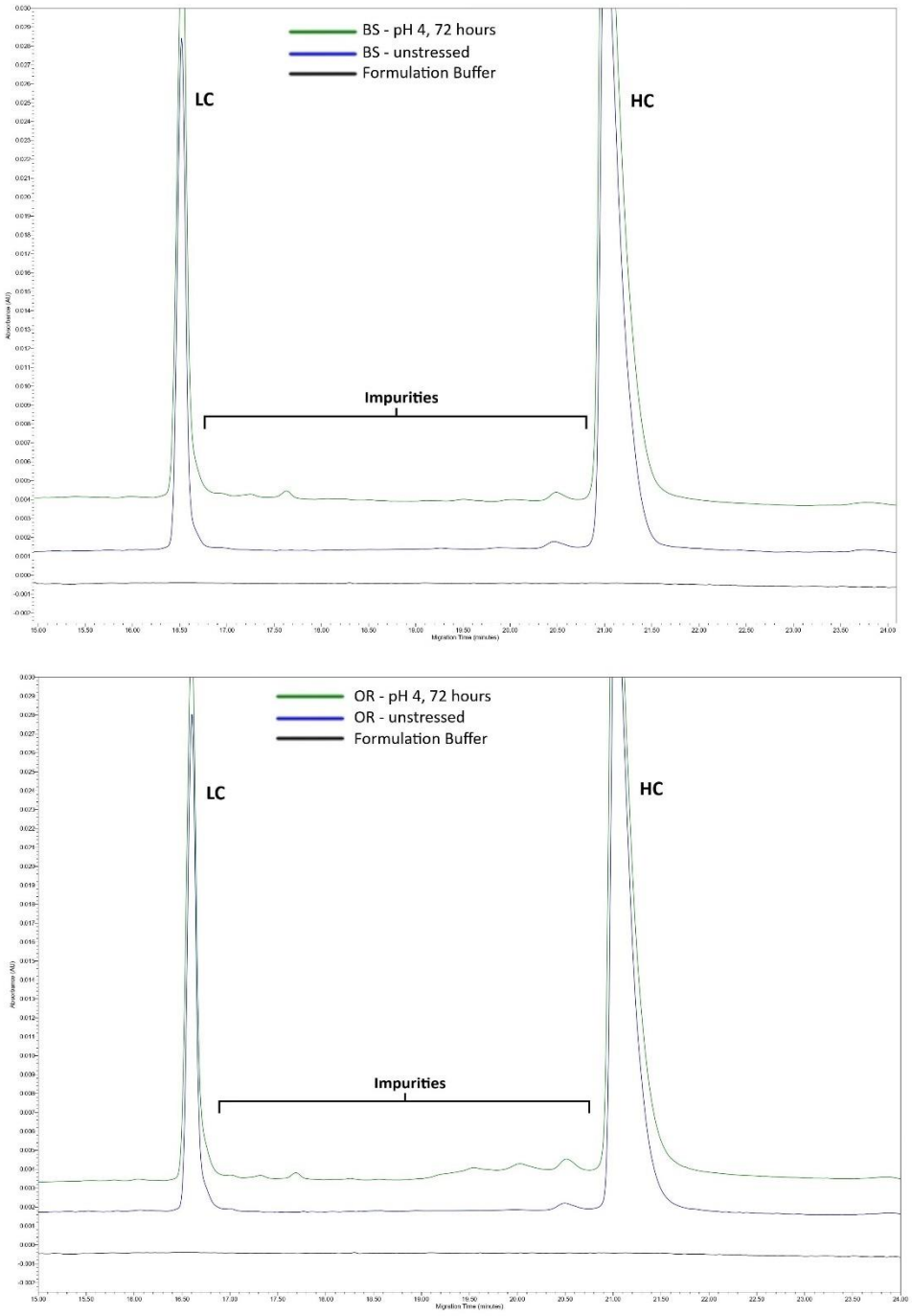

Figure 63: rCE-SDS electrograms of BS (top) and OR (bottom) for pH 4 acidic stress

The differences in mean LC+HC % area values between BS and OR samples exposed to pH 9 basic stress and their controls were determined as 1.67% and 1.96%, respectively. Linear curves of the LC+HC % area values of the samples were generated separately. The slopes of the obtained BS and OR linear curves were compared. The differences between the slopes are not significant (p=0.1246). Curves are given in Figure 64.

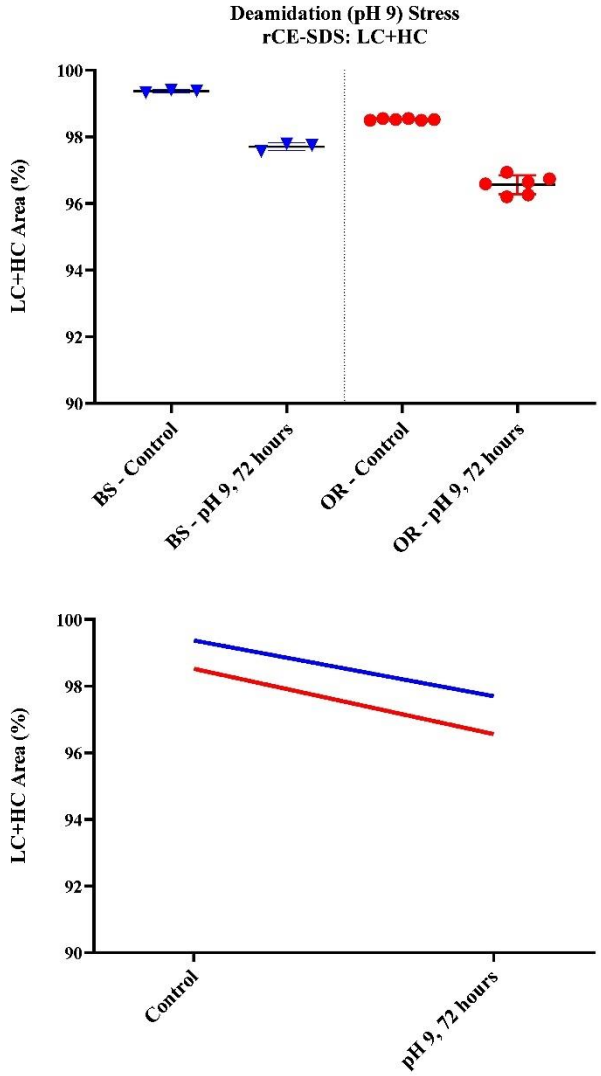

Figure 64: pH 9 basic stress, LC+HC area % results obtained by rCE-SDS. The results are grouped as mean ± SD (top) and linear curves (bottom).

Overlaying rCE-SDS electrograms of pH 9 basic stressed BS and OR samples, stressed FB, and unstressed BS and OR samples are given in Figure 65. It is seen that the amount of LC+HC decreased, and the level of impurities increased in BS and OR samples.

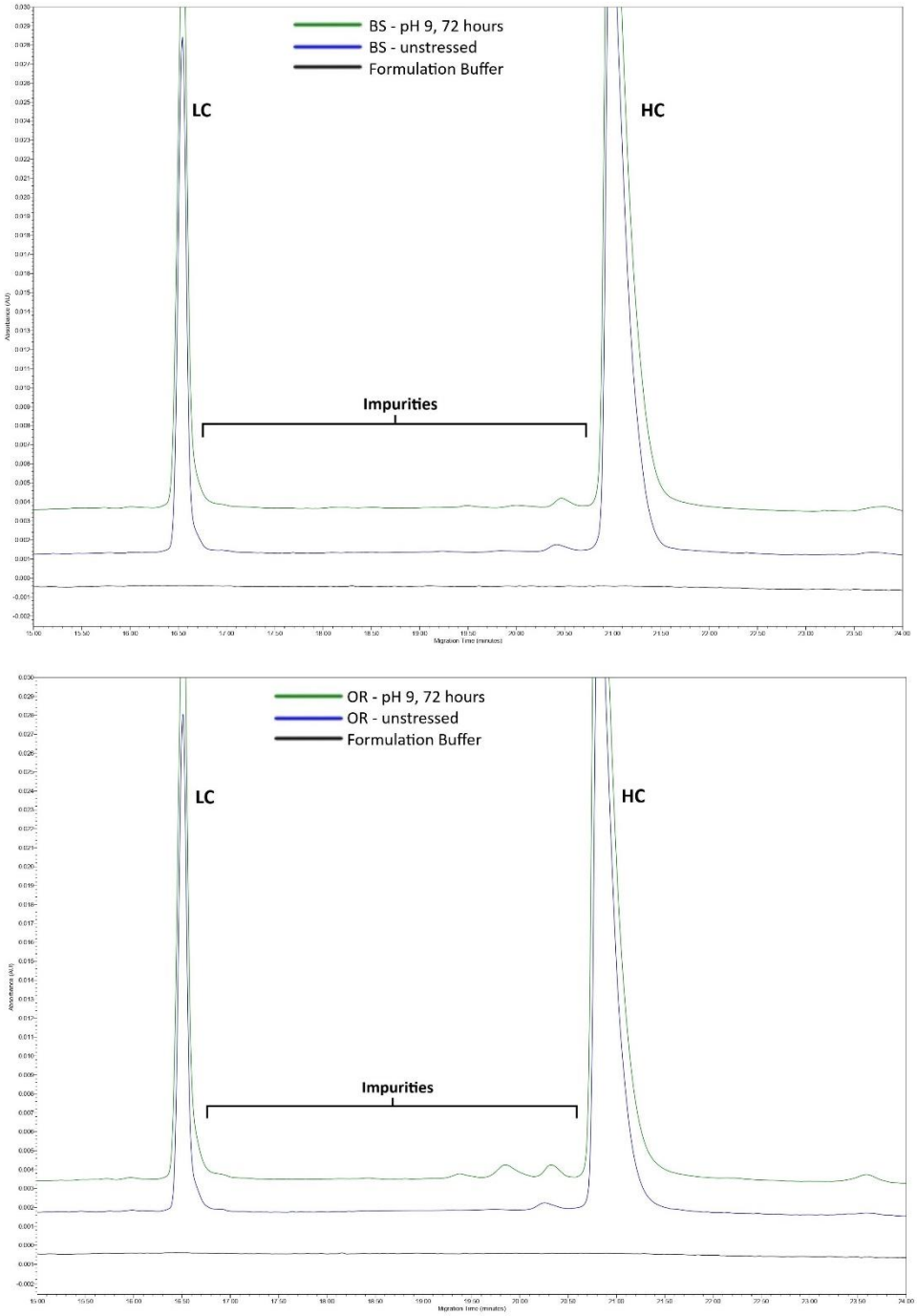

Figure 65: rCE-SDS electrograms of BS (top) and OR (bottom) for pH 9 basic stress

4.2.3.3.2 Non-Reduced CE-SDS

Triplicate results of the BS sample (n=3) and triplicate results of two different OR samples (n=6) were grouped and compared.

The differences in mean IgG % area values between BS and OR exposed to pH 4 acidic stress and their controls were determined as 0.98% and 1.16%, respectively. Linear curves of the IgG % area values of the samples were generated separately. The slopes of the obtained BS and OR linear curves were compared and are given in Figure 66. The differences between the slopes are not quite significant (p=0.0896).

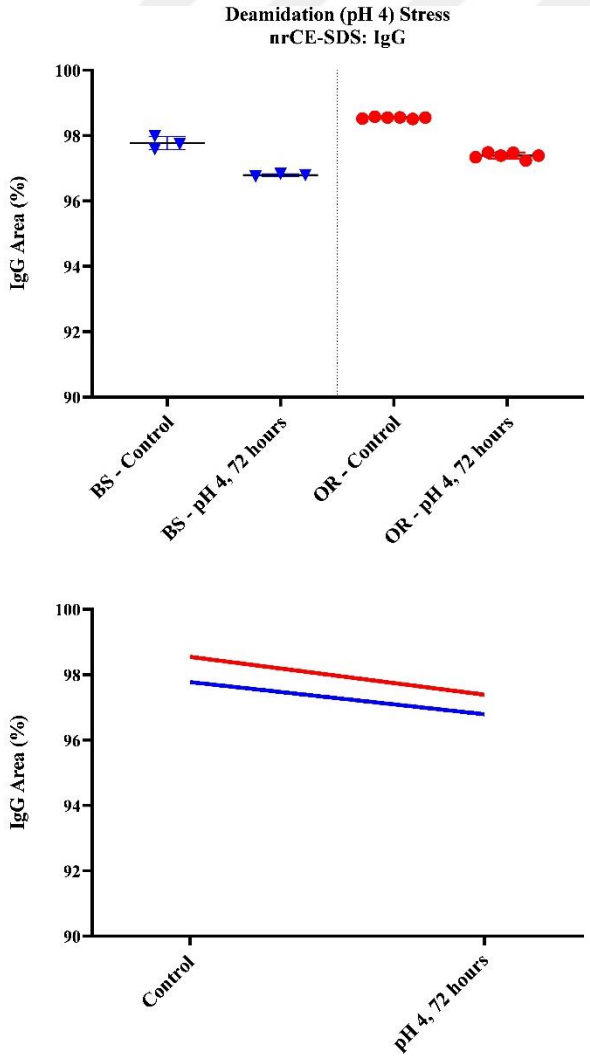

Figure 66: pH 4 acidic stress, IgG area % results obtained by nrCE-SDS. The results are grouped as mean ± SD (top) and linear curves (bottom).

Overlaying nrCE-SDS electrograms of pH 4 acidic stressed BS and OR samples, stressed FB, and unstressed BS and OR samples are given in Figure 67.

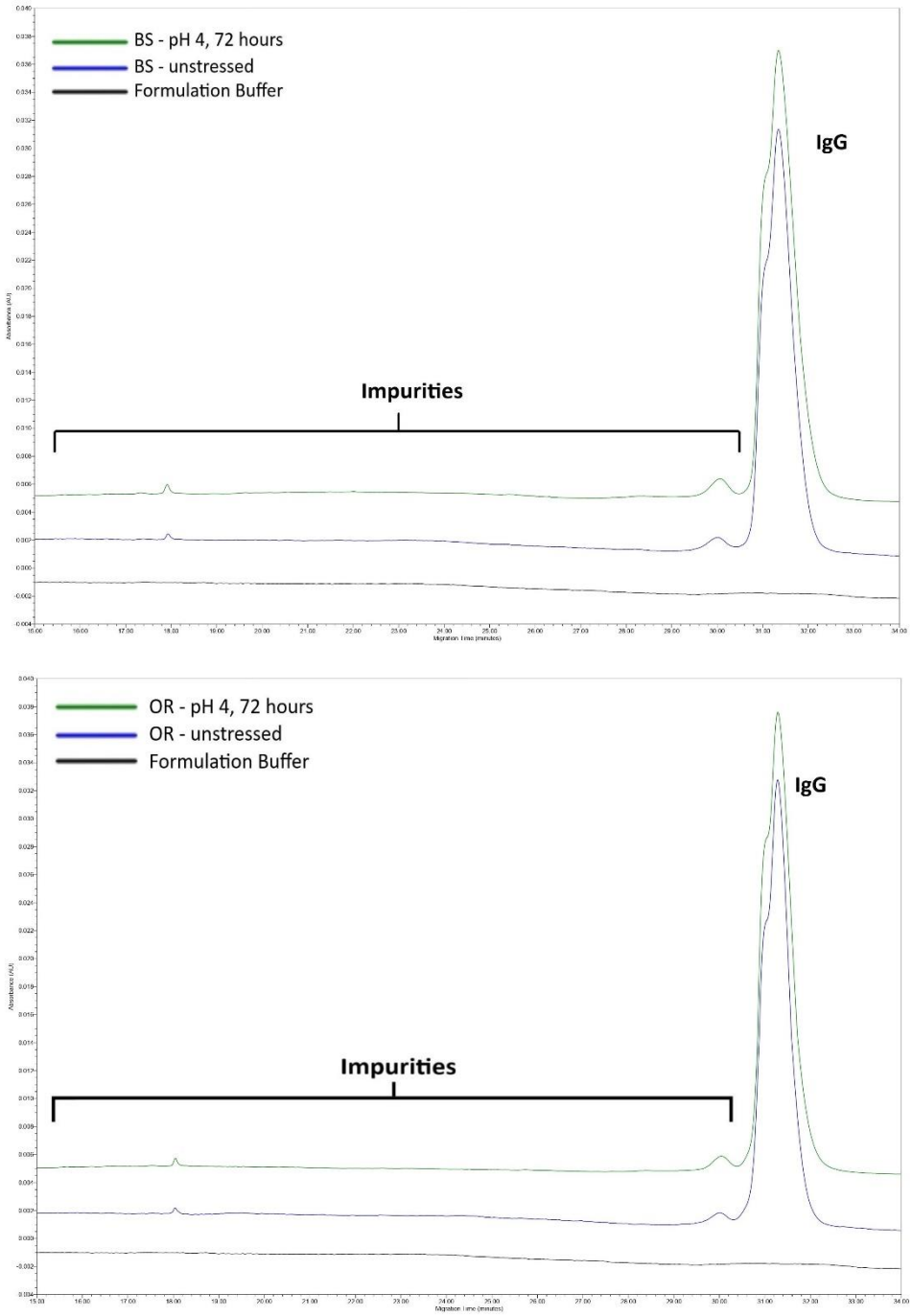

Figure 67: nrCE-SDS electrograms of BS (top) and OR (bottom) for pH 4 stress

The differences in mean IgG % area values between BS and OR samples exposed to pH 9 basic stress and their controls were determined as 0.60% and 0.77%, respectively. Linear curves of the IgG % area values of the samples were generated separately. The slopes of the obtained BS and OR linear curves were compared. The differences between the slopes are not quite significant (p=0.0598). Curves are given in Figure 68.

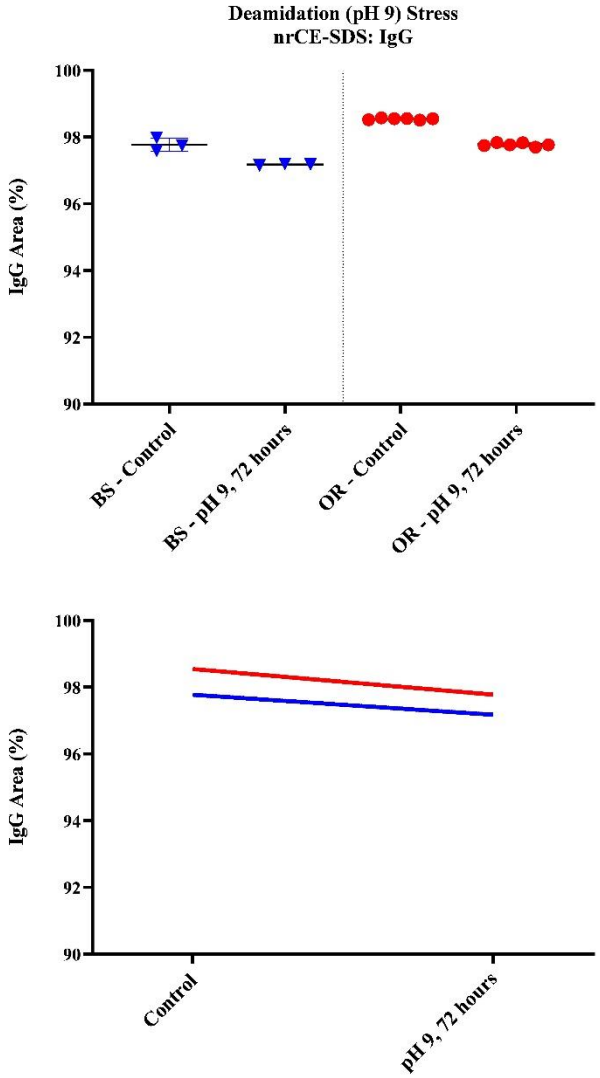

Figure 68: pH 9 basic stress, IgG area % results obtained by nrCE-SDS. The results are grouped as mean ± SD (top) and linear curves (bottom).

Overlaying nrCE-SDS electrograms of pH 9 basic stressed BS and OR samples, stressed FB, and unstressed BS and OR samples are given in Figure 69.

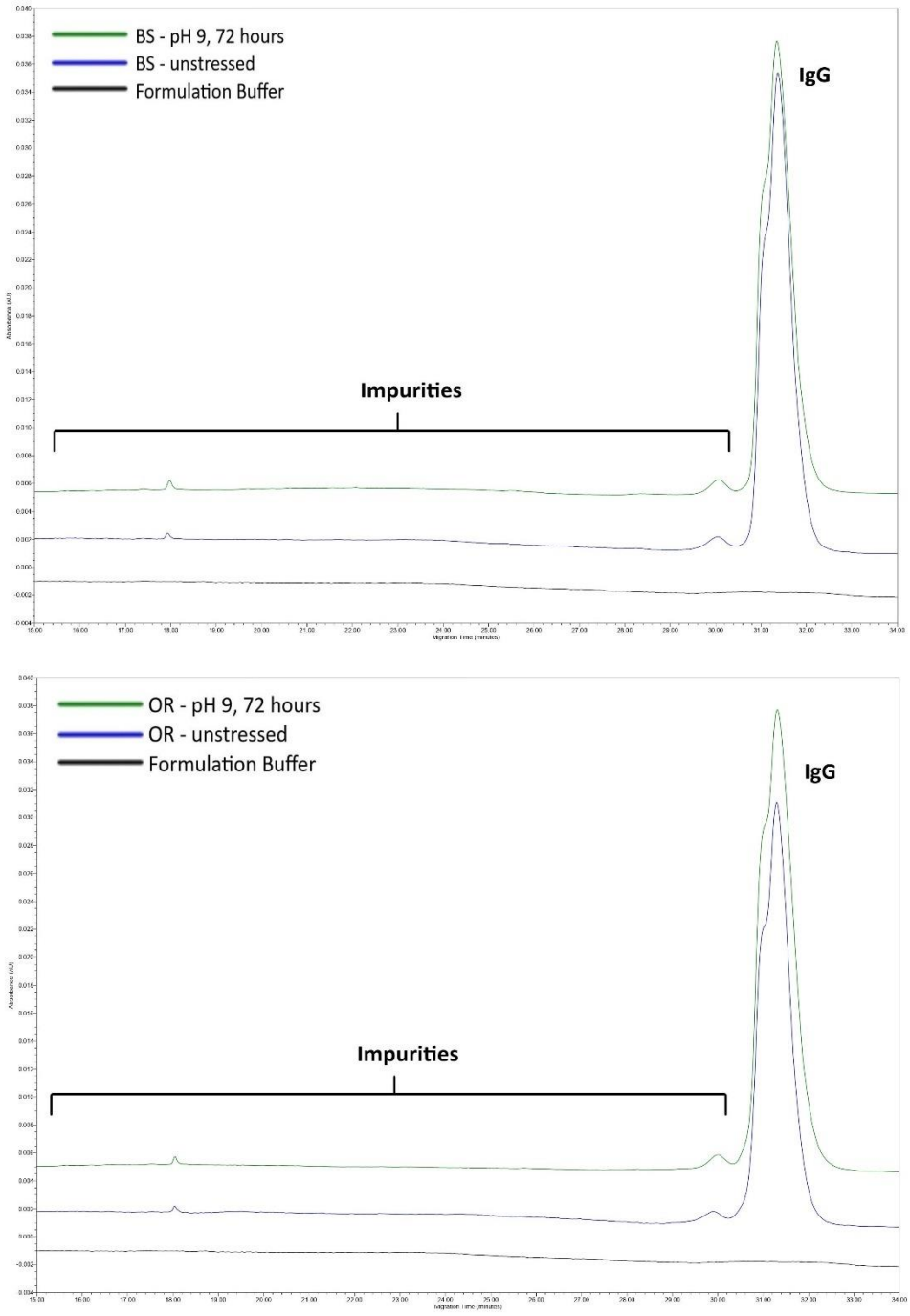

Figure 69: nrCE-SDS electrograms of BS (top) and OR (bottom) for pH 4 acidic stress

4.2.3.4 Complement assay

Relative potencies were evaluated by the complement assay (ELISA), which quantitates the amount of neoantigen (C5b-C9) in the presence of human serum.

As it was the harshest condition, only pH 4 acidic stress samples were analyzed. Percent of the relative potency of the acidic stressed BS and OR was calculated against the unstressed BS as an interim reference standard.

Relative potency results for the BS and OR samples show similar results to each other. The results are given in Table 21.

Table 21: pH 4 acidic stress % relative potency results for BS and OR samples.

Sample Name	**% Relative Potency**	**Average % Relative Potency**
BS (unstressed)	NA	
BS - pH 4 acidic stress, 72 hours	87.55%	
OR lot #1 - pH 4 acidic stress, 72 hours	85.43%	OR - pH 4 acidic stress, 72 hours 87.61%
OR lot #2 - pH 4 acidic stress, 72 hours	89.79%	

4.2.4 Freeze/thaw stress

In freeze/thaw study, aliquoted samples were cooled from 2-8˚C to ≤-65˚C, held at ≤-65˚C for two hours, thawed to 2-8˚C, and stored for two hours at 2-8˚C. The freeze/thaw cycle was repeated five times in total. After five freeze-thaw cycles, SE-UPLC, rCE-SDS, nrCES-SDS and icIEF analyzes were performed. A summary of the analyzes performed is given in Table 22.

Table 22: Freeze/thaw stress % area results for BS and OR samples. Percentages are given as mean ± SD.

Freeze/Thaw Stress		**BS**			**OR**		
		Control	5 Cycle F&T	p-value	Control	5 Cycle F&T	p-value
SE-UPLC	Monomer	97.94 ±0.01	91.92 ±0.01	0.0769	98.05±0.02	92.05±0.01	0.0068*
	HMW	1.19 ±0.01	7.22 ±0.01	0.0767	1.03±0.02	7.08±0.01	0.0068*
CE-SDS	rCE-SDS LC+HC	99.37 ±0.04	98.42 ±0.23	0.2155	98.52 ±0.02	97.58 ±0.17	0.0187*
	nrCE-SDS IgG	97.77 ±0.02	97.26 ±0.06	0.5022	98.55 ±0.03	97.89 ±0.06	0.0461*
icIEF	Main Variants	59.63 ±0.24	57.63 ±0.01	>0.9999	52.76 ±0.21	51.18 ±0.16	0.2333
	Acidic Variants	28.59 ±0.30	30.17 ±0.03	>0.9999	34.57 ±0.29	35.76 ±0.14	0.2333
	Basic Variants	11.79 ±0.53	12.21 ±0.04	>0.9999	12.67 ±0.23	13.07 ±0.03	0.2333

*Statistically meaningful

No significant differences were observed for BS sample compared to the control sample for all analyzes. Significant differences were observed for OR samples in all analyzes compared to the control except the icIEF results.

4.2.4.1 Size Exclusion Ultra-Performance Liquid Chromatography (SE-UPLC)

Triplicate results of the BS sample (n=3) and triplicate results of two different OR samples (n=6) were grouped and compared.

The differences between the mean monomer % area values of the BS and OR, which were subjected to 5-cycle freeze/thaw stress, from their control monomer % area value, were determined as 6.02% and 6.00%, respectively. The differences in mean HMW % area values between BS and OR exposed to freeze/thaw stress and their controls were determined as 6.03% and 6.05%, respectively.

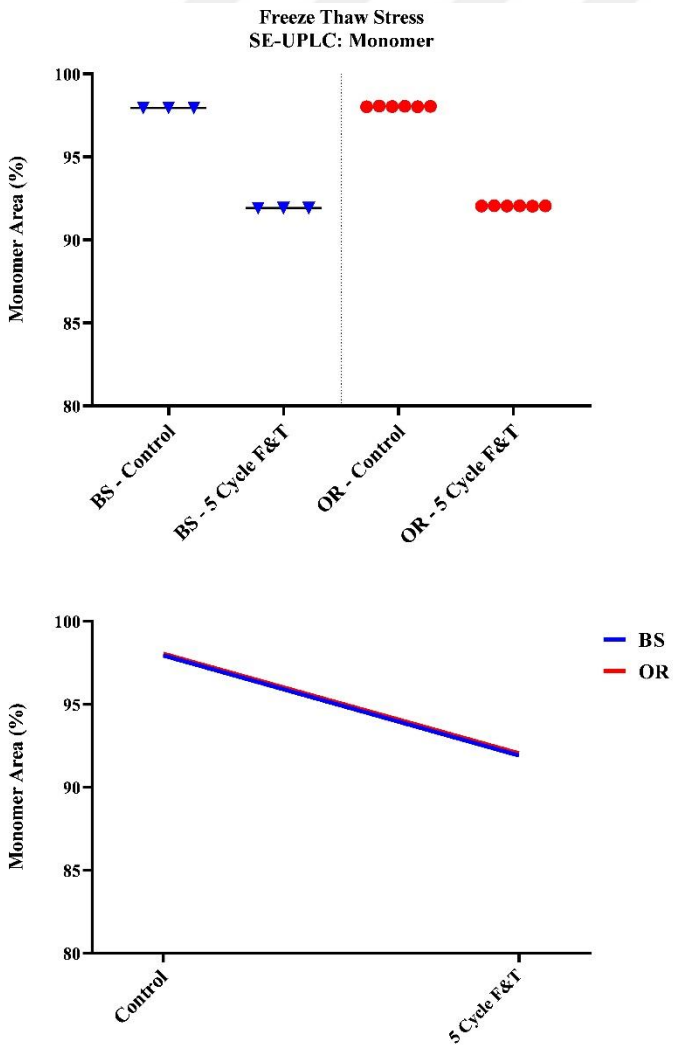

Figure 70: Freeze/thaw stress, monomer area % results obtained by SE-UPLC. The results are grouped as mean ± SD (top) and linear curves (bottom).

Linear curves of the monomer % area values of the freeze and thaw stress applied samples were generated separately and are given in Figure 70. The slopes of the obtained BS and OR linear curves were compared. The differences between the slopes are not quite significant (p=0.0561). The slopes of the linear curves of the HMW % area values of the samples subjected to freeze and thaw stress were compared. The differences between the slopes are not significant (p=0.1984). Curves are given in Figure 71.

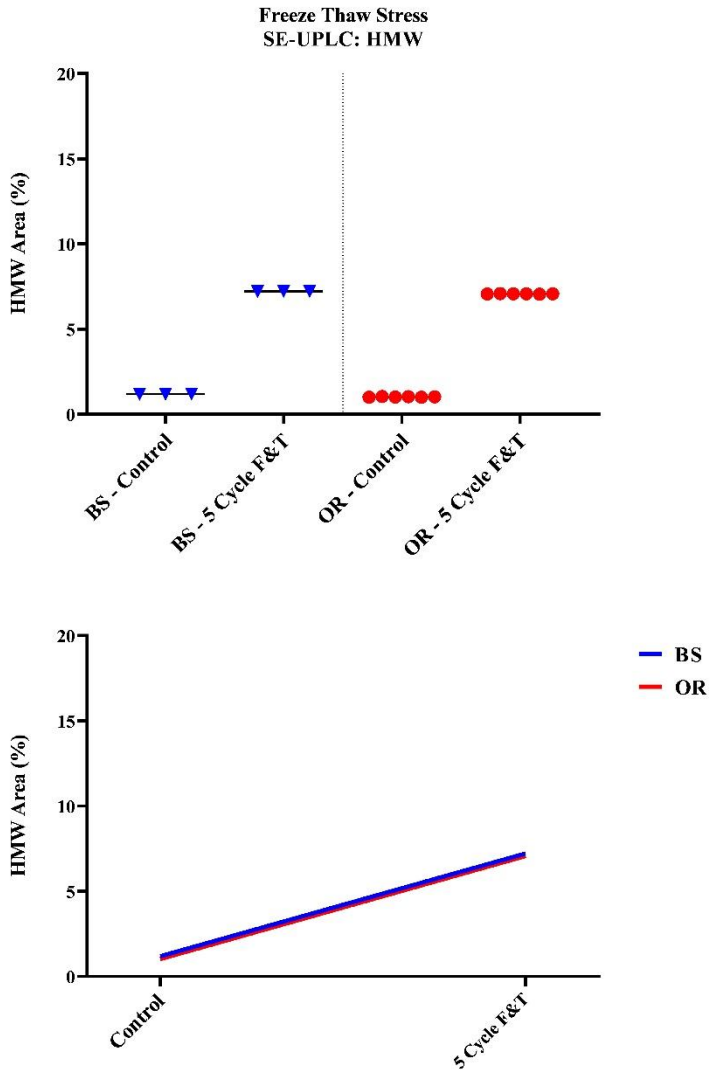

Figure 71: Freeze/thaw stress, HMW area % results obtained by SE-UPLC. The results are grouped as mean ± SD (top) and linear curves (bottom).

Overlaying SE-UPLC chromatograms of freeze/thaw stressed BS and OR samples, stressed FB and unstressed BS and OR samples are given in Figure 72. In BS and OR samples, it is observed that the amount of HMW increases.

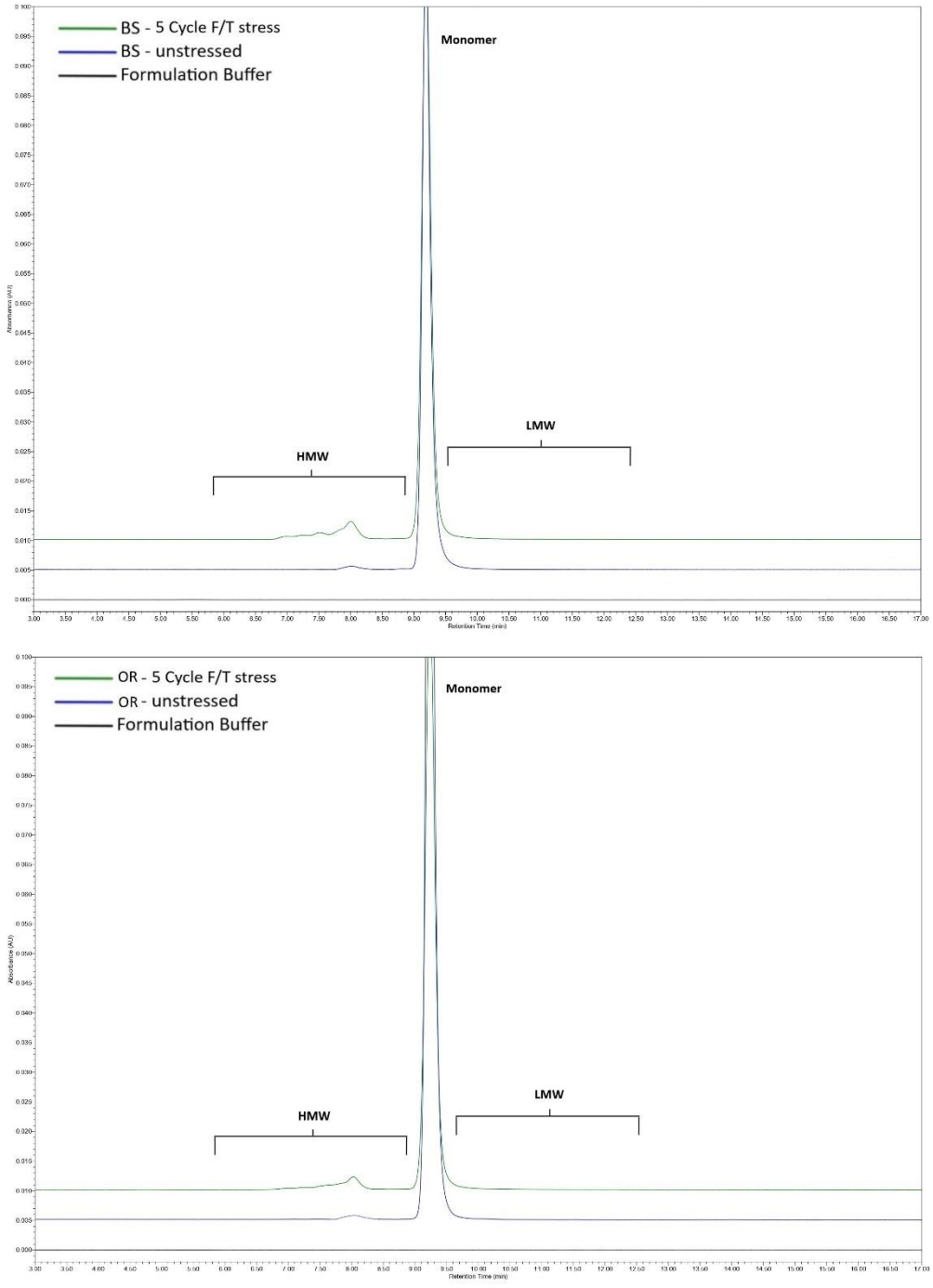

Figure 72: SE-UPLC chromatograms of BS (top) and OR (bottom) subjected to freeze/thaw stress

4.2.4.2 Imaged Capillary Isoelectric Focusing (icIEF)

Duplicate results of the BS sample (n=2) and duplicate results of two different OR samples (n=4) were grouped and compared separately for the 5-cycle freeze and thaw stress.

The differences in mean main charge variant % area values between BS and OR samples exposed to freeze and thaw stress for 5 cycles and their controls were determined as 2.00% and 1.58%, respectively. Linear curves of the BS and OR samples were generated and compared. The differences between the slopes are not quite significant (p=0.0936). The results and linear curves are given in Figure 73.

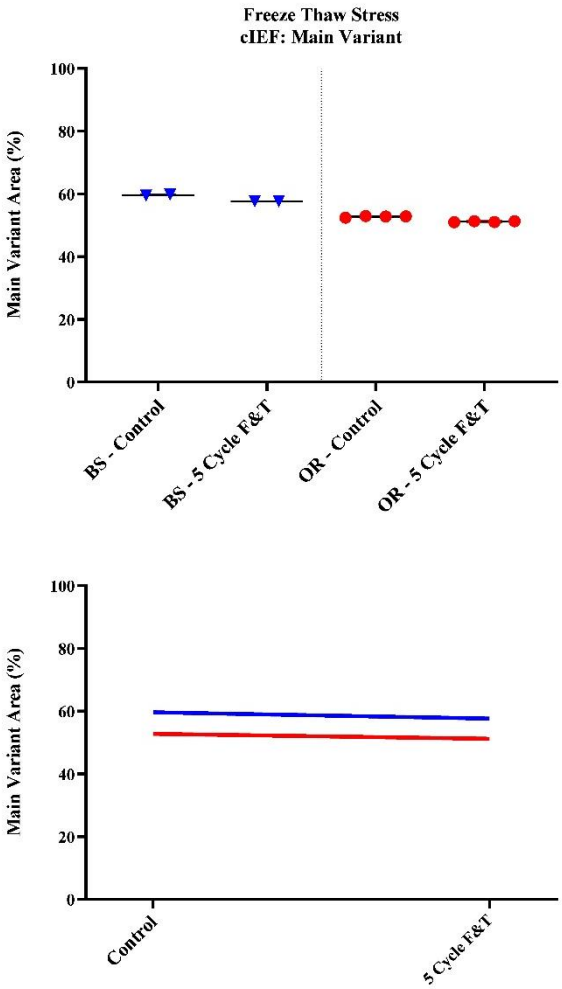

Figure 73: Freeze/thaw stress, main charge variant area % results obtained by icIEF. The results are grouped as mean ± SD (top) and linear curves (bottom).

The differences in mean acidic charge variant % area values between BS and OR samples exposed to freeze and thaw stress for 5 cycles and their controls were determined as 1.58% and 1.19%, respectively. Linear curves of the BS and OR samples were generated and compared. The differences between the slopes are not significant (p=0.1905). The results and linear curves are given in Figure 74.

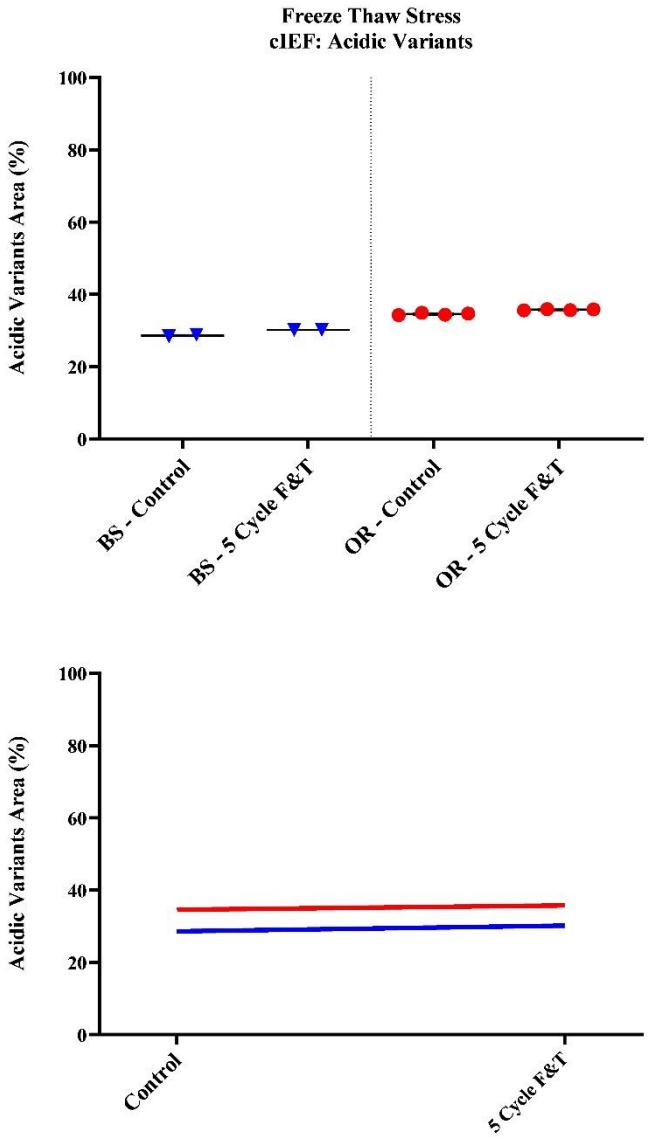

Figure 74: Freeze/thaw stress, acidic charge variant area % results obtained by icIEF. The results are grouped as mean ± SD (top) and linear curves (bottom).

The differences in mean basic charge variant % area values between BS and OR samples exposed to freeze and thaw stress for 5 cycles and their controls were determined as 0.42% and 0.40%, respectively. Linear curves of the BS and OR samples were generated and compared. The differences between the slopes are not quite significant (p=0.9333). The results and linear curves are given in Figure 75.

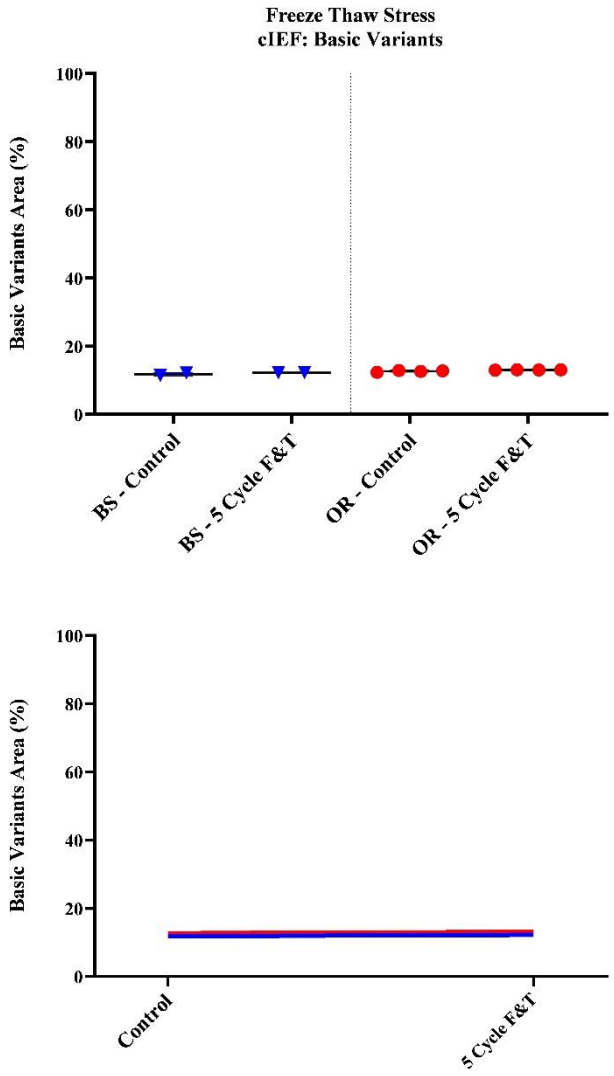

Figure 75: Freeze/thaw stress, basic charge variant area % results obtained by icIEF. The results are grouped as mean ± SD (top) and linear curves (bottom).

Overlaying icIEF electrograms of freeze/thaw BS and OR samples, stressed FB and unstressed BS and OR samples are given in Figure 76. In stressed BS and OR samples, it is observed that the amount of acidic and basic charge variants slightly increased.

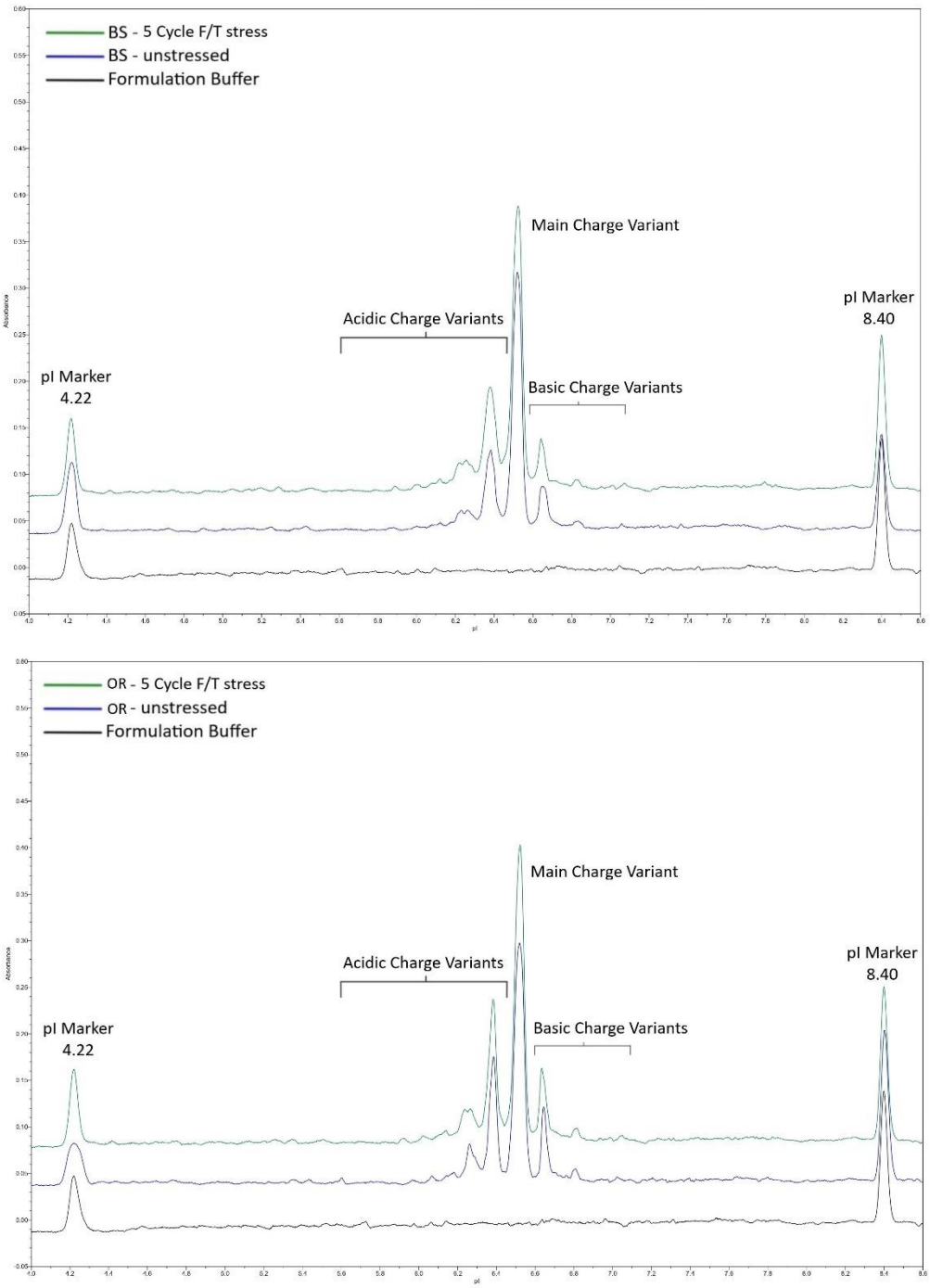

Figure 76: icIEF electrograms of BS (top) and OR (bottom) for freeze/thaw stress

4.2.4.3 Capillary Electrophoresis-Sodium Dodecyl Sulfate (CE-SDS)

4.2.4.3.1 Reduced CE-SDS

Triplicate results of the BS sample (n=3) and triplicate results of two different OR samples (n=6) were grouped and compared.

The differences in mean LC+HC % area values between BS and OR samples exposed to F/T stress for 5 cycles and their controls were determined as 0.95% and 0.94%, respectively. Linear curves of the F/T stress-applied samples were generated and are given in Figure 77. The slopes of the obtained BS and OR linear curves were compared. The differences between the slopes are not significant (p=0.9223).

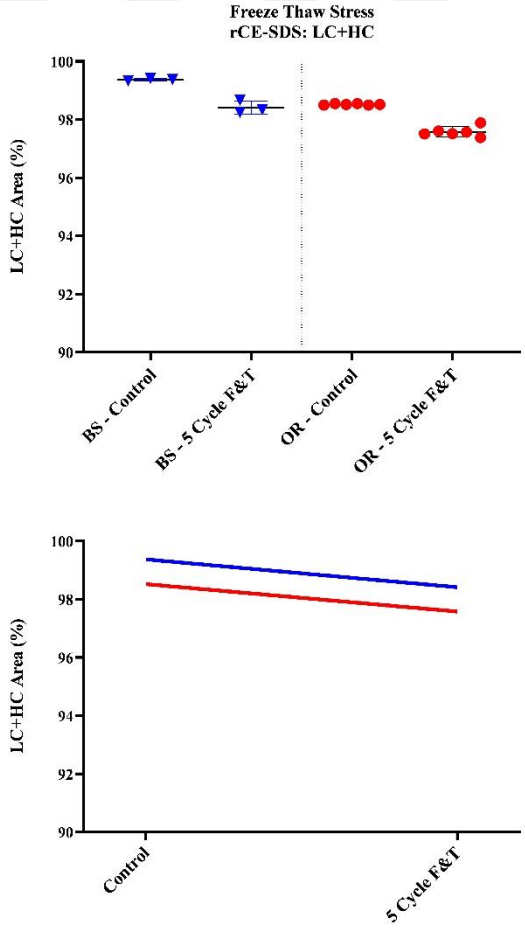

Figure 77: Freeze/thaw stress, LC+HC area % results obtained by rCE-SDS. The results are grouped as mean ± SD (top) and linear curves (bottom).

Overlaying rCE-SDS electrograms of F/T stressed BS and OR samples, stressed FB, and unstressed BS and OR samples are given in Figure 78. The amount of impurities is slightly increased in BS and OR samples.

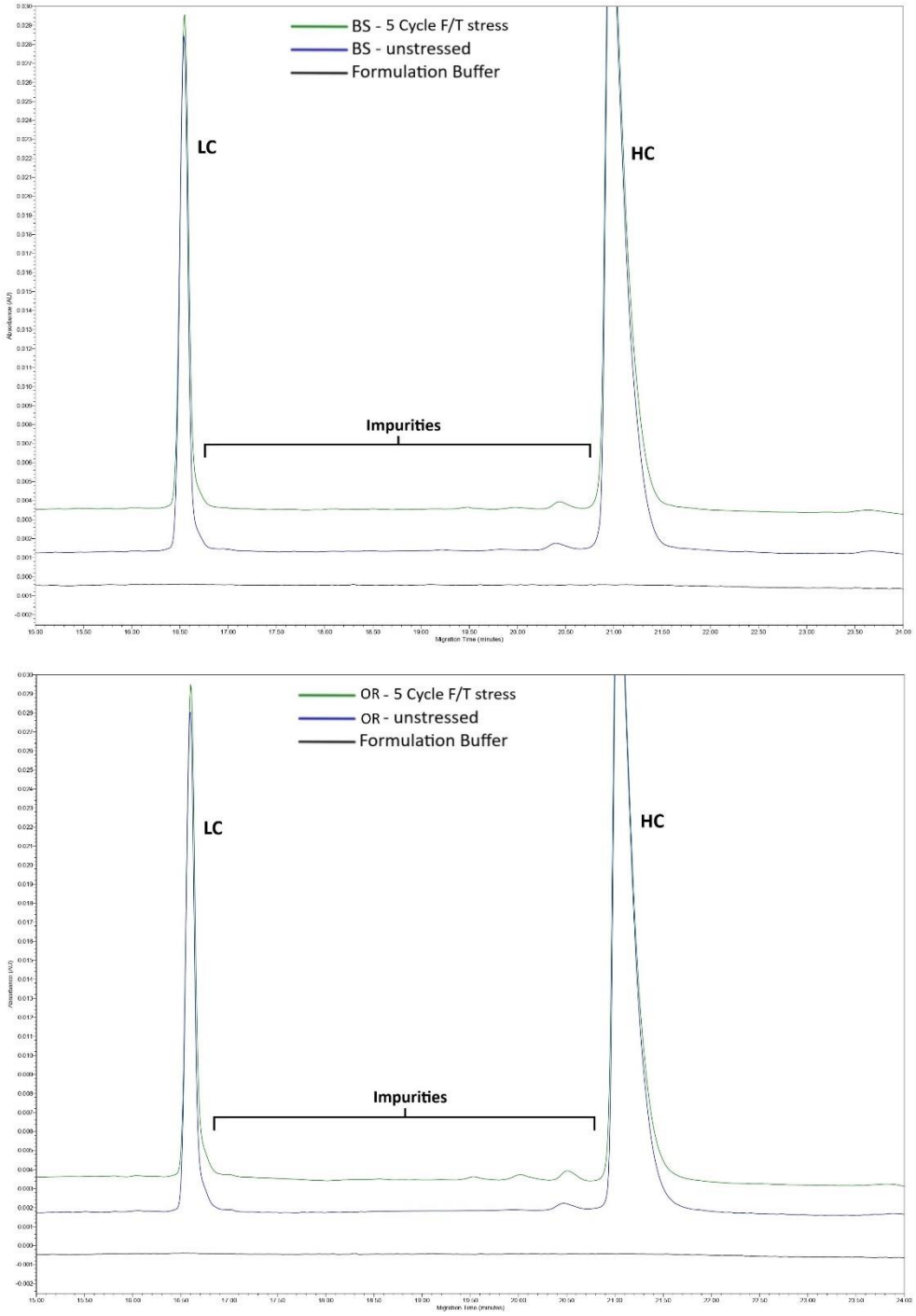

Figure 78: rCE-SDS electrograms of BS (top) and OR (bottom) for freeze/thaw stress

4.2.4.3.2 Non-Reduced CE-SDS

Triplicate results of the BS sample (n=3) and triplicate results of two different OR samples (n=6) were grouped and compared.

The differences in mean IgG % area values between BS and OR samples exposed to F/T stress and their controls were determined as 0.51 % and 0.66%, respectively. Linear curves of the IgG % area values of the F/T stress-applied samples were generated separately. The slopes of the obtained BS and OR linear curves were compared. The differences between the slopes are not significant (p=0.1368). Curves are given in Figure 79.

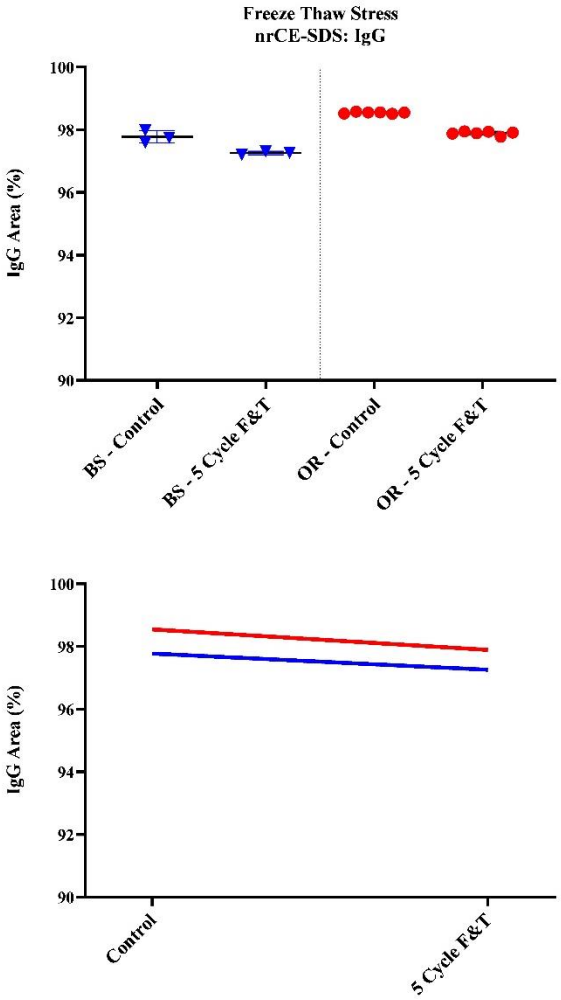

Figure 79: Freeze/thaw stress, IgG area % results obtained by nrCE-SDS. The results are grouped as mean ± SD (top) and linear curves (bottom).

Overlaying nrCE-SDS electrograms of F/T stressed BS and OR samples, stressed FB, and unstressed BS and OR samples are given in Figure 80. It is observed that the amount of IgG decreased in BS and OR samples.

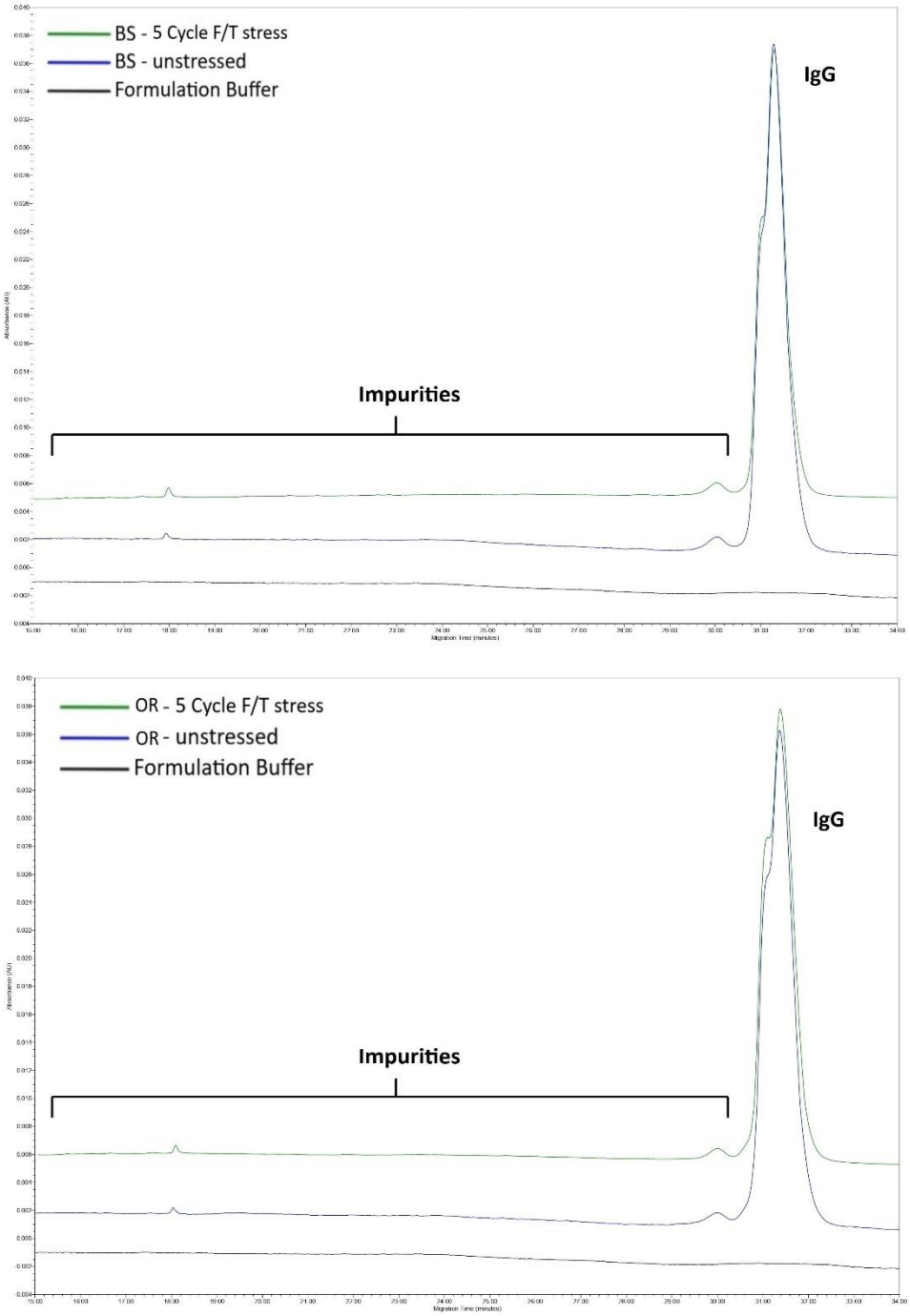

Figure 80: nrCE-SDS electrograms of BS (top) and OR (bottom) subjected to freeze/thaw stress

4.2.5 Oxidation stress

The oxidation stress was performed by incubation of the samples at RT. The samples were pulled for testing after 24 hours. The pulled samples were buffer exchanged back into FB and stored at 2-8˚C until analysis. SE-UPLC, rCE-SDS, nrCES-SDS, and icIEF analyzes were performed. The complement assay analysis provided additional information for the oxidation stress. A summary of the results of the performed analyses is given in Table 23.

Table 23: Oxidation stress % area results for BS and OR samples. Percentages are given as mean ± SD.

Oxidation Stress		**BS**			**OR**		
		Control	0.5% H_2O_2	p-value	Control	0.5% H_2O_2	p-value
SE-UPLC	Monomer	97.94 ±0.01	96.44 ±0.01	0.0775	98.05±0.02	96.79 ±0.19	0.0069*
	HMW	1.19 ±0.01	2.84 ±0.02	0.0775	1.03±0.02	2.42 ±0.21	0.0069*
CE-SDS	rCE-SDS LC+HC	99.37 ±0.04	98.48 ±0.06	0.1312	98.52 ±0.02	98.03 ±0.42	0.0216*
	nrCE-SDS IgG	97.77 ±0.02	91.21 ±0.07	0.0777	98.55 ±0.03	92.05 ±0.14	0.0070*
icIEF	Main Variants	59.63 ±0.24	47.53 ±0.27	0.1922	52.76 ±0.21	40.49 ±0.17	0.0372*
	Acidic Variants	28.59 ±0.30	40.46 ±0.11	0.1922	34.57 ±0.29	46.30 ±0.25	0.0372*
	Basic Variants	11.79 ±0.53	12.02 ±0.16	>0.9999	12.67 ±0.23	13.12 ±0.09	0.2333

*Statistically meaningful

No significant differences were observed for BS sample compared to the control sample for all analyzes. Significant differences were observed for OR samples in all analyzes compared to the control sample.

4.2.5.1 Size Exclusion Ultra-Performance Liquid Chromatography (SE-UPLC)

Triplicate results of the BS sample (n=3) and triplicate results of two different OR samples (n=6) were grouped and compared.

The differences in mean monomer % area values between BS and OR exposed to oxidation stress and their controls were determined as 1.50% and 1.26%, respectively. The differences in mean HMW % area values between stressed BS and OR samples and their controls were determined as 1.65% and 1.39%, respectively.

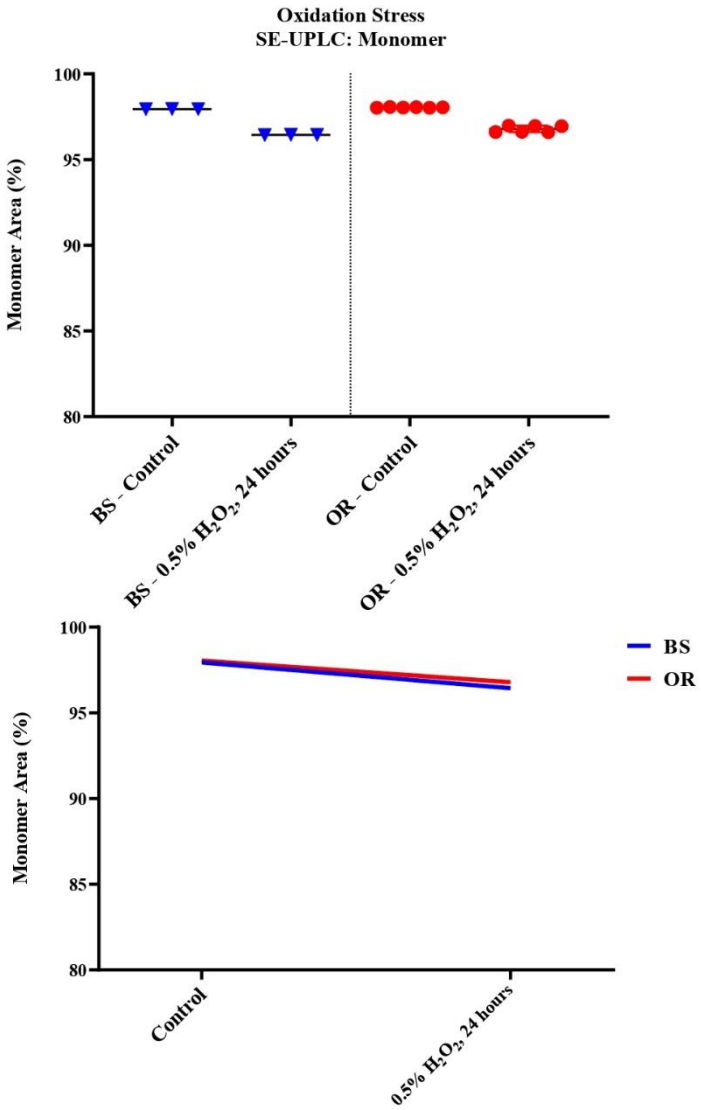

Figure 81: Oxidation stress, monomer area % results obtained by SE-UPLC. The results are grouped as mean ± SD (top) and linear curves (bottom).

Linear curves of the monomer % area values of the oxidation stress applied samples were generated separately and are given in Figure 81. The slopes of the obtained BS and OR linear curves were compared. The differences between the slopes are not significant (p=0.0552). The slopes of the linear curves of the HMW % area values of the samples subjected to oxidation stress were compared. The differences between the slopes are not significant (p=0.0566). Curves are given in Figure 82.

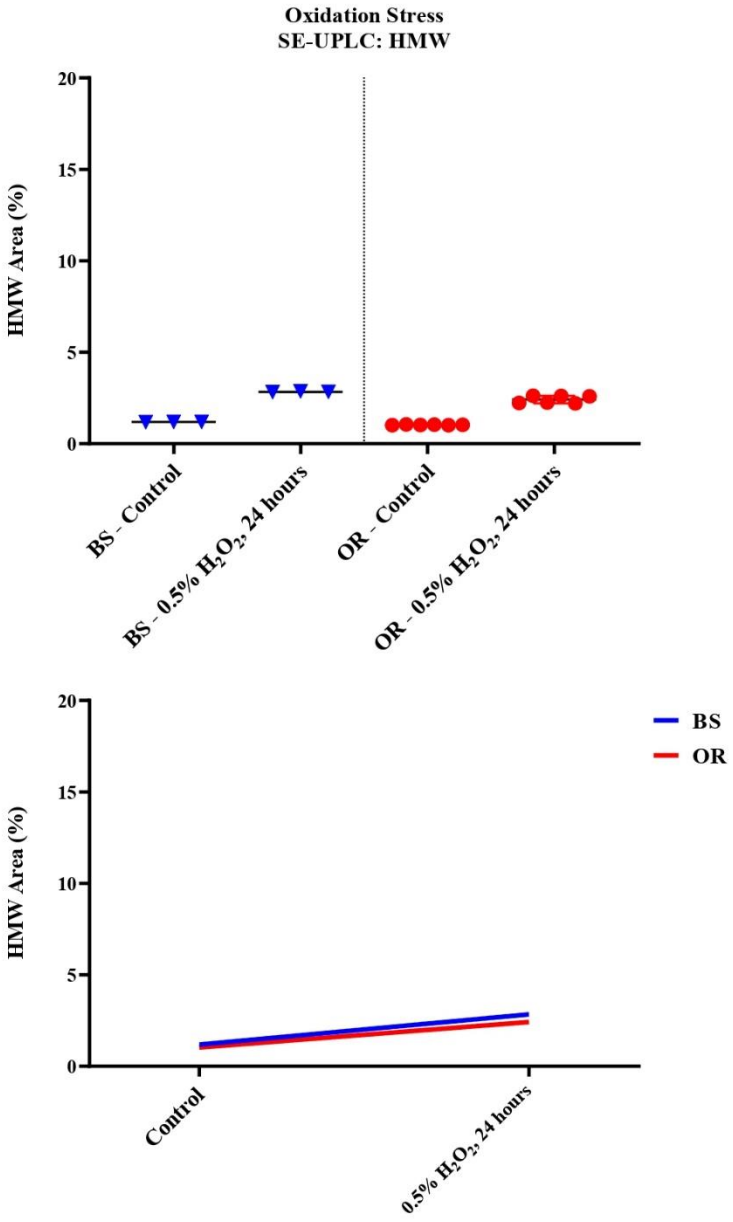

Figure 82: Oxidation stress, HMW area % results obtained by SE-UPLC. The results are grouped as mean ± SD (top) and linear curves (bottom).

Overlaying SE-UPLC chromatograms of oxidation stressed BS and OR samples, stressed FB and unstressed BS and OR samples are given in Figure 83. In BS and OR samples, it is observed that the amount of HMW increases.

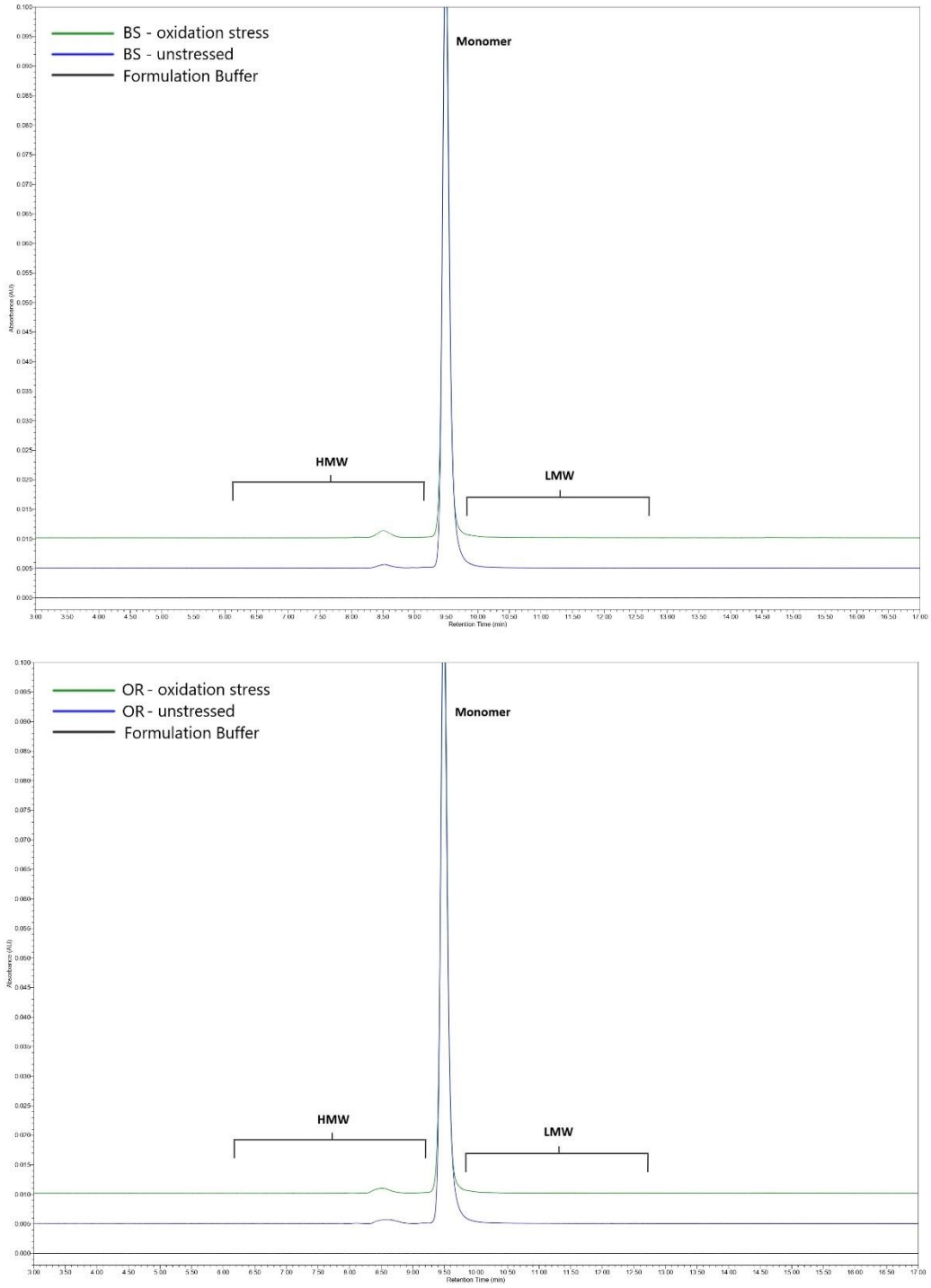

Figure 83: SE-UPLC chromatograms of BS (top) and OR (bottom) subjected to oxidation stress

4.2.5.2 Imaged Capillary Isoelectric Focusing (icIEF)

Duplicate results of the BS sample (n=2) and duplicate results of two different OR samples (n=4) were grouped and compared separately for the oxidation stress.

The differences in mean main charge variant % area values between BS and OR samples exposed to oxidation stress and their controls were determined as 12.10% and 12.27%, respectively. Linear curves of the BS and OR samples were generated and compared. The differences between the slopes are not significant (p=0.5251). The results and linear curves are given in Figure 84.

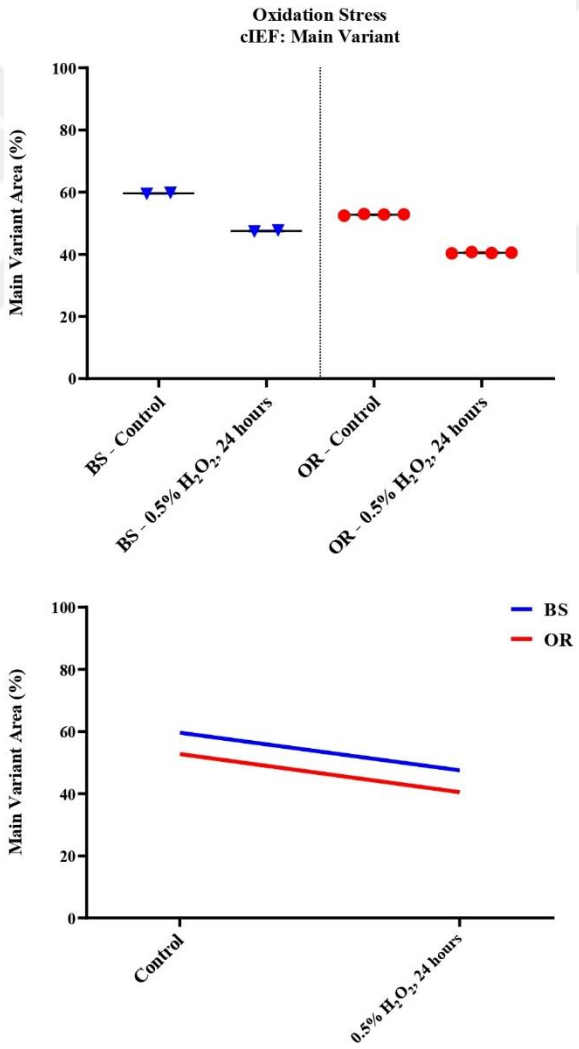

Figure 84: Oxidation stress, main charge variant area % results obtained by icIEF. The results are grouped as mean ± SD (top) and linear curves (bottom).

The differences in mean acidic charge variant % area values between BS and OR samples exposed to oxidation stress and their controls were determined as 11.87% and 11.73%, respectively. Linear curves of the BS and OR samples were generated and compared. The differences between the slopes are not significant (p=0.6818). The results and linear curves are given in Figure 85.

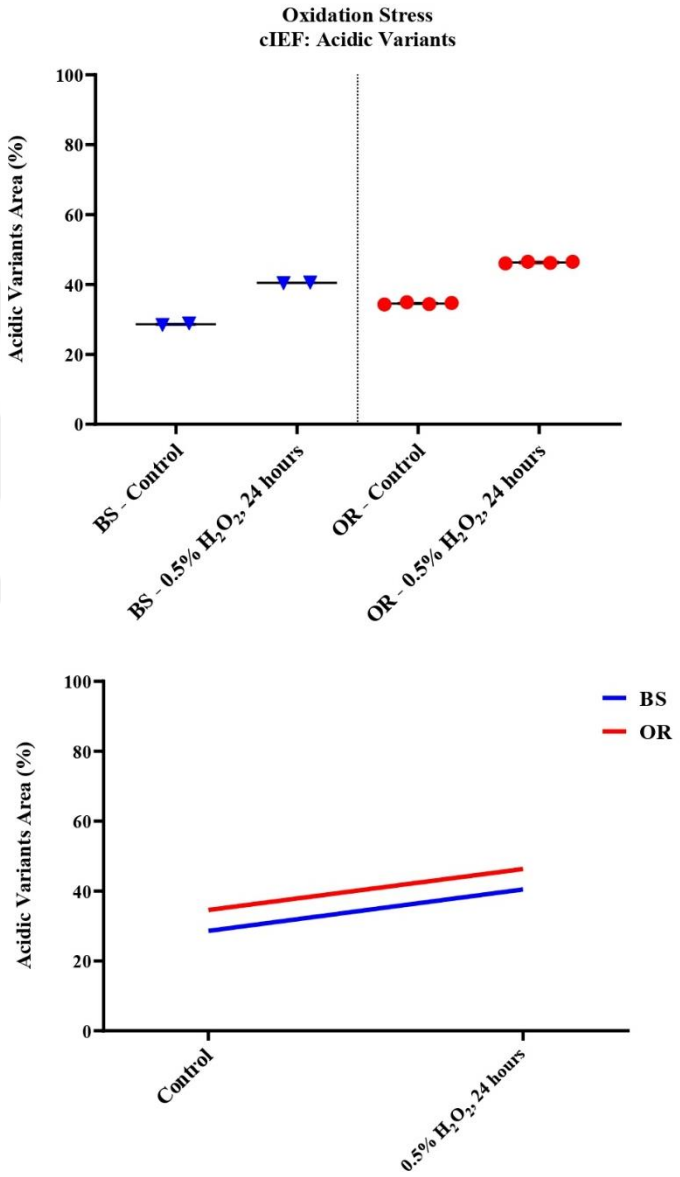

Figure 85: Oxidation stress, acidic charge variant area % results obtained by icIEF. The results are grouped as mean ± SD (top) and linear curves (bottom).

The differences in mean basic charge variant % area values between BS and OR samples exposed to oxidation stress and their controls were determined as 0.23% and 0.45%, respectively. Linear curves of the BS and OR samples were generated and compared. The differences between the slopes are not significant (p=0.3390). The results and linear curves are given in Figure 86.

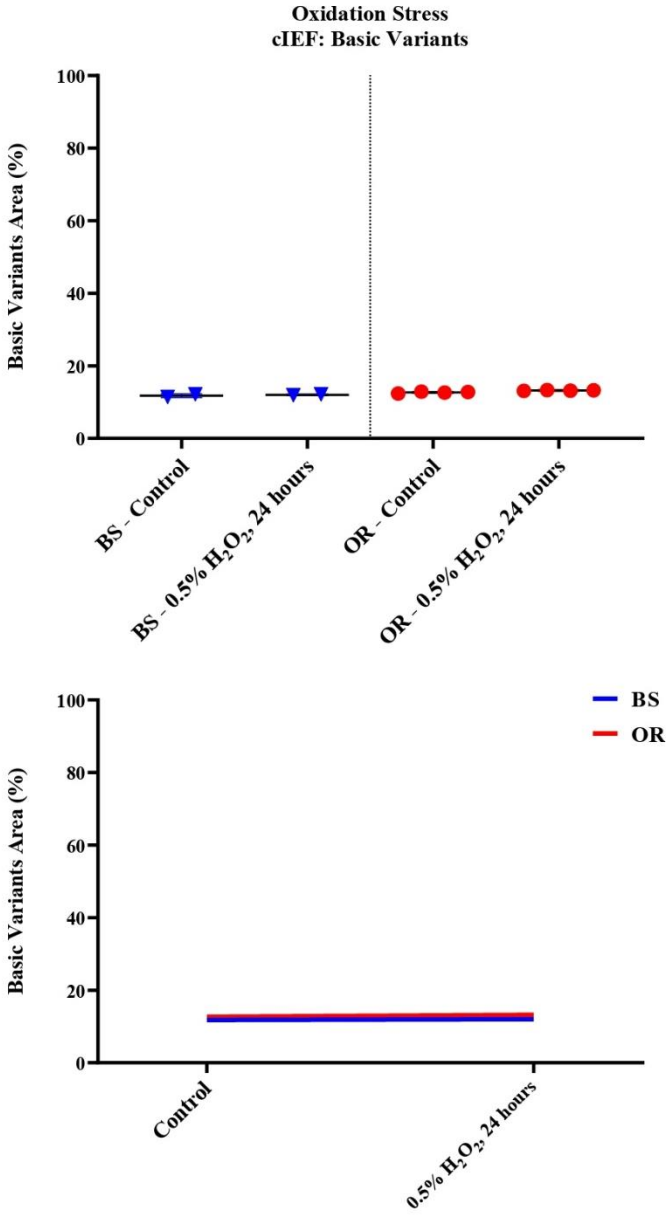

Figure 86: Oxidation stress, basic charge variant area % results obtained by icIEF. The results are grouped as mean ± SD (top) and linear curves (bottom).

Overlaying icIEF electrograms of oxidation stressed BS and OR samples, stressed FB and unstressed BS and OR samples are given in Figure 87. In stressed BS and OR samples, it is observed that the amount of main charge variants decreased while acidic charge variants increased.

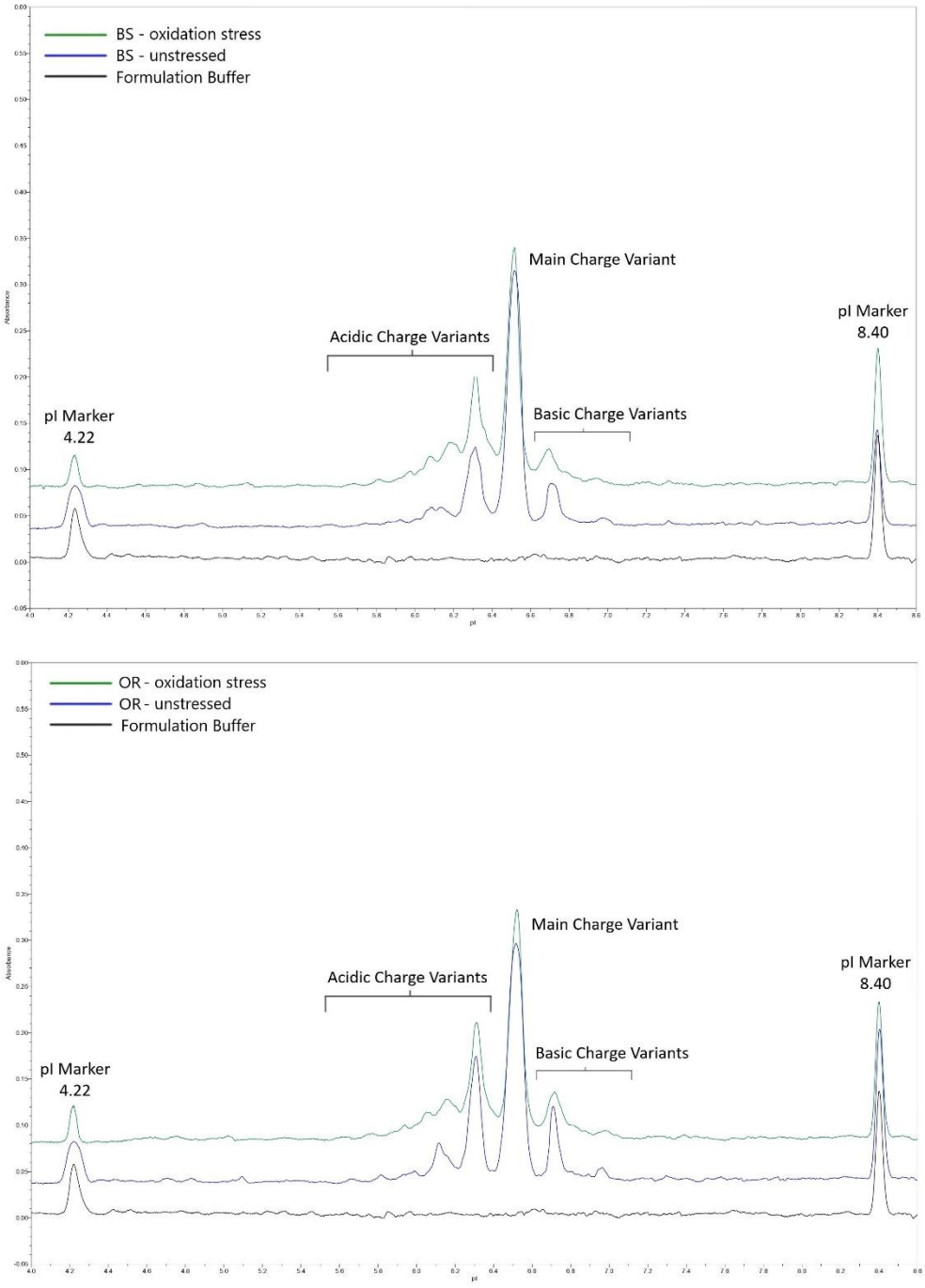

Figure 87: icIEF electrograms of BS (top) and OR (bottom) for oxidation stress

4.2.5.3 Capillary Electrophoresis-Sodium Dodecyl Sulfate (CE-SDS)

4.2.5.3.1 Reduced CE-SDS

Triplicate results of the BS sample (n=3) and triplicate results of two different OR samples (n=6) were grouped and compared.

The differences in mean LC+HC % area values between BS and OR samples exposed to oxidation stress and their controls were determined as 0.89% and 0.49%, respectively. Linear curves of the oxidation stress-applied samples were generated and are given in Figure 88. The slopes of the obtained BS and OR linear curves were compared. The differences between the slopes are not significant (p=0.1318).

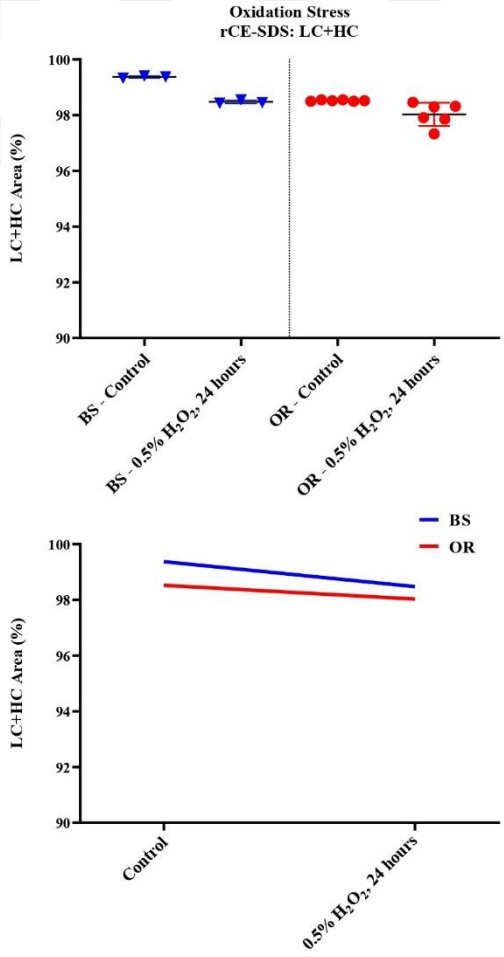

Figure 88: Oxidation stress, LC+HC area % results obtained by rCE-SDS. The results are grouped as mean ± SD (top) and linear curves (bottom).

Overlaying rCE-SDS electrograms of oxidation stressed BS and OR samples, stressed FB, and unstressed BS and OR samples are given in Figure 89. The amount of impurities is slightly increased in BS and OR samples.

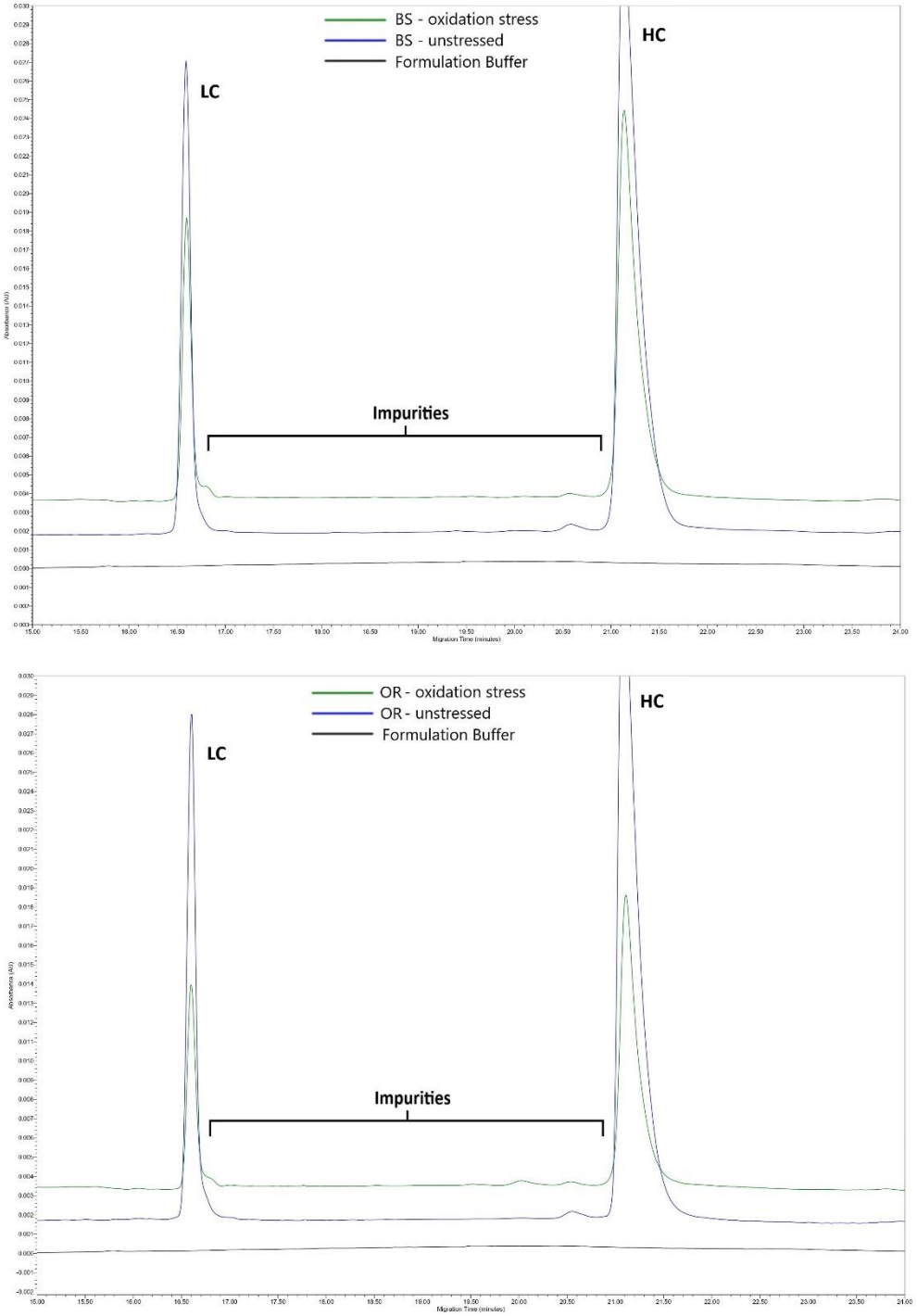

Figure 89: rCE-SDS electrograms of BS (top) and OR (bottom) for oxidation stress

4.2.5.3.2 Non-Reduced CE-SDS

Triplicate results of the BS sample (n=3) and triplicate results of two different OR samples (n=6) were grouped and compared.

The differences in mean IgG % area values between BS and OR samples exposed to oxidation stress and their controls were determined as 6.56% and 6.50%, respectively. The slopes of the BS and OR linear curves were compared and given in Figure 90. The differences between the slopes are not significant (p=0.5245).

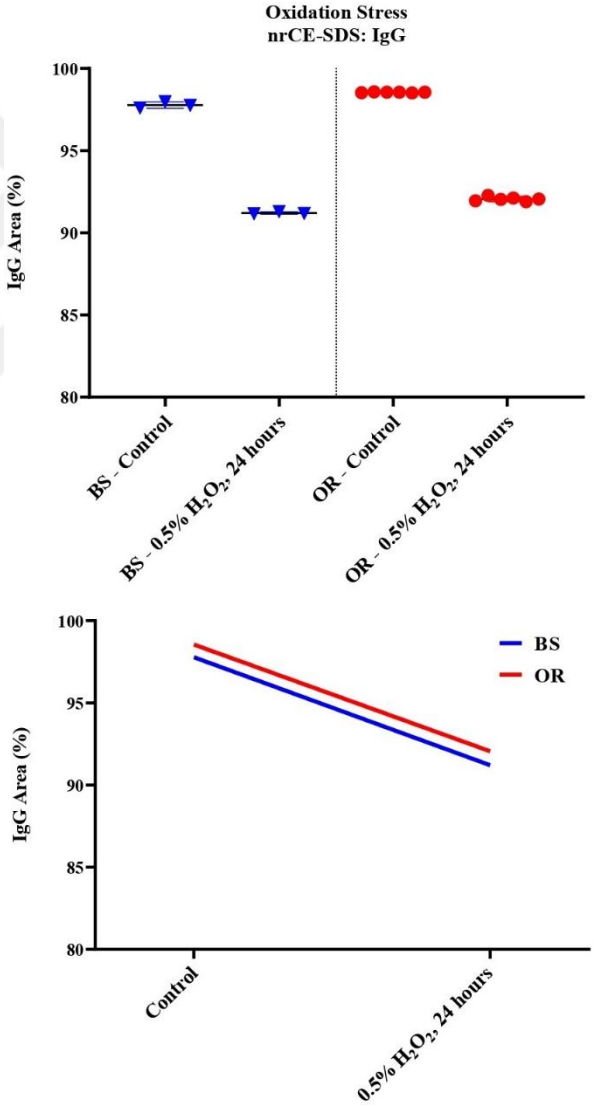

Figure 90: Oxidation stress, IgG area % results obtained by nrCE-SDS. The results are grouped as mean ± SD (top) and linear curves (bottom).

Overlaying nrCE-SDS electrograms of oxidation stressed BS and OR samples, stressed FB, and unstressed BS and OR samples are given in Figure 91. It is observed that the amount of impurities increased in BS and OR samples.

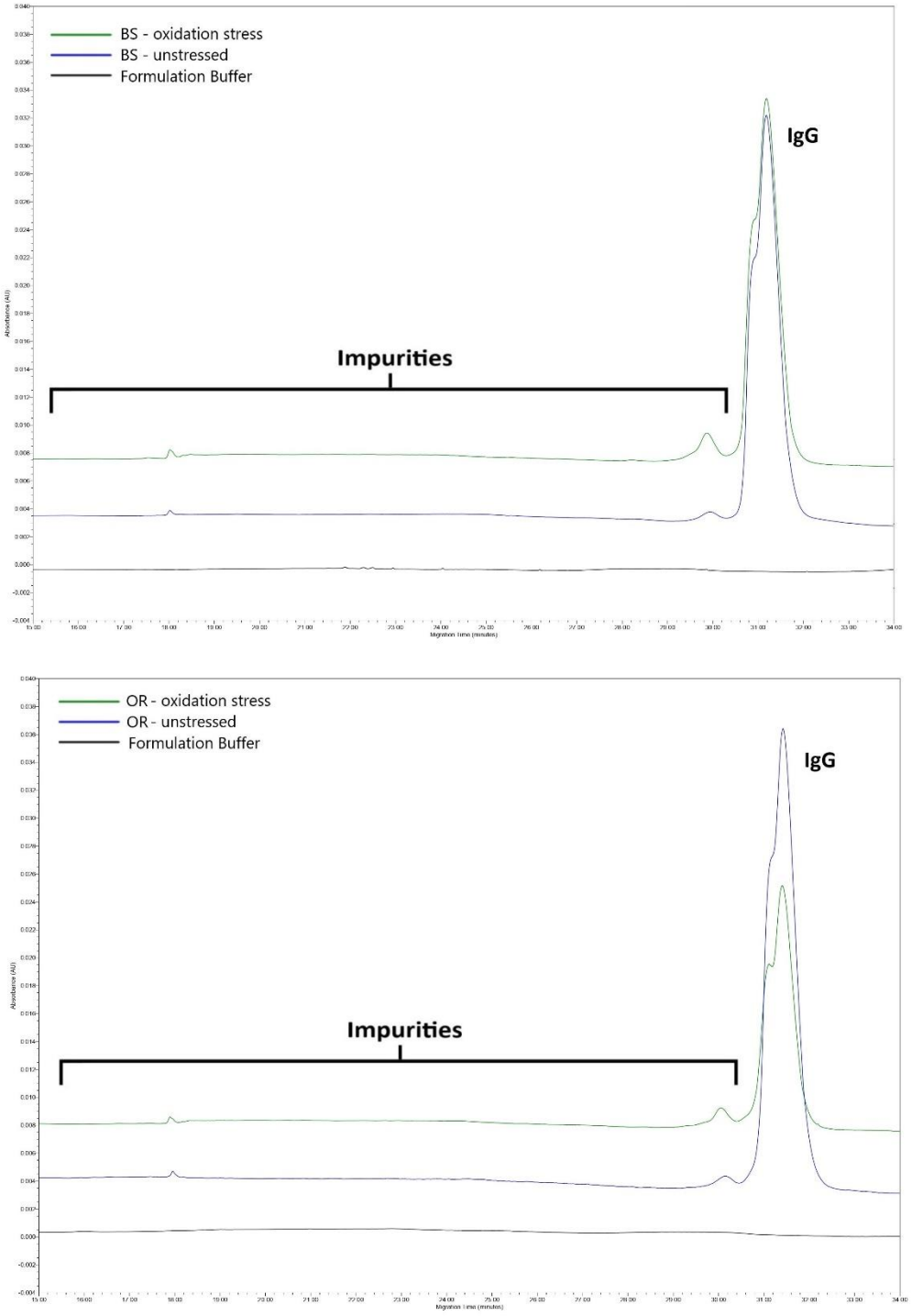

Figure 91: nrCE-SDS electrograms of BS (top) and OR (bottom) subjected to oxidation stress

4.2.5.4 Complement assay

Relative potencies were evaluated by the complement assay. Percent of the relative potency of the oxidation stressed BS and OR was calculated against the unstressed BS as an interim reference standard.

Relative potency results for the BS and OR samples show similar results to each other. The results are given in Table 24.

Table 24: Oxidation stress % relative potency results for BS and OR samples.

Sample Name	**% Relative Potency**
BS (unstressed)	NA
BS - oxidation stress, 24 hours	86.27%
OR lot #1 - oxidation stress, 24 hours	74.72%

5 DISCUSSION

As a result of Stability and Forced Degradation Studies, changes in BS and OR samples were determined by SE-UPLC, icIEF, nrCE-SDS, rCE-SDS and complement assay analyses. The results obtained were evaluated in themselves and by comparing them with previous studies in the literature.

5.1 Stability Study

The stability study aimed to examine the behavior of biosimilar mAb stored long-term under different temperature conditions. The results provide valuable information about the change in physicochemical and biological properties of the biosimilar mAb, which is stored for a long time under different storage conditions.

General tests of the BS sample were performed at each time point. When samples were pulled for analysis, visual appearance tests were performed first. The BS sample at each storage condition remained clear and colorless throughout the stability study, and no visible particles were observed. For all samples, the expected protein concentration is between 8-12 mg/ml. The 5.0±3.0˚C and the ≤-65°C conditions showed similar concentration profiles and were in the range. For the 25±2°C/60±5%RH condition, measured concentrations tend to be higher than expected. This seems to be attributed to the evaporation of the sample during long-term storage at 25°C (41). The pH values of the BS for all storage conditions are within the range. The BS osmolality results for 5.0±3.0˚C and ≤-65°C storage conditions are similar, but the osmolality results tend to increase for 25±2°C/60±5%RH storage conditions. Osmolality and pH are components of chemical stability and were monitored due to the clinical impact they could have on the patient during the infusion (116). Aside from the clinical effects, pH changes can cause mAb degradation, potentially leading to aggregation. The obtained pH and osmolality results meet the acceptability criteria throughout the study and for all storage conditions (117).

The BS samples were analyzed by SE-UPLC at predetermined intervals to obtain aggregate profiles (Appendix 1, Table 25). Throughout the stability study, there was no significant change in the percentage of total aggregate (HMW) or the monomer for BS stored at 5.0±3.0˚C. At the end of the 24th month of stability, the BS sample at 5.0±3.0˚C storage condition meets the test acceptance criteria (Monomer peak: ≥ 95.0%) in Table 6. Also, BS at 25±2°C/60±5%RH storage condition meets the test acceptance criteria until the end of the 12th month. However, a significant decrease in monomer peak and an increase in aggregate level are observed ≤-65°C storage condition. This result is important for BS development because it indicates that the product is not suitable for freezing storage (≤-65°C).

The BS samples analyzed by icIEF with and without CpB treatment at predetermined intervals to obtain charge variant profiles (Appendix 2, Table 26). Through the digestion of samples with CpB, which cleaves the C-terminal lysine and results in a reduction in the basic charge variants, the contribution of the C-terminal lysine variant to the total basic charge variants was assessed (118). Following CpB digestion, there was a slight decrease in the basic species, indicating that the C-terminal lysine variant had a minor impact on the charge profile of BS. There was no significant change in the percentage of all charge variants for BS stored at 5.0±3.0˚C and ≤-65°C storage conditions. In 25±2°C/60±5%RH storage conditions, the percentage of the main charge variants decreased while the percentage of the acidic charge variants increased.

The BS samples were analyzed by rCE-SDS at predetermined intervals. Under reducing conditions, the LC+HC value gives the purity level, and the remaining values give the impurity level (Appendix 3, Table 27). There was no significant change in the percentage of purity level for BS stored at 5.0±3.0˚C and ≤-65°C storage conditions. In 25±2°C/60±5%RH storage condition, the percentage of purity level started to decrease after six months. All storage conditions meet test acceptance criteria.

nrCE-SDS is used to analyze the purity of intact mAb and product-related impurities. The total main (IgG) value is important for non-reducing conditions (Appendix 3, Table 27). There was no significant change in the percentage of total main for BS stored at 5.0±3.0˚C and ≤-65°C storage conditions until 18 months. In 25±2°C/60±5%RH storage condition, the percentage of purity level started to decrease after nine months. All storage conditions meet test acceptance criteria.

Complement assay results for all storage conditions of the BS are very close to each other at all time points. The results of all samples in the analysis performed at all time points are within the specification range (Appendix 4, Table 28). All storage conditions meet test acceptance criteria.

The recommended shelf storage condition of the OR sample is 5.0±3.0°C. Therefore, as additional data, the OR sample was stored at 5.0±3.0°C for 24 months and compared with the BS 5.0±3.0°C product. As a result of SE-UPLC, icIEF, rCE-SDS, nrCE-SDS, and complement assay analyses, no significant change was observed between the 5.0±3.0°C condition of BS and OR samples in all analysis results considering $p<0.05$. Stability result data of SE-UPLC, icIEF, rCE-SDS, nrCE-SDS, and complement assay analyses and 5.0±3.0°C condition graphs of BS and OR samples are given in the Appendix (Table 25 to Table 28). These BS and OR samples at 5.0±3.0°C storage condition comparison results are important because they show the same degradation profile over 24 months, even though they are produced from different cell lines (CHO and NS0, respectively).

5.2 Forced Degradation Study

The BS and OR samples were subjected to various stress conditions. Each stress was chosen because it mimics the potential stress that a mAb therapeutic drug would encounter during the manufacture, shipping, and storage of its lifetime. SE-UPLC, icIEF, nrCE-SDS, rCE-SDS, and complement assay results obtained from BS and OR samples were compared both with their control samples and with each other for each stress condition.

5.2.1 Thermal stress

Two temperature conditions were chosen for thermal stress studies, one of which is 37°C, which is the most preferred temperature for stress studies (119). The BioPhorum Development Group surveyed 12 companies on forced degradation studies between 2016 and 2017. As a result of this survey, companies choose thermal stress temperatures high enough to degrade the product in the desired time frame without reaching the molecule's melting temperature (T_m). Most companies do not check the relative humidity as part of the thermal stress assessment for forced degradation (98).

In studies with anti-C5 antibody biosimilars and originators (EU and USA series), it has been stated that melting temperatures are in the range of 70.0-70.2°C (120). It was suggested that stress application should be carried out at temperatures 10-20°C lower than these values, since the application of stress at temperature levels close to the melting temperature has a greater effect on molecules (121). As the applied temperature in thermal stress approaches the melting temperatures, the mAb structure begins to unfold, and the opened intermediates begin accumulating. This can initiate self-aggregation or degradation, resulting in increased aggregation levels (106,122). Therefore, 50°C was applied as the second thermal stress condition.

The monomer level was decreased as 1.32% in the BS sample and 1.2% in the OR sample after 14 days of incubation at 37°C (Table 16). After 14 days of incubation at 50°C, monomer levels decreased by 8.35% in the BS sample and 11.61% in the OR sample (Table 17). As expected, more significant monomer degradation was observed in the BS and OR samples after thermal stress of 50°C. As observed in previous studies, the degradation of the monomer and the formation of HMW variants lead to a decrease in monomer levels (104,106,123). When the degradation rates of monomer levels were compared using linear curves, no significant difference was observed between the curves formed at 37°C ($p=0.6555$). However, a significant difference was observed between linear curves at 50°C, where the degradation was more pronounced ($p<0.0001$).

A recent study showed that the increase in HMWs observed during different stress treatments applied to mAbs, including the thermal stress condition, resulting in a significant reduction in mAb activity (124). After 14 days of incubation at 37°C, an increase in aggregation at 37°C was observed as 1.19% for BS samples and 1.22% for OR samples. The increase in HMW amounts as a result of incubation at 50°C for the same period was observed as 7.78% for BS samples and 11.16% for OR samples.

When the charge variant changes due to thermal stress were examined, it was observed that there was a significant difference between 37°C and 50°C conditions (Table 16 and Table 17). After 14 days of incubation, the main charge variants of the BS and OR samples decreased by 9.83% and 9.25% at 37°C, respectively; decreased by 34.54% and 33.14% while at 50°C, respectively. It was observed that the decrease in the main charge variant was due to the increase in the acidic charge variants. At the end of 14 days of incubation, the acidic charge variants of BS and OR samples increased by 11.50% and 10.84% at 37°C, respectively, and by 38.96% and 38.72% at 50°C, respectively. At the end of 14 days of incubation of BS and OR samples, it was observed that basic charge variants decreased by 1.68% and 1.59%, respectively, at 37°C and decreased by 4.42% and 5.58%, respectively, at 50°C.

When the charge variant levels at the end of the incubation were compared with the levels of the control samples, statistically significant differences were observed only during the 14 days of incubation of both temperature conditions of the OR sample. As a result of the comparison of the slopes of the linear curves based on the changes of the main, acidic, and basic charge variants, it is seen that the charge variant change rates are statistically similar in both temperature conditions. Still, there is a difference only in the basic charge variants at 50°C condition. It is common to observe these variations in charge variant distributions between biosimilar and originator mAbs (125–127). Because C-terminal Lys, which acts on the presence of basic charge variants, is quickly cleared by proteases after administration, basic charge variants typically have little impact on mAb safety or efficacy (128). On the other hand, acidic charge variants may reduce mAb efficacy because the deamidation of asparagine residues in CDR regions reduces antigen binding affinity (129,130).

Under reducing conditions, the LC+HC value gives the purity level, and the remaining values give the impurity level. When the LC+HC levels measured on the 3rd and 7th days of both temperature incubations were compared with the control sample levels, no significant difference was observed for the BS samples, while there was a significant difference on the 7th day in the OR sample. In addition, it was observed that LC+HC levels of BS and OR samples for both temperatures decreased significantly at the end of the 14th day compared to the control samples ($p=0.0102$ and $p<0.0001$, respectively). The changes in LC+HC levels of BS and OR samples on day 14 of incubation at 50°C were 7.21% and 7.90%, respectively (Table 17). When the LC+HC levels were compared using linear curves, no significant difference was observed between curves formed at 37°C ($p=0.5733$). However, a significant difference was observed between linear curves at 50°C, where the impurity levels in the samples increased in direct proportion to time ($p=0.0158$). Thermal stress application is one of the stress conditions in which the HMW rate increases the most (9). However, no variants with higher molecular weights than HC were observed as a result of the rCE-SDS analysis.

When the measured IgG levels of both temperature incubations were compared with the control sample levels, no significant difference was observed for the BS and OR samples. After 14 days of incubation at 50°C only, there was a significant difference in the OR sample ($p=0.0013$). After 14 days of incubation at 37°C, the differences between samples and controls were 1.35% for BS and 1.08% for OR, while after 14 days of incubation at 50°C, the differences were 1.34% for BS and 1.72% for OR. IgG levels were compared using linear curves, and no significant difference was observed between the slopes for both temperature conditions.

The result of the rCE-SDS and nrCE-SDS studies shows that the HMW variants detected during the SE-UPLC analysis are not covalently linked as they were not detected in the CE-SDS analyses (131). In a study, it was stated that fragment increases that could not be seen in detail in SEC analysis were examined with nrCE-SDS and rCE-SDS analyzes (9). It was stated that fragments of different sizes, which were low before the application of thermal stress, increased; based on the absence of

HMW in the rCE-SDS result, it has been suggested that there are disulfide bond changes. In addition, in the same study, it was stated that the different impurity levels in the initial conditions of infliximab biosimilar and originator samples, which were subjected to thermal stress, did not affect the impurity increase rate (9).

Increasing the temperature from 37°C to 50°C resulted in a decrease in biological activity. However, it is observed that the results in the complement assay still maintain an acceptable range, despite the increased aggregation level and acidic charge variants in BS and OR. In a thermal stress study with adalimumab for 4 weeks at 37°C, the receptor binding ELISA assay results complied with the SE-HPLC analysis results. It was found that the degradation under thermal stress follows the reaction kinetics (108).

5.2.2 Agitation stress

Agitation stress is one of the important physical stresses encountered by the mAbs during purification, formulation, filtration, fill and finish, shipping, and handling, and can accelerate the rate of aggregate formation (92). Agitation stress is an easy way to monitor and assess the robustness of biopharmaceutical formulations. Nonionic surfactant polysorbate is commonly used in mAb formulations to prevent mechanically induced aggregation. It accumulates at the air-liquid interface and protects the mAb from agitation stress. A study reported that 0.005% w/v concentration of polysorbate prevented aggregate formation (132,133).

Another potential degradation pathway caused by agitation stress is oxidation. mAbs are subjected to a variety of stress factors during agitation stress testing, including exposure to liquid-air and liquid-container interfaces, which can cause oxidation. Physical and chemical instability can result from these stressors. Agitation increases the frequency of protein exposure to hydrophobic surfaces or air/water interfaces, resulting in aggregate formation (101,103). In a study to evaluate the effects of agitation stress on cetuximab, the mAb was incubated at 4 °C and 25 °C for 48 hours while subjected to shaking at intensities of 150 and 250 rpm. The

applied stress did not lead to the formation of any degraded products and had no adverse effect on the chromatograms of the stressed samples compared to the control. Furthermore, the evaluation of the charge variants of the cetuximab showed no new acidic or basic variant changes in the charge variant profile of the stressed samples compared to the control sample (132).

After 400 rpm agitation stress for 24 hours, the monomer level decreased by 0.63% in the BS and 0.48% in the OR, and the aggregation levels increased by 0.69% and 0.51, respectively (Table 19). After 400 rpm agitation stress for 72 hours, the monomer levels decreased by 0.66% for BS and 0.52% for OR. The aggregation levels increased by 0.71% and 0.53%, respectively (Table 19). The linear curves of the BS and OR samples were compared, and no significant difference was observed between the slopes (for monomer p=0.4758, for aggregation p=0.4261).

After agitation stress, it was observed that while the main charge variants were slightly decreased, acidic and basic charge variants were increased. At each time point, no significant difference was observed when the charge variant levels of BS and OR were compared with their control samples.

When the LC+HC levels were compared with the control sample levels at both time points, no significant differences were observed for the BS samples, while there were significant differences for the OR samples. The changes in LC+HC levels after 24 hours were 1.01% for BS and 0.94% for OR, while after 72 hours, they were 1.05% and 1.06%, respectively. No significant difference was observed between slopes when the LC+HC levels were compared using linear curves (p=0.9437).

When the measured IgG levels were compared to the control sample levels, no significant difference was observed for the BS and OR samples, except for 72 hours of 400 rpm stress for the OR sample. The changes in IgG levels after 24 hours were 0.34% for BS and 0.56% for OR, while after 72 hours, they were 0.55% and 0.79%, respectively. No significant difference was observed between slopes when the IgG levels were compared using linear curves (p=0.1732).

5.2.3 pH stress

The pH of the environment in which the mAbs are found affects their stability. Due to the disruption of the intermolecular or intramolecular forces forming their structure, mAbs under extremely acidic or alkaline pH conditions may aggregate or become permanently denatured (47,94,124). Degradations such as aggregation, fragmentation, and deamidation occur due to applied pH stress, followed by higher-order structural modifications and reduction in bioactivity (9). Besides, choosing a pH closer to pl can cause solubility issues, complicating the interpretation of degradation data (10,119). In some studies, pH stress is carried out at 40°C and above to increase pH-induced degradation. However, RT is preferred to avoid thermal stress, which complicates the pH stress study's degradation pathways (98).

Incubation of the BS product at pH 4, which is close to the lowest pH value reached during the purification stages, for 72 hours was determined as the stress condition. At the end of 72 hours of incubation at acidic pH 4, the monomer levels of the BS and OR samples decreased to a very low level, and the aggregate levels increased (Table 20). As a result of incubation in acidic pH 4 condition, the monomer level of the BS sample decreased by 44.39%, while the aggregate level increased by 44.39%. In the OR sample, while the monomer level decreased by 67.80%, the aggregate level increased by 67.78%. When the slopes of the monomer and aggregate linear curves created separately using the results of acidic pH stress were compared, it was observed that there were significant differences ($p<0.0001$).

As a result of incubation in the basic pH 9 condition, the monomer level of the BS and OR samples decreased by 1.04% for both, while their aggregation levels increased by 0.97% and 0.95%, respectively. At the end of the basic pH 9 incubation, no significant difference was observed as a result of the comparison of the linear curve slopes obtained by using the monomer and aggregation values of the BS and OR samples. Significant differences in monomer and aggregate levels were observed in both pH stress conditions of the OR sample compared to the control sample.

At the end of the acidic pH 4 incubation, it was observed that the main and acidic charge variants decreased, and the basic charge variant amounts increased in the BS and OR samples (Table 20). In the BS sample, the main charge variant decreased by 8.08% and the acidic charge variant by 2.37%, while the basic charge variant increased by 10.45%. Under the same stress condition, in the OR sample, the main charge variant decreased by 6.60% and the acidic variant by 8.35%, while the basic charge variant increased by 14.95%. Significant differences were observed at all charge variant levels of the OR compared to the control sample. Basic charge variants increased under acidic pH conditions, and mAb acquired basic properties. These results show that there is a transition from the main charge and acidic variants to the basic charge variants in the BS and OR samples.

At the end of the basic pH 9 incubation, it was observed that the main charge variant decreased and especially the acidic charge variants amount increased in the BS and OR samples. No significant changes were observed in the basic charge variants. After 72 hours of basic pH 9.0 stress incubation, the main charge variant decreased by 3.72%, while the acidic charge variants increased by 3.89% in the BS sample. Under the same stress condition, the main charge variant decreased by 4.03% in the OR sample, while the acidic charge variants increased by 4.12%. Acidic charge variants increased under basic pH condition, and the mAbs acquired acidic properties. These results show that most of the main charge variants were transformed into acidic charge variants in the BS and OR.

Compared to controls of BS and OR, measured LC+HC levels decreased by 2.30% and 2.22% at acidic pH 4 incubation, respectively, and by 1.67% and 1.96% at basic pH 9 incubation, respectively. Compared to control samples of BS and OR, measured IgG levels decreased by 0.98% and 1.16% at acidic pH 4.0 incubation, respectively, and by 0.60% and 0.77% at basic pH 9.0 incubation, respectively. Although these changes were relatively low, both %LC+HC and %IgG levels of the OR showed significant differences compared to the control sample in both pH stress conditions. Linear curves of the LC+HC and IgG levels of the samples were generated separately. The differences between the slopes are not significant.

In most cases, aggregate formation causes mAb instability. Aggregates exhibit either reduced or no biological activity and, may be immunogenic. In general, the aggregates have little or no biological activity and may be immunogenic (134). The formation of mAb aggregates has been described under a variety of stress conditions that occur during manufacturing. It has been demonstrated that exposure to low pH during purification procedures, such as residual Protein A chromatography and low-pH virus inactivation, can cause IgG to aggregate (135,136). In the results obtained by changing the pH, the decrease in antibody activity observed as a result of the complement assay analysis supports each other with the increased aggregation of mAbs that can elicit the immunological response.

5.2.4 Freeze/thaw stress

After five cycles of F/T stress (Table 22), monomer amounts of BS and OR samples were decreased by 6.02% and 6.00%, respectively, when compared to control samples. Under the same conditions, it was observed that the amounts of HMW increased by 6.03% for BS and 6.05% for OR. mAbs can be subjected to a number of stresses during freeze-thawing, all of which can cause aggregation. Cold denaturation of the mAb-containing solution during F/T, pH changes due to the crystallization of the buffer, and formation of the ice-solution surface may disrupt protein conformation (107,137). Increased salt concentration caused by freezing can reduce intermolecular repulsion between protein molecules, resulting intermolecular interactions that lead to aggregation (137,138).

CE-SDS analyses were performed to elucidate whether the aggregates formed were composed of covalently or noncovalently linked monomers. The results indicate that the aggregates formed in F/T samples were noncovalent. One study characterized the structural properties of aggregates formed after thermal and F/T stress of IgG1 mAb by SDS-PAGE. It was found that aggregates formed by thermal stress were partially covalently bonded, while aggregates formed by F/T were non-covalently bonded (104).

No significant differences were observed as a result of the comparison of the charge variant levels of both BS and OR samples with their control samples. A decrease of 2.00% for BS and 1.58% for OR was observed in main charge variant levels. An increase of 1.58% and 1.19% was observed for the acidic charge variants of the BS and OR, and 0.42% and 0.40% for the basic charge variants, respectively.

One of the approaches used to compare the degradation rates of BS and OR samples under stress conditions is to construct and compare linear curves that show the change between the results obtained after the application of stress and the control samples (9,108). As a result of the comparison of the linear curve slopes obtained from the forced degradation studies, no statistically significant difference was observed except for the monomer and HMW results of the 50°C thermal and pH 4 stress applications, where aggregation increase was noticeable. Accordingly, it was concluded that the degradation rates of BS and OR samples were similar.

5.2.5 Oxidation stress

In BioPhorum's survey, most companies used oxidation stress to understand the degradation mechanisms of mAbs and form CoAs. Most companies use H_2O_2 as an oxidizing agent at varying concentrations (from 0.001% v/v to as high as 0.5% v/v) from a few hours to 3 days. In oxidation stress, the incubation temperature of 25°C is mostly preferred, and buffer change is required after incubation (98).

After incubation of BS and OR samples with 0.5% H_2O_2 (v/v) for oxidation stress, the % monomer levels decreased by 1.50% for BS and 1.26% for OR. The aggregate level increased almost as much as the decreased level of monomer. In a study, in which BS and OR samples were subjected to oxidative stress with 3.0% H_2O_2 for 24 hours at 25°C, it was stated that aggregate levels increased by 2.0% for BS and 3.0% for OR (99). As observed in the result of the nrCE-SDS analysis, degradation rather than aggregation was observed in the BS and OR samples as a result of oxidation stress.

As a result of oxidation stress, the IgG% amount decreased by 6.56% in BS samples and 6.50% in OR samples compared to control samples. A decrease in LC+HC% was also observed when oxidation stress was applied. Compared to the control samples, the LC+HC% amount decreased by 0.89% in BS samples and by 0.49% in OR samples.

In the distribution of charge variants, the main peak decreased by 12.10% for BS and 12.27% for OR. The level of acidic peaks increased almost as much as the decreased level of the main peak. In the oxidation stress study in which 0.02% H_2O_2 was applied to the mAb sample for 24 hours, no decrease in monomer level was observed; acidic charge variants increased by 9.6%, and basic charge variants decreased by 4.5% (129). In another study, it was stated that oxidations in the Fc region led to the formation of basic variants, while oxidations in the F(ab')2 region led to the formation of acidic variants (139).

Exposure of the BS and OR samples to oxidation stress resulted in a decrease in biological activity. However, it is observed that the results in the complement assay still maintain an acceptable range, despite the decrease in IgG% and increase in acidic charge variants. In an oxidation stress study with adalimumab and its biosimilar, exposure to H_2O_2 caused a negative effect on biological activity by increasing aggregate formation (99).

In conclusion, studies on forced degradation and long-term stability that were completed as part of this thesis helped to characterize the structure and biological activity of anti-C5 mAb. These studies, which can be used to evaluate product stability, guide formulation studies, comprehend product degradation pathways, and produce CQAs, are beneficial at all product life cycle stages. The lack of studies in the literature and their incompleteness demonstrates the novelty of this thesis. This study will bring the long-term stability and forced degradation studies of the biosimilar mAb candidate to the literature and pave the way for further research on developing such biopharmaceutical drug candidates.

6 CONCLUSION

Changes in product size and charge variant profile and what these changes mean for the product are of primary concern in the long-term stability and forced degradation studies. Analytical release methods such as SE-UPLC, CE-SDS, and icIEF are mainly used to understand the impact of these changes on the product.

The stability study aimed to examine the behavior of biosimilar mAb stored long-term under different temperature conditions. The results provide valuable information about the change in physicochemical and biological properties of the biosimilar mAb, which is stored for a long time under different storage conditions.

The force degradation study aimed to assess the similarity between the biosimilar mAb and the originator product in the degradation profile. High-resolution physicochemical and biological characterization methods evaluated acidic and basic charged variants, aggregates, and biological activities. The results support the conclusion that biosimilar mAb is analytically similar to the originator product in critical parameters related to efficacy and safety under different stress conditions. Besides, the correlation of physicochemical analysis results with complement assay analysis results is significant in showing the effect of stress conditions on the overall activity of the drug product. Another achievement of this study is demonstrating that the analytical methods used are suitable for the production, stability, and quality evaluation of biosimilar mAb products exposed to various stress conditions. It has been shown that the degradation products formed under different stress conditions can be determined by the methods used and can also be compared quantitatively.

Future studies, it is planned to expand the scope of this study. Replicating the results obtained with more biosimilar mAb production and originator product series, expanding the data set, and examining the products under more stressful conditions will provide important information before future clinical trials. In addition, LC-MS peptide mapping can also be used to understand degradation in stressed molecules further.

7 REFERENCES

1. Taylor D. The Pharmaceutical Industry and the Future of Drug Development. Issues Environ Sci Technol. 2016;(41):1–33.
2. IEIS. Turkish Pharmaceutical Market [Web]. http://www.ieis.org.tr/ieis/en/indicators/33/turkish-pharmaceutical-market. 2021.
3. Walsh G. Biopharmaceutical benchmarks 2018. Nat Biotechnol. 2018;36(12):1136–45.
4. Vulto AG, Jaquez OA. The process defines the product: what really matters in biosimilar design and production? Vol. 56, Rheumatology. 2017. p. 14–29.
5. Moorkens E, Jonker-Exler C, Huys I, Declerck P, Simoens S, Vulto AG. Overcoming barriers to the market access of biosimilars in the European union: The case of biosimilar monoclonal antibodies. Front Pharmacol. 2016;7(193).
6. Crommelin D, Bermejo T, Bissig M, Damiaans J, Krämer I, Rambourg P, et al. Pharmaceutical evaluation of biosimilars: important differences from generic low-molecular-weight pharmaceuticals. Eur J Hosp Pharm. 2005;11(1):11–7.
7. Gaughan CL. The present state of the art in expression, production and characterization of monoclonal antibodies. Mol Divers. 2016;20(1):255–70.
8. Blessy M, Patel RD, Prajapati PN, Agrawal YK. Development of forced degradation and stability indicating studies of drugs - A review. Vol. 4, J. Pharm. Anal. 2014. p. 159–65.
9. Pisupati K, Benet A, Tian Y, Okbazghi S, Kang J, Ford M, et al. Biosimilarity under stress: A forced degradation study of Remicade and Remsima. MAbs. 2017;9(7):1197–209.
10. Tamizi E, Jouyban A. Forced degradation studies of biopharmaceuticals: Selection of stress conditions. Eur J Pharm Biopharm. 2016;98:26–46.
11. YRKM S, N SK, A D, SY A, G S. A Review on Biotechnology and Its Commercial and Industrial Applications. J Biotechnol Biomaterial. 2011;01(07).
12. Padhyet al I, Padhy I, K Mahapatra AP, Saraswat D, Song J. Role Of Biotechnology in Pharmaceutical Research: A Comprehensive Review. Indo Am J P Sci. 2020;07(05):472–86.
13. Zhang K, Liu W. The Current Status, Trend, and Development Strategies of Chinese Biopharmaceutical Industry With a Challenging Perspective. Sage Open. 2020;10(1):1–16.
14. Chekol C, Gebreyohannes M. Application and Current Trends of Biotechnology: a Brief Review. Austin J Biotechnol Bioeng. 2018;5(1).
15. McCamish M, Woollett G. Worldwide experience with biosimilar development. MAbs. 2011;3(2):209–17.
16. Agrawal P. Biopharmaceuticals: An emerging trend in Drug Development. Vol. 2, SOJ Pharm Pharm Sci. 2015. p. 1–2.
17. Parr MK, Montacir O, Montacir H. Physicochemical characterization of biopharmaceuticals. J Pharm Biomed. 2016;130:366–89.
18. Singh Sekhon B. Biopharmaceuticals: an overview. Thai J Pharm Sci. 2010;34:1–19.

19. Covic A, Cannata-Andia J, Cancarini G, Coppo R, Frazão JM, Goldsmith D, et al. Biosimilars and biopharmaceuticals: What the nephrologists need to know - A position paper by the ERA-EDTA Council. Nephrol Dial Transplant. 2008;23(12):3731–7.
20. Kesik-Brodacka M. Progress in Biopharmaceutical Development. Biotechnol Appl Biochem. 2018;65(3):306–22.
21. Mellstedt H, Niederwieser D, Ludwig H. The challenge of biosimilars. Vol. 19, Ann. Oncol. 2008. p. 411–9.
22. U.S. Food & Drug Administration (FDA). Biological Product Definitions [Internet]. 2017 [cited 2022 Apr 13]. Available from: https://www.fda.gov/drugs/biosimilars/biosimilar-and-interchangeable-products
23. European Medicines Agency (EMA). Guideline on similar biological medicinal products [Internet]. 2014 [cited 2022 Apr 14]. Available from: https://www.ema.europa.eu/en/documents/scientific-guideline/guideline-similar-biological-medicinal-products-rev1_en.pdf
24. Kirchhoff CF, Wang XZM, Conlon HD, Anderson S, Ryan AM, Bose A. Biosimilars: Key regulatory considerations and similarity assessment tools. Vol. 114, Biotechnol. Bioeng. 2017. p. 2696–705.
25. European Medicines Agency (EMA). Human medicine European public assessment reports on authorized biosimilars, 2022. [Internet]. [cited 2022 Apr 17]. Available from: https://www.ema.europa.eu/en/medicines/search_api_aggregation_ema_medicine_types/field_ema_med_biosimilar
26. Sivendran R, Ramírez J, Ramchandani M, Liu J. Scientific and statistical considerations in evaluating the analytical similarity of ABP 501 to adalimumab. Vol. 10, Immunotherapy. 2018. p. 1011–21.
27. Zhang E, Xie L, Qin P, Lu L, Xu Y, Gao W, et al. Quality by Design–Based Assessment for Analytical Similarity of Adalimumab Biosimilar HLX03 to Humira®. AAPS J. 2020;22(3).
28. Lee N, Lee JAJ, Yang H, Baek S, Kim S, Kim S, et al. Evaluation of similar quality attribute characteristics in SB5 and reference product of adalimumab. MAbs. 2019;11(1):129–44.
29. Beck A, Reichert JM. Approval of the first biosimilar antibodies in Europe: A major landmark for the biopharmaceutical industry. Vol. 5, mAbs. 2013. p. 621–3.
30. Botzanowski T, Hernandez-Alba O, Malissard M, Wagner-Rousset E, Deslignière E, Colas O, et al. Middle-level IM-MS and CIU experiments for improved therapeutic immunoglobulin isotype fingerprinting. Anal Chem [Internet]. 2020;92(13):8827–35. Available from: https://doi.org/10.1101/2020.01.20.911750
31. Ansar W, Ghosh S. Monoclonal Antibodies: A Tool in Clinical Research. J Indian Acad Clin Med. 2013;4:9–21.
32. Lu RM, Hwang YC, Liu IJ, Lee CC, Tsai HZ, Li HJ, et al. Development of therapeutic antibodies for the treatment of diseases. J Biomed Sci. 2020;27(1):1–30.

33. Buss NAPS, Henderson SJ, McFarlane M, Shenton JM, de Haan L. Monoclonal antibody therapeutics: History and future. Vol. 12, Curr Opin Pharmacol. 2012. p. 615–22.
34. Shukla AA, Hubbard B, Tressel T, Guhan S, Low D. Downstream processing of monoclonal antibodies—Application of platform approaches. Vol. 848, J. Chromatogr. B. 2007. p. 28–39.
35. AlDeghaither D, Smaglo BG, Weiner LM. Beyond peptides and mAbs - Current Status and Future Perspectives for Biotherapeutics with Novel Constructs. J Clin Pharmacol. 2015;55(03):S4–20.
36. Coghlan J, He H, Schwendeman AS. Overview of Humira® Biosimilars: Current European Landscape and Future Implications. Vol. 110, J. Pharm. Sci. 2021. p. 1572–82.
37. Lee CC, Perchiacca JM, Tessier PM. Toward aggregation-resistant antibodies by design. Trends Biotechnol. 2013;31(11):612–20.
38. Tiller KE, Tessier PM. Advances in Antibody Design. Annu Rev Biomed Eng. 2015;17:191–216.
39. Wang W, Singh S, Zeng DL, King K, Nema S. Antibody structure, instability, and formulation. J Pharm Sci. 2007;96(1):1–26.
40. Fekete S, Gassner AL, Rudaz S, Schappler J, Guillarme D. Analytical strategies for the characterization of therapeutic monoclonal antibodies. Trends Anal Chem. 2013;42:74–83.
41. Fukuda J, Iwura T, Yanagihara S, Kano K. Factors to Govern Soluble and Insoluble Aggregate-formatin in Monoclonal Antibodies. Anal Sci. 2015;31(12):1233–40.
42. Chiu ML, Goulet DR, Teplyakov A, Gilliland GL. Antibody Structure and Function: The Basis for Engineering Therapeutics. Antibodies. 2019;8(4):55.
43. Hmiel LK, Brorson KA, Boyne MT. Post-translational structural modifications of immunoglobulin G and their effect on biological activity. Vol. 407, Anal. Bioanal. Chem. 2015. p. 79–94.
44. Liu B, Guo H, Xu J, Qin T, Xu L, Zhang J, et al. Acid-induced aggregation propensity of nivolumab is dependent on the Fc. MAbs. 2016;8(6):1107–17.
45. Lau C, McAdam MB, Bergseth G, Grevys A, Bruun JA, Ludviksen JK, et al. NHDL, a recombinant VL/VH hybrid antibody control for IgG2/4 antibodies. MAbs. 2020;12(1).
46. An Z, Forrest G, Moore R, Cukan M, Haytko P, Huang L, et al. IgG2m4, an engineered antibody isotype with reduced Fc function. MAbs. 2009;1(6):572–9.
47. Kim J, Kim YJ, Cao M, de Mel N, Albarghouthi M, Miller K, et al. Analytical characterization of coformulated antibodies as combination therapy. MAbs. 2020;12(1).
48. Ma F, Raoufi F, Bailly MA, Fayadat-Dilman L, Tomazela D. Hyphenation of strong cation exchange chromatography to native mass spectrometry for high throughput online characterization of charge heterogeneity of therapeutic monoclonal antibodies. MAbs. 2020;12(1).
49. Ambrogelly A, Gozo S, Katiyar A, Dellatore S, Kune Y, Bhat R, et al. Analytical comparability study of recombinant monoclonal antibody therapeutics. Vol. 10, mAbs. Taylor and Francis Inc.; 2018. p. 513–38.

50. Montacir O, Montacir H, Springer A, Hinderlich S, Mahboudi F, Saadati A, et al. Physicochemical Characterization, Glycosylation Pattern and Biosimilarity Assessment of the Fusion Protein Etanercept. Protein J. 2018 Apr 1;37(2):164–79.
51. Martínez VPM, Tierrablanca-Sánchez L, Espinosa-de la Garza CE, Juárez-Bayardo LC, Piña-Lara N, Santoyo GG, et al. Functional analysis of glycosylation in Etanercept: Effects over potency and stability. Eur J Pharm Sci. 2020 Oct 1;153.
52. Holland M, Yagi H, Takahashi N, Kato K, Savage COS, Goodall DM, et al. Differential glycosylation of polyclonal IgG, IgG-Fc and IgG-Fab isolated from the sera of patients with ANCA-associated systemic vasculitis. Biochim Biophys Acta. 2006;1760(4):669–77.
53. Reily C, Stewart TJ, Renfrow MB, Novak J. Glycosylation in health and disease. Nat Rev Nephrol. 2019;15(6):346–66.
54. Spiro RG. Protein glycosylation: nature, distribution, enzymatic formation, and disease implications of glycopeptide bonds. Glycobiology. 2002;12(4):43R-56R.
55. Costa AR, Rodrigues ME, Henriques M, Oliveira R, Azeredo J. Glycosylation: impact, control and improvement during therapeutic protein production. Crit Rev Biotechnol. 2014 Dec 6;34(4):281–99.
56. Read EK, Park JT, Brorson KA. Industry and regulatory experience of the glycosylation of monoclonal antibodies. Biotechnol Appl Biochem. 2011;58(4):213–9.
57. Hermeling S, Crommelin DJA, Schellekens H, Jiskoot W. Structure-Immunogenicity Relationships of Therapeutic Proteins. Pharm Res. 2004 Jun;21(6):897–903.
58. Bertolotti-Ciarlet A, Wang W, Lownes R, Pristatsky P, Fang Y, McKelvey T, et al. Impact of methionine oxidation on the binding of human IgG1 to FcRn and Fcγ receptors. Mol Immunol. 2009 May;46(8–9):1878–82.
59. Holzmann J, Hausberger A, Rupprechter A, Toll H. Top-down MS for rapid methionine oxidation site assignment in filgrastim. Anal Bioanal Chem. 2013 Aug 6;405(21):6667–74.
60. Liu D, Ren D, Huang H, Dankberg J, Rosenfeld R, Cocco MJ, et al. Structure and Stability Changes of Human IgG1 Fc as a Consequence of Methionine Oxidation. Biochem. 2008 May 1;47(18):5088–100.
61. Liu H, Gaza-Bulseco G, Xiang T, Chumsae C. Structural effect of deglycosylation and methionine oxidation on a recombinant monoclonal antibody. Mol Immunol. 2008 Feb;45(3):701–8.
62. Salas-Solano O, Kennel B, Park SS, Roby K, Sosic Z, Boumajny B, et al. Robustness of iCIEF methodology for the analysis of monoclonal antibodies: An interlaboratory study. J Sep Sci. 2012 Nov;35(22):3124–9.
63. Zhang T, Bourret J, Cano T. Isolation and characterization of therapeutic antibody charge variants using cation exchange displacement chromatography. J Chromatogr A. 2011 Aug;1218(31):5079–86.
64. Vlasak J, Ionescu R. Heterogeneity of Monoclonal Antibodies Revealed by Charge-Sensitive Methods. Curr Pharm Biotechnol. 2008 Dec 1;9(6):468–81.

65. Sydow JF, Lipsmeier F, Larraillet V, Hilger M, Mautz B, Mølhøj M, et al. Structure-Based Prediction of Asparagine and Aspartate Degradation Sites in Antibody Variable Regions. PLoS One. 2014 Jun 24;9(6).
66. Chelius D, Rehder DS, Bondarenko P v. Identification and Characterization of Deamidation Sites in the Conserved Regions of Human Immunoglobulin Gamma Antibodies. Anal Chem. 2005 Sep 1;77(18):6004–11.
67. Liu YD, van Enk JZ, Flynn GC. Human antibody Fc deamidation in vivo. Biologicals. 2009 Oct;37(5):313–22.
68. Nepomuceno AI, Gibson RJ, Randall SM, Muddiman DC. Accurate Identification of Deamidated Peptides in Global Proteomics Using a Quadrupole Orbitrap Mass Spectrometer. J Proteome Res. 2014 Feb 7;13(2):777–85.
69. Mamula MJ, Gee RJ, Elliott JI, Sette A, Southwood S, Jones PJ, et al. Isoaspartyl Post-translational Modification Triggers Autoimmune Responses to Self-proteins. J Biol Chem. 1999 Aug;274(32):22321–7.
70. Lyubarskaya Y, Houde D, Woodard J, Murphy D, Mhatre R. Analysis of recombinant monoclonal antibody isoforms by electrospray ionization mass spectrometry as a strategy for streamlining characterization of recombinant monoclonal antibody charge heterogeneity. Anal Biochem. 2006 Jan;348(1):24–39.
71. Dick LW, Qiu D, Mahon D, Adamo M, Cheng KC. C-terminal lysine variants in fully human monoclonal antibodies: Investigation of test methods and possible causes. Biotechnol Bioeng. 2008 Aug 15;100(6):1132–43.
72. Cai B, Pan H, Flynn GC. C-terminal lysine processing of human immunoglobulin G2 heavy chain in vivo. Biotechnol Bioeng. 2011 Feb;108(2):404–12.
73. Antes B, Amon S, Rizzi A, Wiederkum S, Kainer M, Szolar O, et al. Analysis of lysine clipping of a humanized Lewis-Y specific IgG antibody and its relation to Fc-mediated effector function. J Chromatogr B. 2007 Jun;852(1–2):250–6.
74. Wang B, Gucinski AC, Keire DA, Buhse LF, Boyne II MT. Structural comparison of two anti-CD20 monoclonal antibody drug products using middle-down mass spectrometry. Analyst. 2013;138(10):3058–65.
75. Beck A, Wagner-Rousset E, Ayoub D, van Dorsselaer A, Sanglier-Cianférani S. Characterization of Therapeutic Antibodies and Related Products. Anal Chem. 2013 Jan 15;85(2):715–36.
76. Beck A, Sanglier-Cianférani S, van Dorsselaer A. Biosimilar, Biobetter, and Next Generation Antibody Characterization by Mass Spectrometry. Anal Chem. 2012 Jun 5;84(11):4637–46.
77. Quan C, Alcala E, Petkovska I, Matthews D, Canova-Davis E, Taticek R, et al. A study in glycation of a therapeutic recombinant humanized monoclonal antibody: Where it is, how it got there, and how it affects charge-based behavior. Anal Biochem. 2008 Feb;373(2):179–91.
78. Vrdoljak A, Trescec A, Benko B, Hecimovic D, Simic M. In vitro glycation of human immunoglobulin G. Clin Chim Acta. 2004 Jul;345(1–2):105–11.

79. Fischer S, Hoernschemeyer J, Mahler H. Glycation during storage and administration of monoclonal antibody formulations. Eur J Pharm Biopharm. 2008 Sep;70(1):42–50.
80. Jairajpuri DS, Fatima S, Saleemuddin M. Immunoglobulin glycation with fructose: A comparative study. Clin Chim Acta. 2007 Mar;378(1–2):86–92.
81. Goetze AM, Liu YD, Arroll T, Chu L, Flynn GC. Rates and impact of human antibody glycation in vivo. Glycobiology. 2012 Feb 1;22(2):221–34.
82. Liu H, May K. Disulfide bond structures of IgG molecules. MAbs. 2012 Jan 27;4(1):17–23.
83. Zhang T, Zhang J, Hewitt D, Tran B, Gao X, Qiu ZJ, et al. Identification and Characterization of Buried Unpaired Cysteines in a Recombinant Monoclonal IgG1 Antibody. Anal Chem. 2012 Aug 21;84(16):7112–23.
84. Li X, Xiao L, Kochert B, Donnelly DP, Gao X, Richardson D. Extended characterization of unpaired cysteines in an IgG1 monoclonal antibody by LC-MS analysis. Anal Biochem. 2021 Jun;622:114172.
85. Chelius D, Jing K, Lueras A, Rehder DS, Dillon TM, Vizel A, et al. Formation of Pyroglutamic Acid from N-Terminal Glutamic Acid in Immunoglobulin Gamma Antibodies. Anal Chem. 2006 Apr 1;78(7):2370–6.
86. Liu YD, Goetze AM, Bass RB, Flynn GC. N-terminal Glutamate to Pyroglutamate Conversion in Vivo for Human IgG2 Antibodies. J Biol Chem. 2011 Apr;286(13):11211–7.
87. Lee JAJ, Yang J, Lee C, Moon Y, Ahn S, Yang J. Demonstration of functional similarity of a biosimilar adalimumab SB5 to Humira ®. Biologicals. 2019 Mar 1;58:7–15.
88. Kang J, Kim SY, Vallejo D, Hageman TS, White DR, Benet A, et al. Multifaceted assessment of rituximab biosimilarity: The impact of glycan microheterogeneity on Fc function. Eur J Pharm Biopharm. 2020;146:111–24.
89. Miao S, Fan L, Zhao L, Ding D, Liu X, Wang H, et al. Physicochemical and Biological Characterization of the Proposed Biosimilar Tocilizumab. BioMed Res Int . 2017;2017.
90. Bajaj S, Sakhuja N, Singla D. Stability Testing of Pharmaceutical Products. J Appl Pharm Sci. 2012;02(03):129–38.
91. Laptoš T, Omersel J. The importance of handling high-value biologicals: Physico-chemical instability and immunogenicity of monoclonal antibodies. Exp Ther Med. 2018;15(4):3161–8.
92. Kaur H. Stability testing in monoclonal antibodies. Vol. 41, Crit. Rev. Biotechnol. 2021. p. 692–714.
93. Aashigari S, Goud RG, S S, Uppala V, Potnuri NR. Stability Studies of Pharmaceutical Products. World J Pharm Res [Internet]. 2019;8(1):479–92. Available from: www.wjpr.net
94. Kang J, Halseth T, Vallejo D, Najafabadi ZI, Sen KI, Ford M, et al. Assessment of biosimilarity under native and heat-stressed conditions: rituximab, bevacizumab, and trastuzumab originators and biosimilars. Anal Bioanal Chem. 2020;412(3):763–75.
95. European Medicines Agency (EMA). ICH Topic Q 5 C Quality of Biotechnological Products: Stability Testing of Biotechnological/Biological Products [Internet]. 1996 [cited 2022 May 5]. Available from: https://www.ema.europa.eu/en/documents/scientific-guideline/ich-topic-q-5-

c-quality-biotechnological-products-stability-testing-biotechnological/biological-products_en.pdf

96. European Medicines Agency (EMA). ICH Topic Q 1 A (R2) Stability Testing of New Drug Substances and Products [Internet]. 2003 [cited 2022 Jun 2]. Available from: https://www.ema.europa.eu/en/documents/scientific-guideline/ich-q-1-r2-stability-testing-new-drug-substances-products-step-5_en.pdf
97. Jihyun DP, Jihoon K, Su Y, Park J. Evaluation of the Physico-Chemical and Biological Stability of SB8 (Aybintio), a Proposed Biosimilar to Bevacizumab, Under Ambient and In-Use Conditions. Adv Ther. 2020;37:4308–24.
98. Halley J, Chou YR, Cicchino C, Huang M, Sharma V, Tan NC, et al. An Industry Perspective on Forced Degradation Studies of Biopharmaceuticals: Survey Outcome and Recommendations. Vol. 109, J. Pharm. Sci. 2020. p. 6–21.
99. Shabestari AB, Mojtaba Mostafavi S, Malekzadeh H. Force Degradation Comparative Study on Biosimilar Adalimumab and Humira. Rev Latinoam Hipertens. 2018;13(6):498–509.
100. Nowak C, K. Cheung J, M. Dellatore S, Katiyar A, Bhat R, Sun J, et al. Forced degradation of recombinant monoclonal antibodies: A practical guide. Vol. 9, mAbs. Taylor and Francis Inc.; 2017. p. 1217–30.
101. Hawe A, Wiggenhorn M, van de Weert M, Garbe JHO, Mahler HC, Jiskoot W. Forced Degradation of Therapeutic Proteins. Vol. 101, J. Pharm. Sci. John Wiley and Sons Inc.; 2012. p. 895–913.
102. Das TK, Narhi LO, Sreedhara A, Menzen T, Grapentin C, Chou DK, et al. Stress Factors in mAb Drug Substance Production Processes: Critical Assessment of Impact on Product Quality and Control Strategy. J Pharm Sci. 2020 Jan 1;109(1):116–33.
103. Farjami A, Siahi-Shadbad M, Akbarzadehlaleh P, Roshanzamir K, Molavi O. Evaluation of the physicochemical and biological stability of cetuximab under various stress condition. J Pharm Pharm Sci. 2019;22(1):171–90.
104. Hawe A, Kasper JC, Friess W, Jiskoot W. Structural properties of monoclonal antibody aggregates induced by freeze-thawing and thermal stress. Eur J Pharm Sci. 2009 Sep 10;38(2):79–87.
105. Brych SR, Gokarn YR, Hultgen H, Stevenson RJ, Rajan R, Matsumura M. Characterization of antibody aggregation: Role of buried, unpaired cysteines in particle formation. J Pharm Sci. 2010;99(2):764–81.
106. Zhang A, Singh SK, Shirts MR, Kumar S, Fernandez EJ. Distinct aggregation mechanisms of monoclonal antibody under thermal and freeze-thaw stresses revealed by hydrogen exchange. Pharm Res. 2012;29(1):236–50.
107. Kueltzo LA, Wang W, Randolph TW, Carpenter JF. Effects of solution conditions, processing parameters, and container materials on aggregation of a monoclonal antibody during freeze-thawing. J Pharm Sci. 2008;97(5):1801–12.

108. Hassan LA, Al-Ghobashy MA, Abbas SS. Evaluation of the pattern and kinetics of degradation of adalimumab using a stability-indicating orthogonal testing protocol. Biomed Chromatogr. 2019;33(12).
109. Zheng S, Qiu D, Adams M, Li J, Mantri R v., Gandhi R. Investigating the Degradation Behaviors of a Therapeutic Monoclonal Antibody Associated with pH and Buffer Species. AAPS PharmSciTech. 2017;18(1):42–8.
110. Gaza-Bulseco G, Liu H. Fragmentation of a recombinant monoclonal antibody at various pH. Pharm Res. 2008;25(8):1881–90.
111. Alsante KM, Ando A, Brown R, Ensing J, Hatajik TD, Kong W, et al. The role of degradant profiling in active pharmaceutical ingredients and drug products. Adv Drug Deliv Rev. 2007;59(1):29–37.
112. Chumsae C, Gaza-Bulseco G, Sun J, Liu H. Comparison of methionine oxidation in thermal stability and chemically stressed samples of a fully human monoclonal antibody. Chromatogr B Analyt Technol Biomed Life Sci. 2007 May 1;850(1–2):285–94.
113. Gaza-Bulseco G, Faldu S, Hurkmans K, Chumsae C, Liu H. Effect of methionine oxidation of a recombinant monoclonal antibody on the binding affinity to protein A and protein G. Chromatogr B Analyt Technol Biomed Life Sci. 2008 Jul 1;870(1):55–62.
114. Li X, Xu W, Wang Y, Zhao J, Liu YH, Richardson D, et al. High throughput peptide mapping method for analysis of site specific monoclonal antibody oxidation. J Chromatogr A. 2016 Aug 19;1460:51–60.
115. Sokolowska I, Mo J, Dong J, Lewis MJ, Hu P. Subunit mass analysis for monitoring antibody oxidation. MAbs. 2017 Apr 3;9(3):498–505.
116. Tokhadze N, Chennell P, le Basle Y, Sautou V. Stability of infliximab solutions in different temperature and dilution conditions. J Pharm Biomed Anal. 2018 Feb 20;150:386–95.
117. Chi EY, Krishnan S, Randolph TW, Carpenter JF. Physical Stability of Proteins in Aqueous Solution: Mechanism and Driving Forces in Nonnative Protein Aggregation. Pharm Res. 2003;20(9):1325–36.
118. Gusarova V, Degterev M, Lyagoskin I, Simonov V, Smolov M, Taran S, et al. Analytical and functional similarity of biosimilar Elizaria® with eculizumab reference product. J Pharm Biomed Anal. 2022 Oct;220:115004.
119. Tamizi E, Jouyban A. Forced degradation studies of biopharmaceuticals: Selection of stress conditions. Vol. 98, Eur. J. Pharm. Biopharm. 2016. p. 26–46.
120. Hutterer KM, Ip A, Kuhns S, Cao S, Wikström M, Liu J. Analytical Similarity Assessment of ABP 959 in Comparison with Eculizumab Reference Product. BioDrugs. 2021;35(5):563–77.
121. DeFelippis MR, Harmon BJ, Huang L, Sukumar M. Pharmaceutical Stress Testing. 2nd ed. Baertschi SW, Alsante KM, Reed RA, editors. CRC Press; 2011. 370–390 p.
122. Hernández-Jiménez J, Martínez-Ortega A, Salmerón-García A, Cabeza J, Prados JC, Ortíz R, et al. Study of aggregation in therapeutic monoclonal antibodies subjected to stress and long-

term stability tests by analyzing size exclusion liquid chromatographic profiles. Int J Biol Macromol. 2018 Oct 15;118:511–24.

123. Ito T, Tsumoto K. Effects of subclass change on the structural stability of chimeric, humanized, and human antibodies under thermal stress. Protein Science. 2013 Nov;22(11):1542–51.

124. Bansal R, Dash R, Rathore AS. Impact of mAb Aggregation on Its Biological Activity: Rituximab as a Case Study. J Pharm Sci. 2020;109(9):2684–98.

125. Jung SK, Lee KH, Jeon JW, Lee JW, Kwon BO, Kim YJ, et al. Physicochemical characterization of Remsima®. MAbs. 2014 Sep 3;6(5):1163–77.

126. Lee KH, Lee J, Bae JS, Kim YJ, Kang HA, Kim SH, et al. Analytical similarity assessment of rituximab biosimilar CT-P10 to reference medicinal product. MAbs. 2018 Apr 3;10(3):380–96.

127. Dakshinamurthy P, Mukunda P, Prasad Kodaganti B, Shenoy BR, Natarajan B, Maliwalave A, et al. Charge variant analysis of proposed biosimilar to Trastuzumab. Biologicals. 2017 Mar 1;46:46–56.

128. Khawli LA, Goswami S, Hutchinson R, Kwong ZW, Yang J, Wang X, et al. Charge variants in IgG1: Isolation, characterization, in vitro binding properties and pharmacokinetics in rats. MAbs. 2010 Nov;2(6):613–24.

129. Haberger M, Bomans K, Diepold K, Hook M, Gassner J, Schlothauer T, et al. Assessment of chemical modifications of sites in the CDRs of recombinant antibodies. MAbs. 2014 Mar 17;6(2):327–39.

130. Schmid I, Bonnington L, Gerl M, Bomans K, Thaller AL, Wagner K, et al. Assessment of susceptible chemical modification sites of trastuzumab and endogenous human immunoglobulins at physiological conditions. Commun Biol. 2018 Dec 5;1(1):28.

131. Cho IH, Lee N, Song D, Jung SY, Bou-Assaf G, Sosic Z, et al. Evaluation of the structural, physicochemical, and biological characteristics of SB4, a biosimilar of etanercept. MAbs. 2016 Aug 17;8(6):1136–55.

132. Mahler HC, Friess W, Grauschopf U, Kiese S. Protein aggregation: Pathways, induction factors and analysis. J Pharm Sci. 2009 Sep;98(9):2909–34.

133. Wang W, Wang YJ, Wang DQ. Dual effects of Tween 80 on protein stability. Int J Pharm. 2008 Jan;347(1–2):31–8.

134. Vázquez-Rey M, Lang DA. Aggregates in monoclonal antibody manufacturing processes. Biotechnol Bioeng. 2011 Jul;108(7):1494–508.

135. Shukla AA, Gupta P, Han X. Protein aggregation kinetics during Protein A chromatography. Case study for an Fc fusion protein. J Chromatogr A. 2007 Nov 9;1171(1–2):22–8.

136. Mazzer AR, Perraud X, Halley J, O'Hara J, Bracewell DG. Protein A chromatography increases monoclonal antibody aggregation rate during subsequent low pH virus inactivation hold. J Chromatogr A. 2015 Oct 9;1415:83–90.

137. Gómez G, Pikal MJ, Rodríguez-Hornedo N. Effect of initial buffer composition on pH changes during far-from-equilibrium freezing of sodium phosphate buffer solutions. Pharm Res. 2001;18(1):90–7.
138. Chi EY, Krishnan S, Randolph TW, Carpenter JF. Physical Stability of Proteins in Aqueous Solution: Mechanism and Driving Forces in Nonnative Protein Aggregation. Pharm Res. 2003;20(9):1325–36.
139. Leblanc Y, Ramon C, Bihoreau N, Chevreux G. Charge variants characterization of a monoclonal antibody by ion exchange chromatography coupled on-line to native mass spectrometry: Case study after a long-term storage at +5 °C. J Chromatogr B. 2017 Mar 24;1048:130–9.

APPENDIX

APPENDIX 1: Stability Study Results of SE-UPLC Analysis

Table 25: SE-UPLC stability study % area results

Stability Study			BS			OR
			5.0±3.0˚C	25±2°C/60±5%RH	≤-65°C	5.0±3.0˚C
SE-UPLC	Monomer	0	97.95	97.95	97.95	97.94
		1	97.84	97.63	96.96	97.94
		6	97.74	96.67	95.60	97.88
		9	97.69	96.10	95.05	97.83
		12	97.25	95.11	94.32	97.51
		18	97.37	NT	93.93	97.50
		24	97.30	NT	92.89	97.42
	HMW	0	1.19	1.19	1.19	1.19
		1	1.28	1.45	2.21	1.22
		6	1.56	2.53	3.76	1.54
		9	1.56	2.98	4.10	1.46
		12	1.70	3.67	4.53	1.45
		18	1.81	NT	5.35	1.71
		24	2.03	NT	6.47	1.94

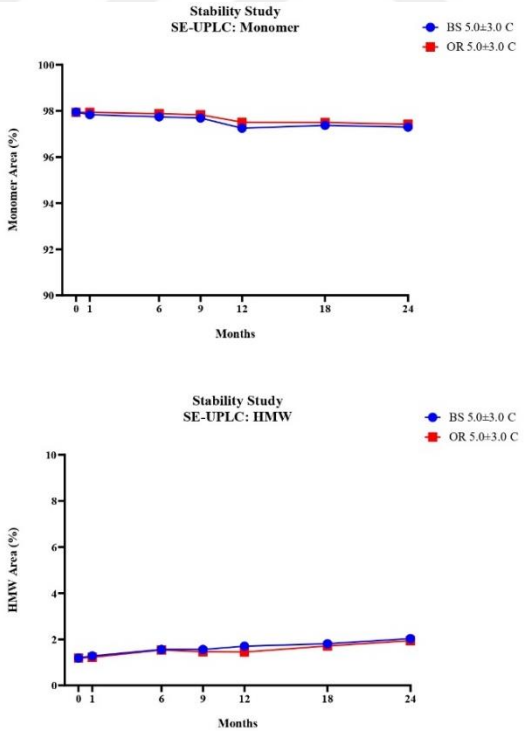

Figure 92: Stability atudy, SE-UPLC analysis results of BS and OR samples at 5.0±3.0°C storage condition

APPENDIX 2: Stability Study Results of icIEF Analysis

Table 26: icIEF stability study % area results

Stability Study			BS						OR	
			5.0±3.0˚C		25±2°C/60±5%RH		≤-65°C		5.0±3.0˚C	
			With CpB	Without CpB	With CpB	Without CpB	With CpB	Without CpB	With CpB	Without CpB
icIEF	Main Variant	0	62.95	59.63	62.95	59.63	62.95	59.63	55.34	54.07
		1	62.50	61.05	60.63	58.65	62.83	60.45	57.14	52.80
		6	62.43	56.55	43.70	42.90	63.03	59.06	55.65	51.92
		9	61.66	58.36	36.32	37.42	61.84	58.94	54.99	52.08
		12	58.31	58.30	30.79	30.47	58.70	58.48	51.57	50.86
		18	57.85	55.91	NT	NT	58.81	56.74	51.60	48.98
		24	56.52	55.02	NT	NT	58.31	56.47	50.17	48.09
	Acidic Variants	0	30.44	28.59	30.44	28.59	30.44	28.59	40.23	32.98
		1	29.99	28.12	33.12	31.80	29.64	28.07	38.32	33.63
		6	30.19	29.99	50.55	47.79	29.17	28.37	38.57	34.73
		9	31.99	29.95	59.04	55.12	28.69	28.18	39.38	34.71
		12	34.68	30.41	64.48	63.83	33.07	28.34	42.90	35.30
		18	34.67	32.88	NT	NT	30.80	29.88	42.00	37.21
		24	36.22	32.60	NT	NT	30.42	29.08	43.64	37.74
	Basic Variants	0	6.63	11.79	6.63	11.79	6.63	11.79	4.44	12.95
		1	7.53	10.84	6.26	9.55	7.53	11.48	4.55	13.57
		6	7.37	13.47	5.76	9.32	7.80	12.57	5.78	13.36
		9	6.36	11.70	4.65	7.48	9.47	12.90	5.64	13.21
		12	7.02	11.31	4.73	5.70	8.23	13.19	5.54	13.84
		18	7.47	11.21	NT	NT	10.29	13.38	6.41	13.82
		24	7.26	12.38	NT	NT	11.23	14.46	6.20	14.18

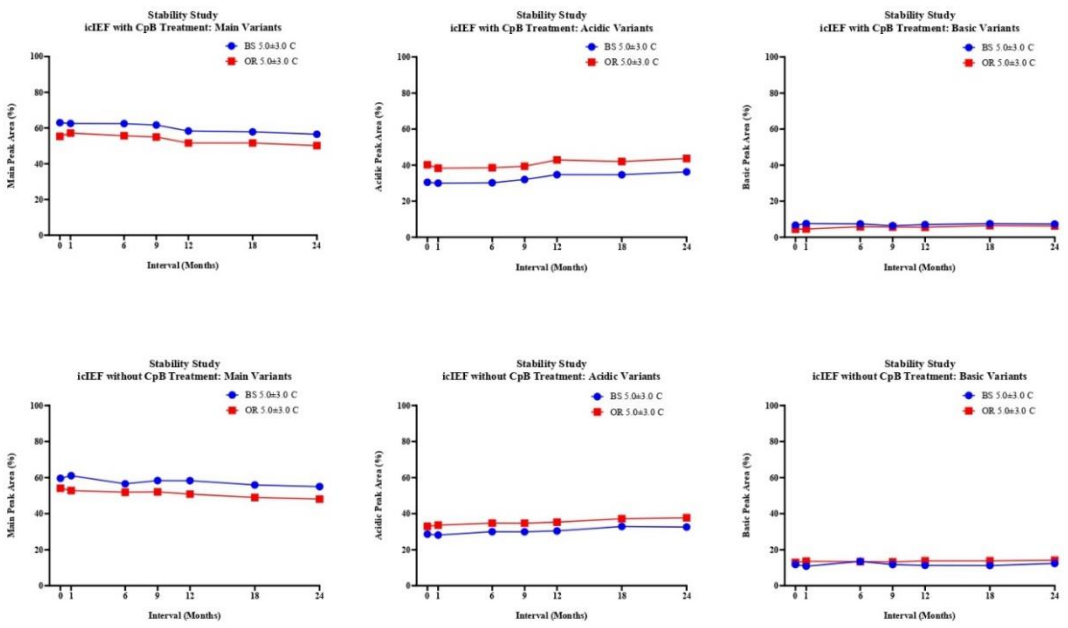

Figure 93: Stability study, icIEF analysis results of BS and OR samples at 5.0±3.0°C storage condition

APPENDIX 3: Stability Study Results of CE-SDS Analysis

Table 27: CE-SDS stability study % area results

Stability Study			BS			OR
			5.0±3.0˚C	25±2°C/60±5%RH	≤-65°C	5.0±3.0˚C
CE-SDS	rCE-SDS LC+HC	0	99.41	99.41	99.41	98.35
		1	99.42	99.39	99.33	98.70
		6	99.46	98.26	99.43	98.61
		9	99.47	97.55	99.48	98.54
		12	99.44	96.48	99.49	98.42
		18	99.46	NT	99.42	98.21
		24	99.38	NT	99.44	98.22
	nrCE-SDS IgG	0	98.35	98.35	98.35	98.44
		1	98.33	98.32	98.32	98.68
		6	98.25	98.24	98.30	98.82
		9	98.21	98.19	98.22	98.59
		12	98.17	97.51	98.19	98.67
		18	97.44	NT	97.40	97.75
		24	97.23	NT	96.87	97.51

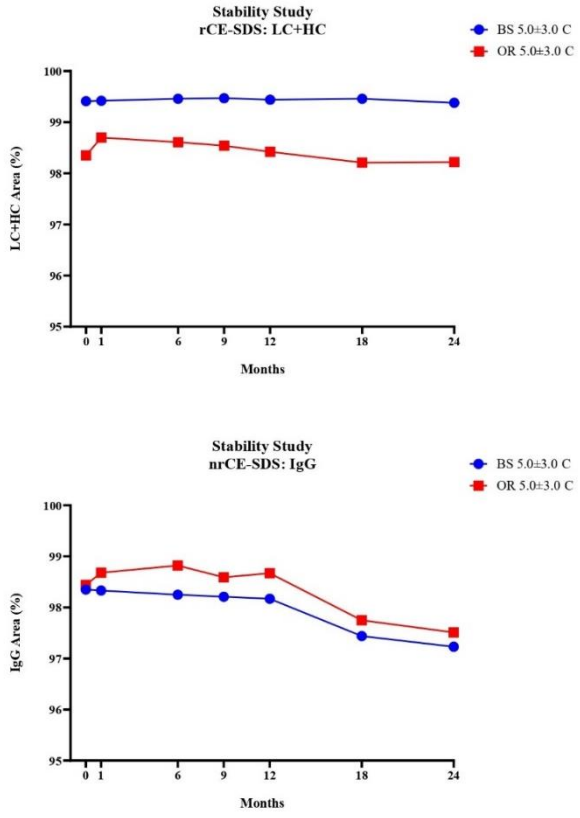

Figure 94: Stability study, CE-SDS analysis results of BS and OR samples at 5.0±3.0°C storage condition

APPENDIX 4: Stability Study Results of Complement Assay Analysis

Table 28: Complement assay stability study relative potency % results

Stability Study			BS			OR
			5.0±3.0˚C	25±2°C/60±5%RH	≤-65°C	5.0±3.0˚C
Complement Assay	Relative Potency %	0	94.34	94.34	94.34	78.79
		1	106.56	104.04	98.30	98.91
		6	88.84	86.98	90.70	93.02
		9	93.54	93.39	93.00	101.17
		12	105.73	106.17	106.17	122.47
		18	90.66	NT	85.04	84.12
		24	99.59	NT	103.85	102.97

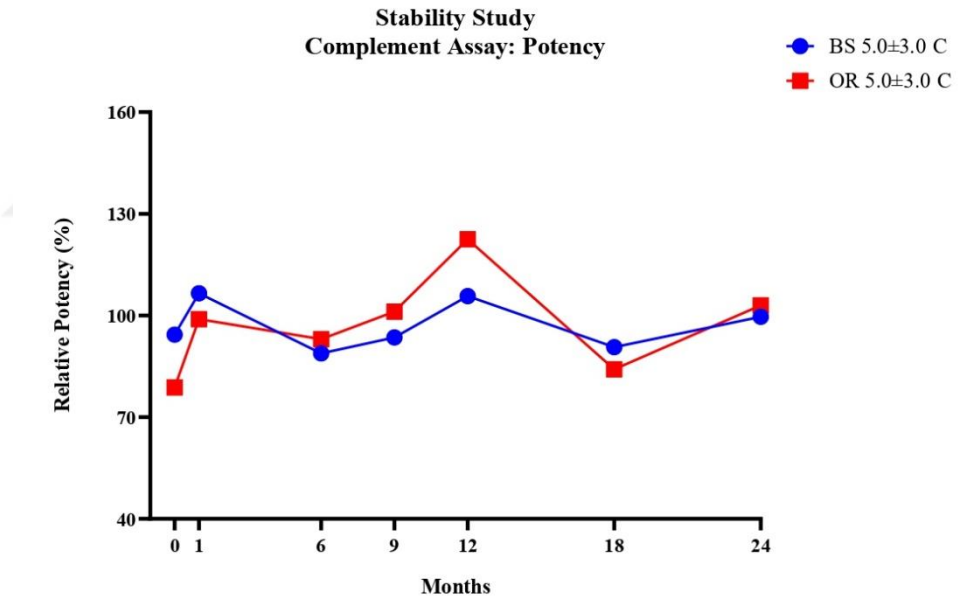

Figure 95: Stability study, complement assay analysis results of BS and OR samples at 5.0±3.0°C storage condition

9 CURRICULUM VITAE